TURKISH REPUBLIC
ERCIYES UNIVERSITY
GRADUATE SCHOOL OF NATURAL AND APPLIED SCIENCE
DEPARTMENT OF MECHANICAL ENGINEERING

NUMERICAL INVESTIGATION OF HEAT TRANSFER ENHANCEMENT ON ADDING (TiO_2) NANOPARTICALES TO WATER FLOW IN NOZZLES ADDED TOA HORIZONTAL TUBE

Prepared By
Natiq Abbas Fadhil AL-AMERI

Supervisior
Prof. Dr. Veysel ÖZCEYHAN

M.Sc. Thesis

December 2017
KAYSERI

TURKISH REPUBLIC
ERCIYES UNIVERSITY
GRADUATE SCHOOL OF NATURAL AND APPLIED SCIENCE
DEPARTMENT OF MECHANICAL ENGINEERING

NUMERICAL INVESTIGATION OF HEAT TRANSFER ENHANCEMENT ON ADDING (TiO_2) NANOPARTICALES TO WATER FLOW IN NOZZLES ADDED TOA HORIZONTAL TUBE

Prepared By
Natiq Abbas Fadhil AL-AMERI

Supervisior
Prof. Dr. Veysel ÖZCEYHAN

M.Sc. Thesis

December 2017
KAYSERI

TURKISH REPUBLIC
ERCIYES UNIVERSITY
GRADUATE SCHOOL OF NATURAL AND APPLIED SCIENCE
DEPARTMENT OF MECHANICAL ENGINEERING

NUMERICAL INVESTIGATION OF HEAT TRANSFER ENHANCEMENT ON ADDING (TiO_2) NANOPARTICALES TO WATER FLOW IN NOZZLES ADDED TOA HORIZONTAL TUBE

(M.Sc. Thesis)

Prepared By
Natiq Abbas Fadhil AL-AMERI

Supervisior
Prof. Dr. Veysel ÖZCEYHAN

This Thesis is supported by Erciyes University Scientific Research Unit with Project Code Number of FYL-2017-7240

December 2017
KAYSERI

SCIENTIFIC ETHICS SUITABILITY

I declare that all information in this work were obtained in accordance with academic and ethical rules. All results and material that not been at the essence of this work are also transferred and expressed by giving reference as required by these rules and behavior.



Natiq Abbas Fadhil AL-AMERI

SUITABILITY FOR GUIDE

The MSc thesis entitled **Numerical Investigation of Heat Transfer Enhancement on Adding (TiO2) Nanoparticles to Water Flow in Nozzles Added to a Horizontal Tube"** has been prepared in accordance with Erciyes University Graduate Education and Teaching Institute Thesis Preparation and Writing Guide.

Student

Natiq Abbas Fadhil AL-AMERI

Supervisor

Prof. Dr. Veysel ÖZCEYHAN

Chairman of the Department of Mechanical Engineering

Prof. Dr. Necdet ALTUNTOP

This study entitled "**Numerical Investigation of Heat Transfer Enhancement on Adding (TiO2) Nanoparticales To Water Flow in Nozzles Added To A Horizontal Tube**" prepared by **Natiq AL-AMERI** under the supervision of **Prof. Dr. Veysel ÖZCEYHAN** was accepted by the jury as MSc. Thesis in Mechanical department.

..25../12 / 2017

JURY:

Supervisor : Prof. Dr. Veysel ÖZCEYHAN .....

Juror : Prof. Dr. Necdet ALTUNTOP .....

Juror : Prof. Dr. Hüseyin AKILLI .....

APPROVAL

That the acceptance of this thesis has been approved by the decision of the Institute's Board of Directors with the 26./12/2017 Date and 2017/55-16 numbered decision.

T.C.

Prof. Dr. Mehmet AKKURT

Director of the Institute

ACKNOWLEDGEMENTS

First, I thank God and praise him for his bounty and grace which guided me and enlightened my way in completing this research.

I would like to express my special appreciation and gratitude to my advisor Prof. Dr. Veysel ÖZCEYHAN who has been a tremendous mentor for me. I would like to thank him for encouraging my research and for allowing me to grow as a research scientist. His advice on both research and my career has been priceless. I would also like to thank my committee members, Prof. Dr. Necdet ALTUNTOP, Prof. Dr. Hüseyin AKILLI, and for serving as my committee members even at hardship. I also want to thank you for letting my defense be an enjoyable moment, and for your brilliant comments and suggestions.

I would especially like to thank Res. Assist. Toygun DAGDEVIR and Res. Assist. Orhan KEKLIKCIOGLU who have always been available to support me when I collected data for my MSc. thesis.

I express special thanks to my family. Words cannot express how grateful I am to my mother, and father for all of the sacrifices that they have made on my behalf. Your prayer for me was what sustained me this far. I also thank my older brother Tariq who was a friend and a fan of me in completing my MSc. In the end, I would like to express my deepest gratitude to my beloved wife and children (Anas, Arwa and Ahmed) who spent sleepless nights with me and was always my support in the moments when there was no one to answer my queries.

Natiq Abbas Fadhil AL-AMERI

Kayseri, December 2017

NUMERICAL INVESTIGATION OF HEAT TRANSFER ENHANCEMENT ON ADDING (TiO_2) NANOPARTICLES TO WATER FLOW IN NOZZLES ADDED TO A HORIZONTAL TUBE

Natiq AL-AMERI

Erciyes University, Graduate School of Natural and Applied Sciences
MSc. Thesis, December -2017
Thesis Supervisors: Prof. Dr. Veysel ÖZCEYHAN

ABSTRACT

This study presents a quantitative investigation regarding the thermal performance of inserting two types of nozzle; (a) Non-drilled nozzles, (b) Drilled nozzle with three different pitch lengths (126, 180 and 315 mm) through a water-based TiO_2 nanofluid flowing into a horizontal tube. The considered nanofluid volume fractions are limited from 0.2% to 2.0%. A uniform constant heat flux of 50 $kW/m^2$was applied onto the outer surface of the tube. The k-ω standard turbulent model was chosen to simulate turbulent flow, and analyses were implemented for the Reynolds number ranging from 4000 to 14,000. The nanofluid flow was modeled using the mixture model as it is more accurate than the single-phase model. The thermophysical properties of nanoparticles and water are considered independent of temperature. The thermophysical properties of the nanofluid were calculated with equations and empirical correlations based on the literature. Thus, as the volume fraction of TiO_2 in both the smooth tube and drilled nozzle inserted tube rise, the heat transfer coefficient increases. While increasing pitch length of the nozzles means decreasing the number of nozzles in the tube, yet when using drilled nozzle, it's higher than the non-drilled nozzle. As such, inserting more nozzles into the tube fosters the heat transfer, but increases the pressure drop penalty. The highest heat transfer coefficient for drilled nozzle is obtained as 72% which is bigger than the non-drilled nozzle, and the heat transfer of non-drilled nozzle is higher than the smooth tube about 54.5% for nanofluid flow through the smooth tube inserted nozzle with a pitch length of 126 and volume fraction of 2.0%, and friction factor increases approximately 5 times more than the smooth tube and less than the non-drilled nozzle approximately 7%.

Keywords: Heat transfer enhancement, TiO_2/Water nanofluid, nozzle, performance enhancement coefficient, CFD.

İÇERİSİNE LÜLE YERLEŞTİRİLMİŞ YATAY BİR BORU İÇİNDEN GEÇEN SUYA TiO_2 NANOPARTİKÜL EKLENMESİNİN ISI TRANSFERİ İYİLEŞTİRİLMESİ SAYISAL ARAŞTIRMASI

Natiq AL-AMERI

Erciyes Üniversitesi Fen Bilimleri Enstitüsü
Yüksek Lisans Tezi, Aralık 2017
Tez Danışmanı: Prof. Dr. Veysel ÖZCEYHAN

ÖZET

Bu tez çalışması, su bazlı TiO_2 nanoakışkanın geçtiği yatay düz bir boru içerisine yerleştirilen farklı adım uzunluklarında (126, 180 ve 315 mm) yerleştirilen iki farklı tipteki lüle elemanların (üzerine delik açılmış ve açılmamış olmak üzere) termal performans etkisinin sayısal araştırmasını sunmaktadır. İncelenen nanoakışkan acimsel fraksiyonlar %0.2 ila %2.0 arasında sınırlandırılmıştır. Borunun dış yüzeyine 50 kW/m^2 değerinde sabit ısı akısı uygulanmıştır. Reynolds sayısının 4000-14000 arasında gerçekleştirilen analizlerde türbülans akışın simulasyon edilmesi için *k-ω standard turbulent* model seçilmiştir. Tek fazlı modelden (single phase model) daha gerçekçi sonuçlar vermesi sebebiyle, nanoakışkan analizlerinde karışım modeli (mixture model) kullanılmıştır. Nano parçacık ve suyun termo-fiziksel özellikleri sıcaklıktan bağımsız olduğu göz önünde bulundurulmuştur. Nanoakışkanın termo-fiziksel özellikleri literatürde yer alan korelasyon ve formüller ile hesaplanmıştır. Sonuçlar, hem boş boruda hem de lüle yerleştirilmiş boruda TiO_2-Su nanoakışkanın hacimsel fraksiyonunun arttıkça taşınımla ısı transfer katsayısının arttığını göstermiştir. Lülelerin adım uzunluğunun azalması, kullanılan lülelerin sayısının artması anlamına gelmektedir ve bu durum ısı transferini arttırdığı gözlemlenmiştir. Ayrıca kullanılan üzerine delik açılmış lülelerin ısı transferi açısından sonuçları, delinmemiş lülelere nazaran daha olumludur. Boru içerisinde lüle kullanımı ısı transferini arttırırken; basınç düşümünü de olumsuz anlamda arttırmaktadır. En yüksek taşınımla ısı transferi sayısı boş boru da su akışı ile kıyaslandığında, en düşük adım uzunluğunda (PL=126 mm) yerleştirilmiş delinmiş lüle ve en yüksek hacimsel fraksiyonlu (φ=2.0 %) nanoakışta yaklaşık olarak %72 daha fazla elde edilmiştir. %2.0 hacimsel fraksiyonlu nanoakışta delinmiş lüle yerine delinmemiş lüle kullanımında ise su akışlı boş boruya nazaran ısı transferi katsayısı %54.5 daha fazla elde edilmiştir. Hidrolik açısından sonuçlar incelendiğinde

ise en düşük adım uzunluğunda delinmemiş lüle kullanımı ile boş boru kıyaslandığında (aynı akışkan için) sürtünme faktörü 5 kat daha fazla ortaya çıkmaktadır. Delinmemiş lüle yerine delinmiş lüle kullanıldığında ise sürtünme faktörü yaklaşık olarak %7 azalmaktadır.

Anahtar Kelimeler: Isı transferi iyileştirmesi, TiO_2/Su nanofluid, lüle, performans iyileşme katsayısı, HAD

TABLE OF CONTENTS

NUMERICAL INVESTIGATION OF HEAT TRANSFER ENHANCEMENT ON ADDING (TiO2) NANOPARTICALES TO WATER FLOW IN NOZZLES ADDED TOA HORIZONTAL TUBE

SCIENTIFIC ETHICS SUITABILITY i

SUITABILITY FOR GUIDE ii

APPROVAL iii

ACKNOWLEDGEMENTS iv

ABSTRACT v

ÖZET vi

TABLE OF CONTENTS viii

LIST OF ABBREVIATIONS xiii

LIST OF TABLES xv

LIST OF FIGURES xvi

INTRODUCTION 1

CHAPTER 1

GENERAL INFORMATION

1. TECHNIQUES OF HEAT TRANSFER ENHANCEMENT 3

1.1. Passive Techniques 3

1.1.1. Treated Surface 3

1.1.2. Rough surface 4

1.1.3. Extended surfaces 4

1.1.4. Displaced enhancement devices: 4

1.1.5. Swirl flow devices: 4

1.1.6. Coiled tubes: 4

1.1.7. Surface tension devices: 5

1.1.8. Additives for liquids: 5

1.1.9. Additives for gases: 5

1.2. Active Techniques **6**
1.2.1. Mechanical aids **7**
1.2.2. Surface vibration **7**
1.2.3. Fluid vibration **7**
1.2.4. Electrostatic fields **7**
1.2.5. Injection **7**
1.2.6. Suction **7**
1.2.7. Jet impingement **7**
1.3. Compound Techniques **8**
1.4. Different Inserts **8**
1.5. The Concept of Nanofluds **10**
1.5.1. Nanoparticle Material Types **12**
1.5.2. Base Liquid Types **14**
1.5.3. Nanofluid Preparation **14**
1.6. IMPORTANCE OF NANOFLUIDS **18**
1.7. APPLICTION OF NANOFLUIDS **19**
1.8. THE OBJECTIVES OF THE PRESENT STUDY **20**
1.9. BENEFITS OF THE STUDY **21**
1.9.1. Scientific Benefits **21**
1.9.2. Technological Benefits **21**
1.9.3. Environmental Benefits **22**
1.9.4. Industrial Benefits **22**
1.9.5. Economical Benefits **22**
2. LITERATURE REVIEW **23**
2.1. INVESTIGATIONS ON USING TURBULATORS **23**
2.2. INVESTIGATIONS ABOUT USING NANOFLUID **29**
2.3. INVESTIGATIONS ON USING BOTH TURBULATOR AND NANOFLUID **36**

CHAPTER 2

METHODOLOGY

2.1. INFLUENTIAL PARAMETERS IN THE INVESTIGATION 45

2.1.1. Boundary Layer (Hydraulic) 45

2.1.2. Thermal Boundary layer 47

2.1.3. Drop Pressure (∆P) 48

2.1.4. Thermal Conductivity (K) 49

2.1.5. Heat Transfer Coefficient (h) 50

2.1.6. Non-Dimensional Number 50

2.1.6.1. Reynolds Number (Re) 50

2.1.6.2. Prandtl Number (Pr) 51

2.1.6.3. Nusselt Number (Nu) 51

2.2. Computational Domain 54

2.3. Method and Governing Equation 56

2.3.1. Governing Equation 56

2.3.1.1. Conservation of mass equation [107]: 57

2.3.1.2. Conservation of momentum equation [107]: 57

2.3.1.3. Energy equation [107]: 57

2.3.2. Determining of the Numerical Methodology 57

2.3.2.1. Determining of the Water Analyses 58

2.3.2.1.1. Turbulence Models (smooth tube) 58

2.3.2.1.2. Mesh Independence 59

2.3.2.2 Validation of Nanofluid Analyses 62

2.3.2.2.1. Property of Nanofluid (Thermo- physical properties) 62

2.3.2.2.1.1. Density 62

2.3.2.2.1.2. Specific Heat 63

2.3.2.2.1.3. Viscosity 63

2.3.2.2.1.4. Thermal Conductivity 63

2.3.2.3. Thermal Performance Factor 64

CHAPTER 3

RESULTS AND DISCUSSION

3.1. Validation **66**

3.1.1. Validation of Water flow: **66**

3.1.1.1. Convective Heat Transfer **66**

3.1.1.2. Friction Factor **67**

3.1.2. Validation of nanofluid flow **68**

3.1.3. Comparison between water and nanofluid flow in smooth tube **72**

3.1.3.1. Convective Heat Transfer **72**

3.1.3.2. Friction Factor **73**

3.2. Non drilled nozzle inserted-Smooth tube **75**

3.2.1. Water flow **75**

3.2.1.1. Convective Heat Transfer **75**

3.2.1.2. Friction factor **76**

3.2.1.3. Performance Enhancement Factor **77**

3.2.2. Nanofluid flow **77**

3.2.2.1. Convective Heat Transfer **77**

3.2.2.2. Pressure Drop **78**

3.2.2.3. Performance Enhancement Factor **79**

3.3. Drilled – non drilled nozzle **83**

3.3.1. Water flow **83**

3.3.1.1. Convective Heat Transfer **83**

3.3.1.2. Friction factor **84**

3.3.1.3. Performance Enhancement Factor **85**

3.3.2. Nanofluid flow **87**

3.3.2.1. Convective Heat Transfer **87**

3.3.2.2. Pressure Drop **88**

3.3.2.3 Performance Enhancement Factor **89**

CHAPTER- 4

CONCLUSION AND RECOMMENDATIONS

4.1. CONCLUSION.....94

4.2. RECOMMENDATIONS.....96

REFERENCES.....98

CURRICULUM VITAE.....110

LIST OF ABBREVIATIONS

b	Base fluid	(-)
C	Specific heat capacity	(kJ/kg.K)
D	Diameter of tube	(mm)
D_1	Big diameter of nozzle	(mm)
D_2	Small diameter of nozzle	(mm)
d	hole diameter	(mm)
f	Friction factor	(-)
h	Convective Heat transfer coefficient	($W/m^2.K$)
I	inserted tube	(-)
in	inlet	(-)
k	Thermal conductivity coefficient	(W/m.K)
κ	Turbulent kinetic energy	($J/kg)=(m^2/s^2$)
L	Length of tube	(mm)
l	Distance between two nozzle	(mm)
l_1	Length of nozzle	(mm)
Nu	Nusselt number	(-)
nf	nanofluid	(-)
np	nanoparticle	(-)
out	outlet	(-)
P.L	Pitch length	(mm)
Pr	Prandtal number	(-)
q	Heat flux	(W/m^2)
Re	Reynolds number	(-)
s	smooth tube	(-)
T_b	Bulk temperature	(℃)
T1	Inlet temperature	(℃)
T2	Outlet temperature	(℃)

t	Tube inserted	(-)
V	Velocity inlet	(m/s)
w		(-)
ω	Dissipation rate	(1/s)
ΔP	Drop pressure	(Pa)
μ	Dynamic viscosity	(kg/m.s)
ρ	Density	(kg/m^3)
φ	Volume fraction	(%)
PEC	Performance enhancement coefficient	(-)
β	Thermal expansion coefficient	(K^{-1})
∇	represents the partial derivative of a quantity with respect to all directions in the chosen coordinate system	

LIST OF TABLES

Table 1.1. Thermal conductivities of different materials 13

Table 1.2. Nanofluids systems reported in literature 17

Table 1.3. The comparison between the micro particles and nanoparticles 18

Table 2.1. The equations that pertain for smooth circular tube in turbulent flow thermohydrolic. 52

Table 2.2. The equations of friction factor for smooth circular tube in turbulent flow 53

Table 2.3. The physical explanation for dimensionless number 54

Table 2.4. Definitions, symbols and magnitudes of the solution geometry and boundary conditions 56

Table 2.5. Thermo-physical properties of water –TiO_2nanofluid 64

Table 4.1. Most advantages and Most Disadvantages for Convective heat transfer coefficient, Pressure drop and Performance Enhancement Factor. 96

LIST OF FIGURES

Figure 1.1. Examples of passive enhancement techniques 6

Figure 1.2. Schema of the various flow zones in an impinging jet 8

Figure 1.3. Tubefitted with conical ring turbulator and twisted tape insert 9

Figure 1.4. Tubefitted with coiled wire inserts 9

Figure 1.5. Tube fitted with conical ring turbulator and twisted tape insert by Promvonge and Eiamsa 10

Figure 1.6. The nozzle-turbulators 10

Figure 1.7. Thermal conductivity of some materials 12

Figure 1.8. An image of dispersed TiO2 nanoparticales in water 16

Figure 1.9. SEM image of dispersed Al2O3 nanoparticle in water 16

Figure 1.10. Typical procedure of two-step method of preparation of nanofluids 17

Figure 2.1. The development of the boundary layer for flow over a flat plate, and the different flow regimes. 46

Figure 2.2. The development of the velocity boundary layer in a tube. (The developed mean velocity profile will be parabolic in laminar flow, as shown, but somewhat blunt in turbulent flow) 47

Figure 2.3. The development of the thermal boundary layer in a tube. (The fluid in the tube is being cooled.) 48

Figure 2.4. The sketch show pressure drop is one of the most general relations in fluid mechanics 49

Figure 2.5. (a) Boundary condition and definition of solution domain for nozzle without hole 54

Figure 2.6. Boundary condition and definition of solution domain for nozzle inserted tube 55

Figure 2.7. Boundary condition and definition of solution domain for nozzle inserted tube 56

Figure 2.8. (a) Comparison of a turbulence model with the effect of Reynolds number and Nusselt number. 58

Figure 2.9. Element types (a) Triangular, (b) Tetrahedral, and (c) Polyhedral.....60

Figure 2.10. Mesh sizes for the grid independence study of the tube and inserted nozzle.....61

Figure 2.11. Grid independence study for the simulation of nozzle inserted tube.....62

Figure 3.1. Comparison of quantitative results with Dittus-Boelter Equation in terms of Nusselt number versus Reynolds number 67

Figure 3.2. Comparison of quantitative results with Blasius Equation in terms of Friction factor versus Reynolds number.....68

Figure 3.3. Validation of nanofluid study in terms of Nusselt number versus Reynolds number in correlation with Pak and Cho, Duangthongsuk & Wongwises and Sajadi & Kazemi at 0.2% TiO2/water nanofluid. 69

Figure 3.4. Validation of nanofluid study in terms of Nusselt number versus Reynolds number in correlation with Pak and Cho, Duangthongsuk & Wongwises and Sajadi & Kazemi at 0.6% TiO2/water nanofluid. 69

Figure 3.5. Validation of nanofluid study in terms of Nusselt number versus Reynolds number in correlation with Pak and Cho, Duangthongsuk & Wongwises and Sajadi & Kazemi at 1 % TiO2/water nanofluid. 70

Figure 3.6. Validation of nanofluid study in terms of Nusselt number versus Reynolds number in correlation with Pak and Cho, Duangthongsuk & Wongwises and Sajadi & Kazemi at 1.5 % TiO2/water nanofluid. 70

Figure 3.7. Validation of nanofluid study in terms of Nusselt number versus Reynolds number in correlation with Pak and Cho, Duangthongsuk & Wongwises and Sajadi & Kazemi at 2 % TiO2/water nanofluid. 71

Figure 3.8. Comparison of friction factor between the quantitative data and the reckoned values from correlation and Duangthongsuk and Wongwises.....71

Figure 3.9. Comparison of Nusselt Number and Reynolds Number for the nanofluid and water for smooth tube 72

Figure 3.10. Comparison of Friction Factor and Reynolds Number for nanofluid and water.....73

Figure 3.11. Effect of nanofluid on smooth tube on thermal performance factor 74

Figure 3.12. Comparison of convective heat transfer coefficient and Reynolds Number for the water between smooth tube and inserted nozzle at varying pitch lengths (126mm, 180mm and 315mm)..... 75

Figure 3.13. Comparison of friction factor and Reynolds Number for water between smooth tube and varying pitch lengths (126mm, 180mm and 315 mm) for non-drilled nozzle 76

Figure 3.14. Effect and comparison of inserted non-drilled nozzle on tube and smooth tube on thermal performance factor for water flow 77

Figure 3.15. Effect of inserted non-drilled nozzles upon the tube with considered pitch length at constant volume fraction of 2.0% in terms of convective heat transfer versus Reynolds number..... 78

Figure 3.16. Effect of inserted non-drilled nozzles into the tube with considered pitch length at constant volume fraction of 2.0% in terms of pressure drop versus Reynolds number..... 79

Figure 3.17. Effect of inserting non-drilled nozzles inside the pipe and volume friction on thermal performance factor for the pitch length of 126 mm and comparison with smooth tube 80

Figure 3.18. Effect of inserting non-drilled nozzles inside the pipe and volume friction on thermal performance factor for the pitch length of 180 mm and comparison with smooth tube 80

Figure 3.19. Effect of inserting non-drilled nozzles inside the pipe and volume friction on thermal performance factor for the pitch length of 315 mm and comparison with smooth tube 81

Figure 3.20. Pressure contours of considered configurations for total pressure (a) smooth tube / water. (b) smooth tube /2% TiO2-water. (c) P.L=126mm / water, (d) P.L=126mm / 2% TiO-water, (e) P.L=180 mm / water, (f) P.L=180mm 2% TiO-water, (g) P.L=315mm / water and (h) P.L=315mm / 2% TiO-water..... 81

Figure 3.21. Temperature contours of considered configurations for total pressure (a).smooth tube / water. (b).smooth tube /2% TiO2-water. (c).P.L=126mm / water, (d).P.L=126mm / 2% TiO-water, (e). P.L=180 mm / water, (f) P.L=180mm 2% TiO-water, (g). P.L=315mm / water and (h). P.L=315mm / 2% TiO-water.....82

Figure 3.22. Comparison of Nusselt number and Reynolds Number for the water at different pitch lengths (126mm, 180mm and 315 mm) between drilled and non-drilled nozzle.....83

Figure 3.23. Comparison of friction factor and Reynolds Number for water between drilled nozzle and non-drilled nozzle at varying pitch length (126mm, 180mm and 315 mm) 84

Figure 3.24. Comparison of drilled nozzle with non-drilled nozzle inserted on tube on thermal performance factor for water flow at pitch length of 126mm 85

Figure 3.25. Comparison of drilled nozzle with non-drilled nozzle inserted on tube on thermal performance factor for water flow at pitch length of 180mm 86

Figure 3.26. Comparison of drilled nozzle with non-drilled nozzle inserted on tube on thermal performance factor for water flow at pitch length of 315mm 86

Figure 3.27. Comparison of drilled nozzle with non-drilled nozzle inserted on tube on thermal performance factor for nanofluid flow at constant volume fraction of 2.0% 87

Figure 3.28. Comparison of drilled nozzle with non-drilled nozzle inserted on for nanofluid flow at constant volume fraction of 2.0% in terms of pressure drop versus Reynolds number 88

Figure 3.29. Comparison of drilled nozzle with non-drilled nozzle inserted on tube on thermal performance coefficient and volume friction on thermal performance factor for pitch length of 126 mm 89

Figure 3.30. Comparison of drilled nozzle with non-drilled nozzle inserted on tube on thermal performance coefficient and volume friction on thermal performance factor for pitch length of 180 mm 90

Figure 3.31. Comparison of drilled nozzle with non-drilled nozzle inserted on tube on thermal performance coefficient and volume friction on thermal performance factor for pitch length of 315mm 90

Figure 3.32. Pressure contours of considered configurations for total pressure (a) Non-drilled- nozzle P.L=126mm/water. (b) Drilled-nozzle P.L=126mm/water. (c) Non-drilled- nozzle P.L=126mm/2% TiO2 nanofluid, (d) Drilled- nozzle P.L=126mm/2% TiO2 nanofluid, (e) Non-drilled- nozzle P.L=180mm/water, (f) Drilled- nozzle P.L=180mm/water., (g) Non-drilled- nozzle P.L=180 mm/2% TiO2 nanofluid, (h) Drilled- nozzle P.L=180mm/2% TiO2 nanofluid, (i) Non-drilled- nozzle P.L=315mm/water, (j) Drilled- nozzle P.L=315 mm/water, (k) Non-drilled- nozzle P.L=315mm/2% TiO2 nanofluid, and (l) Drilled- nozzle P.L=315mm/2% TiO2 nanofluid. 91

Figure 3.33. Temperature contours of considered configurations for total (a) Non-drilled- nozzle P.L=126mm/water. (b) Drilled-nozzle P.L=126mm/water. (c) Non-drilled- nozzle P.L=126mm/2% TiO2 nanofluid, (d) Drilled- nozzle P.L=126mm/2% TiO2 nanofluid, (e) Non-drilled- nozzle P.L=180mm/water, (f) Drilled- nozzle P.L=180mm/water., (g) Non-drilled- nozzle P.L=180 mm/2% TiO2 nanofluid, (h) Drilled- nozzle P.L=180mm/2% TiO2 nanofluid, (i) Non-drilled- nozzle P.L=315mm/water, (j) Drilled- nozzle P.L=315 mm/water, (k) Non-drilled- nozzle P.L=315mm/2% TiO2 nanofluid, and (l) Drilled- nozzle P.L=315mm/2% TiO2 nanofluid. 92

Figure 3.34. Velocity vector (a) Non-drilled nozzle (b) Drilled nozzle for nanofluid flow at 2% TiO2/Water and Reynolds number 14000 93

INTRODUCTION

The heat transfer is a type of energy. This energy is the main factor in many of engineering equipment, including transportations, electrical generation, microelectronics, chemical engineering, aerospace, medical, nuclear reaction and manufacturing. It becomes a challenge Facing the researchers and designers in the industrial area. Their studies on factors affecting, especially economically and technically, and the trend of many of the world's rounds has focused on energy reduction or search for alternatives. Aksoy et al. [6] argue that the problems of energy production affect the environment and increase their prices with regard to the amount of consumption, on the other hand, rapid decline of fossil fuel reserves such as oil and natural gas, ozone tier and greenhouse gas emissions pose a threat over the human life. It is one of the crucial energy problems of today, It has also increased the importance of efficient use of energy and energy resources. With this latest work mentioned, there has been a significant development of consciousness at this point, environment friendly policies in production, resource diversification and consumption and applying the methods to improve the sufficiency by a policy that has been carefully addressed. Supply of energy policies to be safe and sustainable, as easily as it is supposed to be, yet cannot be realized.

The presence of external dependence makes the situation even more troublesome. Energy efficient use has gained a special importance in itself, which will be achieved through the energy recovery in the industry and in the buildings. The amount of savings, given the rates, renewable energy exceeds the amount of energy that can be obtained from its sources. It is vital in terms of energy recovery. Increasing the number and the quality of researches requires the improvement of heating or cooling in an industrial procedure which can render an energy save, diminish the process duration, augment the heat level and extend the lifetime of equipment. Improved heat transfer also influenced

the quality of some procedures. The advent of effective thermal systems regarding the heat transfer betterment has recently gained popularity.. Many studies have been conducted to develop an understanding of the heat transfer performance for their practical applications for the heat transfer improvement. Therefore, the emanation of the high heat current processes has formed a serious demand for new technologies in order to better the heat transfer.

Not only the studies on finding alternatives or reducing fuel, but many of the researchers in the specialty of Thermal engineering seek to discover new ways and mechanisms have evolved to include changing designs of equipment and machinery through several ways, to augment the heat transfer process and work on a significant and ascent improvement between the surface and surrounding liquid [6]. It requires various methods of heat exchangers used in energy recovery processes. The amount of heat transfer might be augmented, and thus the energy is recovered. Energy through the heat exchangers is commonly utilized in engineering applications, the air conditioning used in houses, the large processes in the industrial facilities and the devices that can be provided in many areas. When a number of changes have been made on heat exchangers to obtain large energy gains, it is likely to have a comfortable use and prevent energy consumption, and also the cost is reduced. Hence, increasing the amount of heat transfer provides enough heat transfer to prevent energy consumption and it is essential to develop modifications that will not diminish the sufficiency of the system.

CHAPTER 1
GENERAL INFORMATION

1. TECHNIQUES OF HEAT TRANSFER ENHANCEMENT

The advent of effective thermal heat delivery enhancement has recently gained popularity. Many studies have been conducted to gain an understanding of the heat transfer performance for their practical application to heat transfer enhancement. Therefore, the advent of high heat current processes has created a huge demand for novel technologies to better the heat transfer. Not only studies on finding alternatives or reducing fuel consumption, but many of the researchers in the field of Thermal Engineering dwelling on finding new ways and mechanisms have evolved to include changing the designs of equipment and machinery through several ways, to augment the heat transfer process and been working on a significant and upswing improvement between surface and surrounding liquid. Moreover, this augment of the transfer of the heat is based on theories called mechanisms to enhance the heat transfer by Bergles et al. (1983, 1991, 1995 and 2005) [1, 2]. These mechanisms aim to use such techniques to increase the system's thermodynamic sufficiency, which allows reducing the operating cost. Including passive techniques, active and compound and that is, the effectiveness of any of these methods highly depends on the mode of heat transfer (single-stage, free or forced convection, pool boiling, forced convection boiling or condensation and convective mass transfer) and the process application of heat industrial.

1.1. Passive Techniques

These techniques do not necessitate input of external power. They generally make use of surface or geometrical modifications to the current channel, incorporate an insert, material, or additional device. As shown that in Figure 1.1. [2], it increases the effective heat transfer surface area. Therefore, this technique promotes higher heat transfer

parameters by scattering or shifting the existing current act which includes the following:

1.1.1. Treated Surface

This method is based on the fact that facets includes a fine scale shift to their endpoint or permanent or temporary coating. They are mainly utilized to heat up and concentrating tasks.

1.1.2. Rough surface

These modifications foster turbulence in the current area in the wall section, majorly in single stage currents excluding any rise in the superficial heat transfer range.

1.1.3. Extended surfaces

They supply influential heat transfer enlargement. The latest developments have resulted in modified finned facets that are liable to foster the heat transfer parameter by scattering the current field as well as raising the facet range.

1.1.4 Displaced enhancement devices:

These are the inserts that are mainly used in contracted forced convection, and they enhance energy transfer implicitly at the heat exchange facet by removing the liquid from the hot or cold facet of the duct with bulk liquid off the central current.

1.1.5 Swirl flow devices:

They generate and superimpose swirl current or subordinate recycle on the axial current in a channel. These involve helical strip or cored screw type tube inserts and twisted tapes, which are employed for single stage and twofold stage currents.

1.1.6 Coiled tubes:

These result in slightly neater heat exchangers. It manufactures subordinate currents and vortices which enhance higher heat transfer parameter in single stage currents as well as in most boiling areas.

1.1.7 Surface tension devices:

These are comprised of wicking or grooved facets, which directly and indirectly develop the current of liquid to boiling facets and from condensing facets.

1.1.8 Additives for liquids:

These involve mixing solid granules, soluble trace additives and gas bubbles in single stage currents and trace additives which generally diminish the surface tension of the liquid for boiling systems.

1.1.9 Additives for gases:

These consist of liquid droplets or solid elements, which are included in single-stage gas currents either as dilute stage (gas-solid suspensions) or as intense stage (liquidized beds).

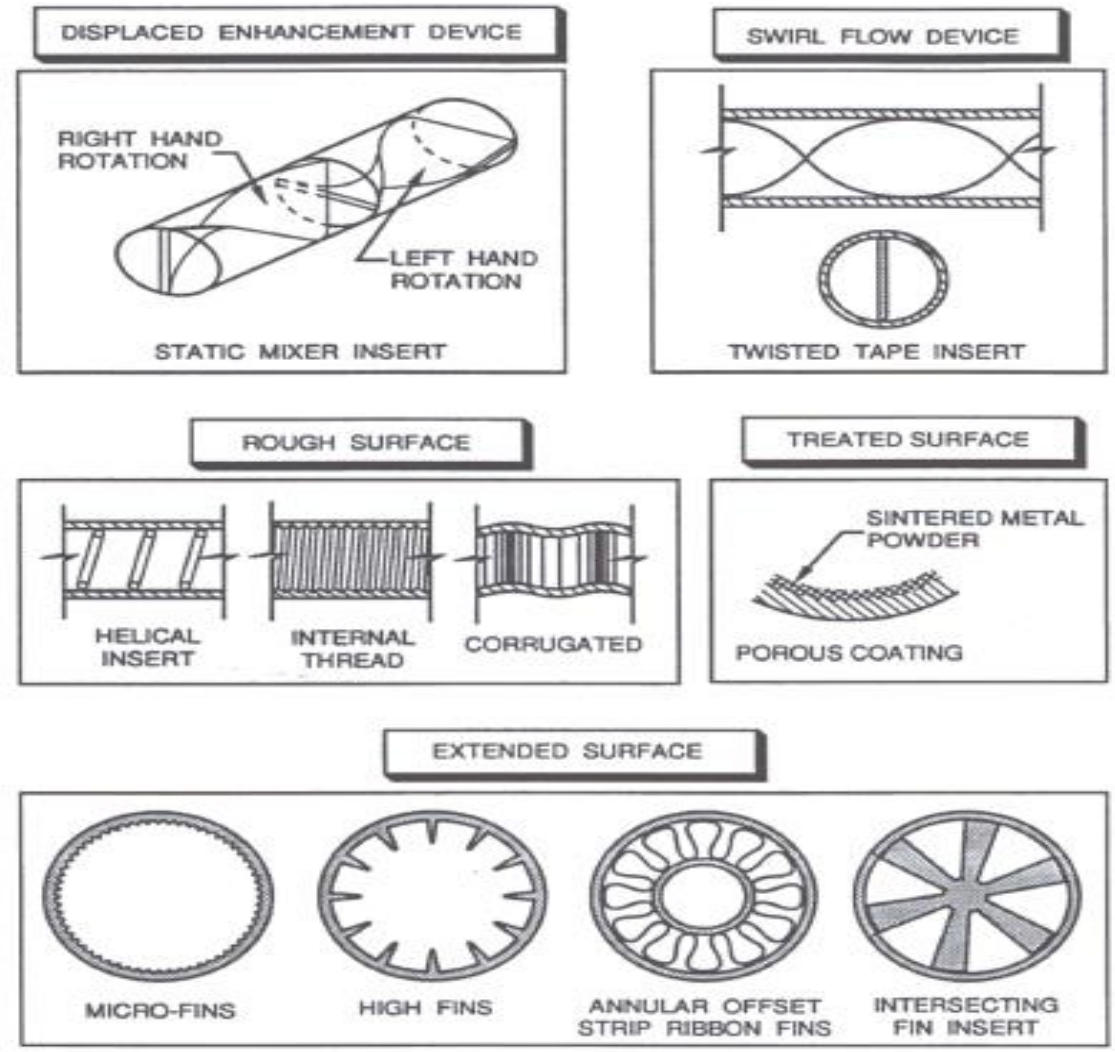


Figure 1.1. Examples of passive enhancement techniques [1, 2]

1.2. Active Techniques

This kind's use of external power essentially eases the desired current modification and the concomitant betterment in the rate of heat transfer. In addition, active techniques have attracted little financial interest due to the costs and the problems that are profitably engaged with vibration or acoustic noise. Special facet geometries contribute to the enhancement by establishing a higher heat transfer parameter ^{x} area per unit base facet area as suggested by Jadhan et al. [3]. The active technique includes the following methods:

1.2.1. Mechanical aids

This method is based on the fact that tools stir the liquidliquid via mechanical ways or by turning the facet. These involve turning the tube heat exchangers and scrapped facet heat and mass exchangers.

1.2.2. Surface vibration

It is employed in single stage currents to attain better heat transfer parameters.

1.2.3. Fluid vibration

These are mainly utilized in single stage currents and are regarded as the most practical type of vibration enhancement technique.

1.2.4. Electrostatic fields

It yields electric or magnetic fields or a set of both from dc or ac sources, which can be implemented in heat exchange systems including dielectric liquid. As for the application, it can also generate larger bulk mixing and trigger forced convection or electromagnetic pumping to improve the heat transfer.

1.2.5. Injection

This method is implemented in single stage current and is compatible to injecting the same or another liquidliquid into the main bulk liquid either through a cellular heat transfer interface or upward current of the heat transfer section.

1.2.6. Suction

It consists of either vapor displacement through a porous heated facet in nucleate or film boiling, or liquidliquid pull via a porous heated facet in single-stage current.

1.2.7. Jet impingement

It includes heating or cooling liquid vertically or laterally to the heat transfer facet which is depicted in Figure 1.2

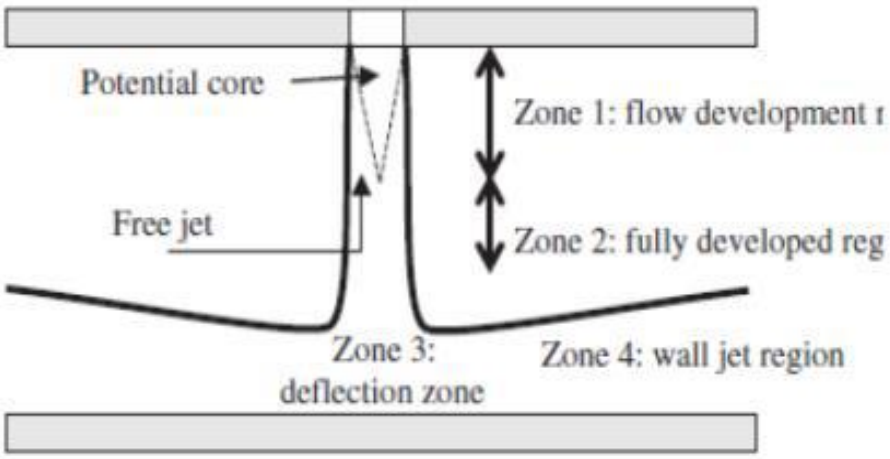


Figure 1.2. Schema of the various flow zones in an impinging jet [3].

1.3. Compound Techniques

This kind use two or more methods (passive and/or active), conjunction constitutes, and may be employed simultaneously to generate an augmentation that is bigger than either of the techniques operating independently. Preliminary studies on compound passive augmentation technique of this kind are quite encouraging. Some examples are rough tube wall with a twisted tape by Bergles (1998) [1] and grooved rough tube having a twisted tape by Usui *et al*., (1984, 1986) [4, 5]. The latter reports a particularly high rise in the heat transfer sufficiency in the combination of an internally grooved rough tube with a tape twisted in the opposite direction of the rotation of the grooves. Besides, this technique consists of a complex design and thus is of restricted applications. For instance:

I. Fins and electric fields (compound of electrostatic fields devices and extended facet devices).

II. Radially grooved rotating disk (mechanical help with facet enhancement).

1.4. Different Inserts

These inserts are an expression turbulator under passive techniques, different inserts are used to increase the heat transfer. These inserts methods are widely employed because of their low cost, easily installation and deportability, implantation capability on existing heat exchangers such as twisted tape, helical wire, nozzle and rings. The effect of opposite current and boundary tier upheaval (dissipation) augment the efficient

heat delivery sufficiencyand the momentum transfer. Many researchers explored the heat transfer augmentation techniques using modified twisted tape, modified conical ring, coil wire, nozzle, etc. shown in Figure 1.3. [7] and 1.4. [8]. Promvonge and Eiamsa [9] suggest that using conical nozzle and the snail can augment the heat transfer rate considerably over that of plain tube using gas current which is depicted in Figure 1.5 (a, b). Also, Akeel et al (2014) [10] argue that the augmentation process is done by using divergent Nozzle-Turbulator arrangement with and without perforation models which can be seen in Figure 1.6. For nozzle embedded, the P.L is the required distance for the tow nozzle added to the length of nozzle according to the following equation.

$$p.l = l_1 + l \quad (1)$$



Figure 1.3. Tubefitted with conical ring turbulator and twisted tape insert [7].

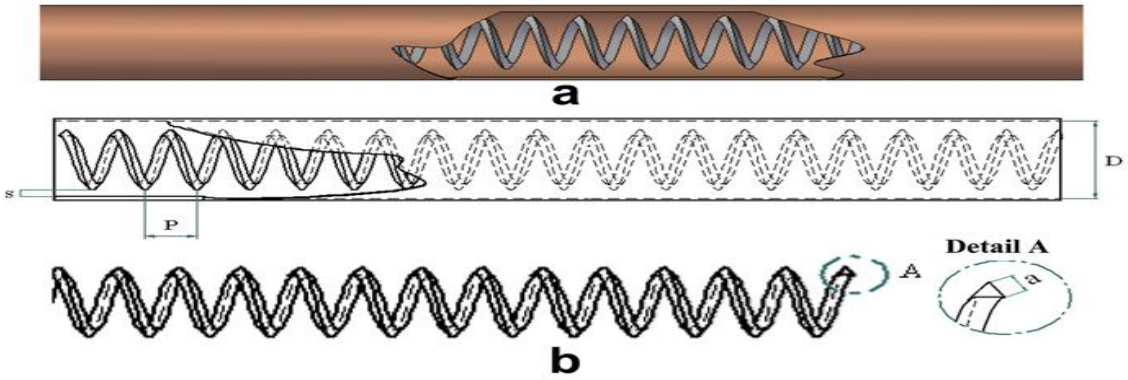
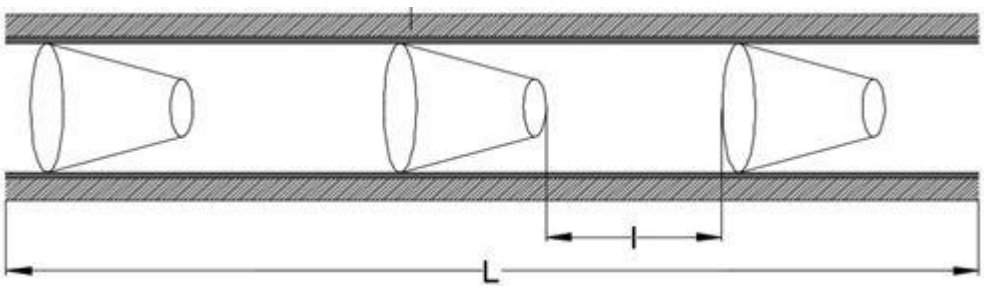
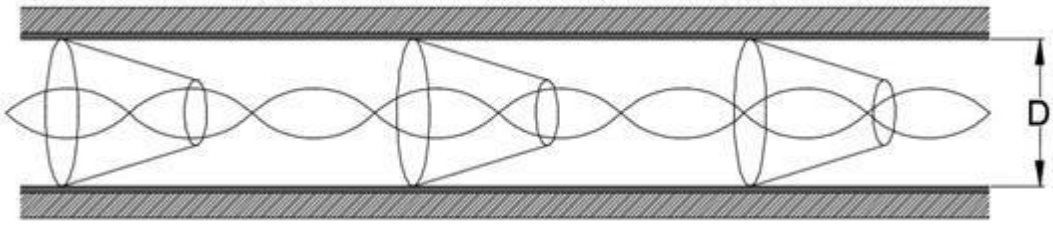


Figure 1.4. Tubefitted with coiled wire inserts [8].



(a)Conical ring arrangement



(b)Tube fitted with conical ring turbulator and twisted tape insert

Figure 1.5. Tube fitted with conical ring turbulator and twisted tape insert by Promvonge and Eiamsa [9]



(a)The nozzle without hole.



(b)The nozzle with circle hole

Figure 1.6. The nozzle-turbulators Akeel.et.al. [10]

1.5. The Concept of Nanofluds

The pivot factor affecting the heat transfer sufficiency of thermal convection is the thermal conductivity of heat transfer liquids, as known by ever body, the low thermal conductivity of conventional liquids such as water, oil and ethylene glycol, which fundamentally constrains the improvement of energy-efficient heat transfer tool, and this can be observed through Figure 1.7. Leading researchers in this field have

discovered an influential method of enhancing thermal conductivity of liquids to delay tiny concrete granules in the liquids so as to alter the transportation features, current and heat transfer properties of the liquids because solid materials have high thermal conductivity compared to the liquids. They expected the innovative concept of nanos which has been proposed as a prospect for these challenges [11]. Maxwell was the first presenter of the theoretical basis to predict a suspension affective conductivity about 140 years ago (1873) [12] and his theory was applied to suspensions with from millimeter to micrometer sized granules. Despite the fact that such solid additives may better heat transfer parameter of liquids, there was a problem regarding size. As the use of solid granules at micrometer-or millimeter-sized is of limited application because of a low fixity of suspension, clogging of current channel, abrasion of conduit, causing pressure drops, nanos are made from generally one type of base liquid and one type of nanoparticles. As explained above, the purpose is to raise the thermal conductivity of the liquid matrix to be utilized in a heat transfer application. Hence, the nanoparticles are usually opted as metallic or metal oxide materials with higher thermal conductivity. Usual metallic and metallic oxide nanoparticles preferred in this area are Alumina (Al2O3), Copper Oxide (CuO), Copper (Cu), Titanium di Oxide (TiO2). Other types of materials such as graphite, carbon and diamond are utilized in the research as well.

In the last two decades, with the quick advent of modern nanotechnology, granules of nanometer with a size smaller than 100 nm started to be used rather than micrometer–size ones for dispersing in base liquids are termed as nanos, which was coined by Choi [13] in 1995.The researchers have found influence of the nanoparticles size diffused within the liquids. The form of granules also influences the thermal conductivity of nano. Murshed et al. [15] report that the metal oxide nanoparticles and metals are typically employed in nanos, such as alumina (Al2O3), copper (Cu) and titanium (TiO2) etc. As well as the effect of the liquid on the base for nanos of thermal conductivity, they are weak such as glycol ethylene, water, oil, and other types. Researchers in the field of nanos make use of the unique features of these small nanoparticles to create fixed and high-thermal-conductivity heat transfer liquids. Stable delay of tiny amounts of small pieces renders traditional heat transfer liquids' cooling more quickly and smaller and lighter thermal conduct systems.

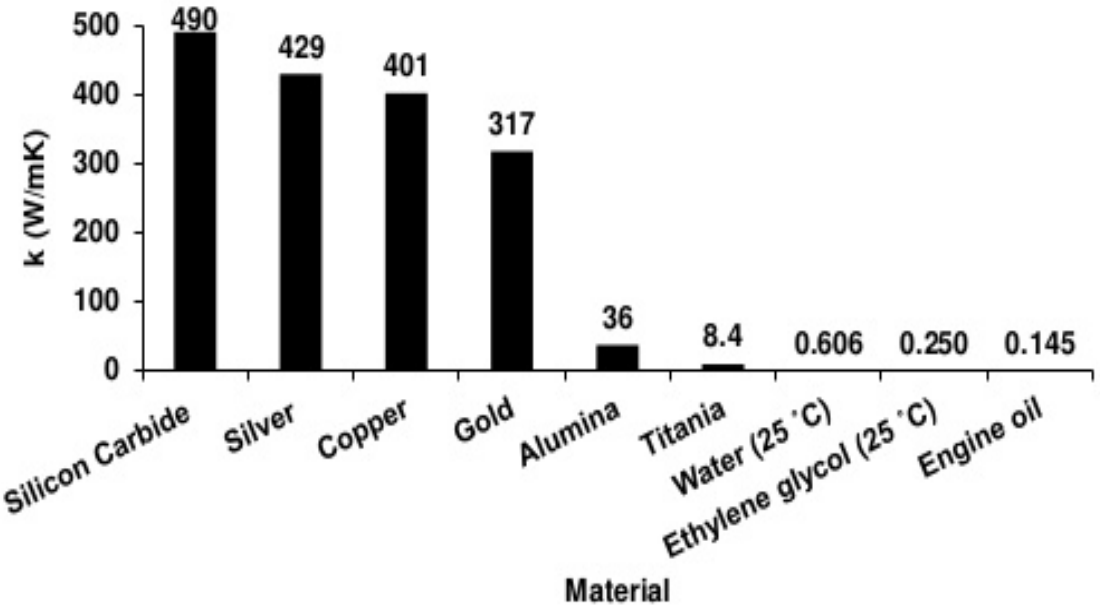


Figure 1.7. Thermal conductivity of some materials [14].

1.5.1. Nanoparticle Material Types

There are various types of nanoparticle materials which are used in nanofluids according to its ability to conduct thermal conductivity as seen in table 1.1 [16, 17] .In addition, there are several factors besides thermal conductivity such as size, shape, physical and chemical effect etc. When nanoparticles are dispersed in liquid medium, two significant interactions are likely: granule-liquid interaction and granule-granule interaction. These interactions are called as first and second electroviscous effects by Timofeeva et al. [18]. As for the shape, virtually all studies on the thermophysical properties of nanos either supposed or alleged that their nanoparticles were in form of spherical except for those working with carbon nanotubes (CNTs) and some other studies on various nanoparticles [19, 20]. Shape factor, which is a measure of all facet area of granules, is engaged with the degree of solid-liquid interactions at the interface as well as the effect of pH. Its pH gets significant in the engineering of nanos given the prospect of data available, highlighting the level of zeta potential on the thermophysical features of nanos. Zeta potential specifies the electro-kinetic capacity of the EDL and this affects the electrostatic act of nanos as reported by Syam Sundar et al. [21]. They can be classified as follows:

(1)- Metal elements (Cu, Al, Fe, Au, and Ag).

(2)- Metallic oxide (Al2O3, CuO, Fe3O4, TiO2, and Sic).

(3)- Non-metallic (carbon nanotube) (single- and multi-wall carbon nanotube (SWCNT and MWCNT), Si, Graphene, etc.).

The high facet area of nanoparticles fosters the heat conduction of nanofluids as the heat transfer takes place on the facet of the granule. The number of atoms existing on the facet of nanoparticles, contrary to the interior, is quite wide. Hence, these unmatched features of nanoparticles can be used to produce nanofluids with an unequalled combination of the two properties which are quite desired for heat transfer systems: extreme fixity and ultrahigh thermal conductivity. Moreover, nanoparticles are so tiny that they may diminish the abrasion and clogging considerably. Other advantages of nanos involve lower demand for pumping power, diminished inventory of heat transfer liquid, and considerable energy savings. These nano sized materials are generally manifactured in the shape of powder which is dispersed in aqueous or organic host fluids for particular practices.

Table 1.1. Thermal conductivities of different materials [14, 15]

Type of Material	Material	Thermal Conductivity (W/m·K)
Metallic	Cu	401
	Al	237
	Ag	428
	Au	318
	Fe	83.5
Metallic oxide	Al2O3	40
	CuO	76.5
	TiO2	10.2
	Sic	270
Non-Metallic	SWCNT	- 3000
	NWCNT	- 6000
Base fluids	H2O	0.613
	EG	0.253
	Engine Oil	0.145

1.5.2. Base Liquid Types

The term “base liquid” refers that it is the foundation which all the enhancements are built on like water, glycol ethylene, water, engine oil, and so on. Many traditional heat transfer liquids have been examined with different nanoparticles, in varying mixing proportions and commonly study of nanos in the literature. Fundamental liquid qualities of density, thermal conductivity, viscosity and pH are certainly part of the factors that influence the all characteristics of nanos such as fixity, thermal conductivity and viscosity. The crucial part of the selection of the base liquid is still dependent on the suitability for a particular heat transfer application. All heat transfer base liquids can be utilized for nanofluid production if they are appropriate for the production techniques. However, it is vital to emphasize that the addition of nanoparticles in a liquid supplies more enhancement if the liquid has poor heat transfer capabilities. In other words, it is much more useful to add the nanoparticle technology when the working base liquid of a system has low thermal conductivity. Researches like Syam Sundar et al. [21] arguing that base liquid characteristics affect the viscosity betterment have not provided any extensive experimental data scrutinizing the limit to which the internal features of base liquids affect the viscosity improvement of nanos.

1.5.3. Nanofluid Preparation

Preparation of nanos is a necessity for their heat transfer application. Usually, there are two fundamental preparation techniques; that is, single-stage and double-stagedouble-stage techniques for nanos.

One-stage technique is implemented by separating nanoparticles into base liquids simultaneously in the course of the production process of nanoparticles for which the nanoparticles are explicitly prepared by Physical Vapor Deposition (PVD) technique or fluid chemical techniques [22]. As Yanjiao et al. [23] outlined, the processes of drying, storage, transportation, and dispersion of nanoparticles are avoided, so the agglomeration of nanoparticles is minimized and the fixity of liquids is augmented. Yet, a disadvantage of this method is that only low vapor pressure liquids are congruent with the process. This restricts the application of the method whereas in double-stage method, the generating and dispersing procedures of nanoparticles are operated on their own. Cooling liquids or chemical reagent solutions in single-stage method do not

generally require base liquids for nanos such as water, oil, or refrigerant etc. Hence, single-stage method is not quite suitable for preparing heat-transfer nanos, but mostly feasible with producing dry nanoparticles.

In other respects, double-stagedouble-stage method has been commonly applied for example in preparing TiO_2 nanos for heat transfer use, as TiO_2 nanoparticles synthesis method has already attained industrial manufacturing scale as shown in Figure1.8. and Figure 1.9 of industrial manufacturing scale Al2O3 nanoparticles. A usual procedure of double-stage method of preparing nanos is illustrated in Figure 1.10. By and large, some additional dispersion tools are employed for better fixities and conveniences for nanos. Hence, agglomeration of nanoparticles can occur in both stages, particularly during the procedure of drying, storage, and transfer of nanoparticles. The agglomeration will both lead to the settlement and clogging of micro channels, and lower the thermal conductivity. Simple methods such as ultrasonic agitation or mixing surfactants to the liquids are frequently utilized to mitigate the granule aggregation and better the dispersion act. As nano powder synthesis methods have already reached up to industrial manufacture levels by many companies, there are probable financial benefits in implementing double-stage synthesis techniques that exploit such powders. However, a considerable problem that requires solution is the stabilization of the suspension designed. So far, many techniques have been exploited to assess the fixity of nanos. The most simple and dependable technique is the sedimentation technique. In this technique, the variation of density or granule dimensions of supernatant granule with sediment time is attained by an exclusive device. And table 1.2 [22, 23] outlines some studies and steps to prepare them.

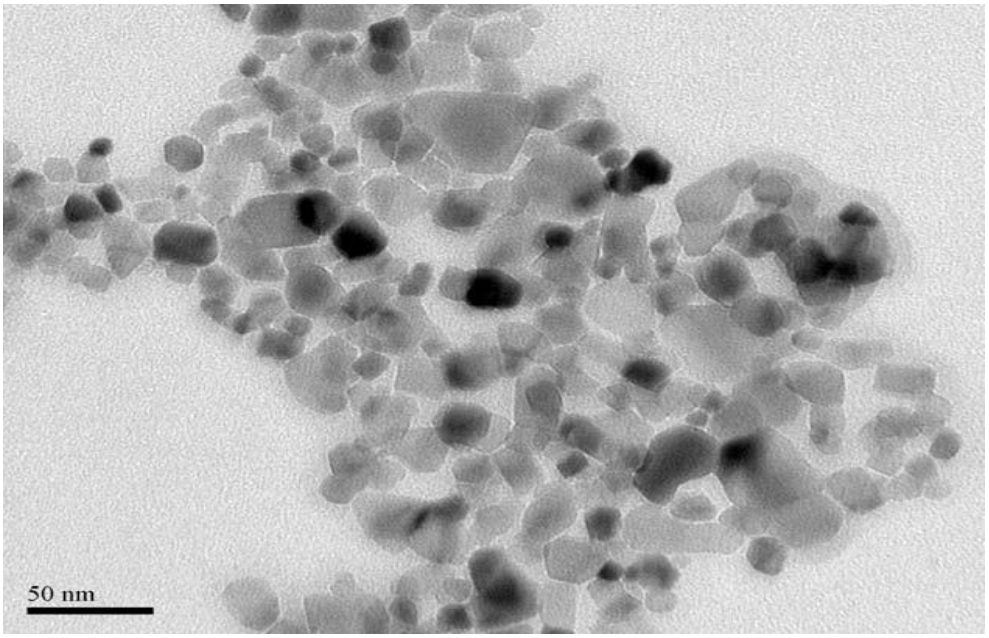


Figure 1.8. An image of dispersed TiO2 nanoparticales in water [64].

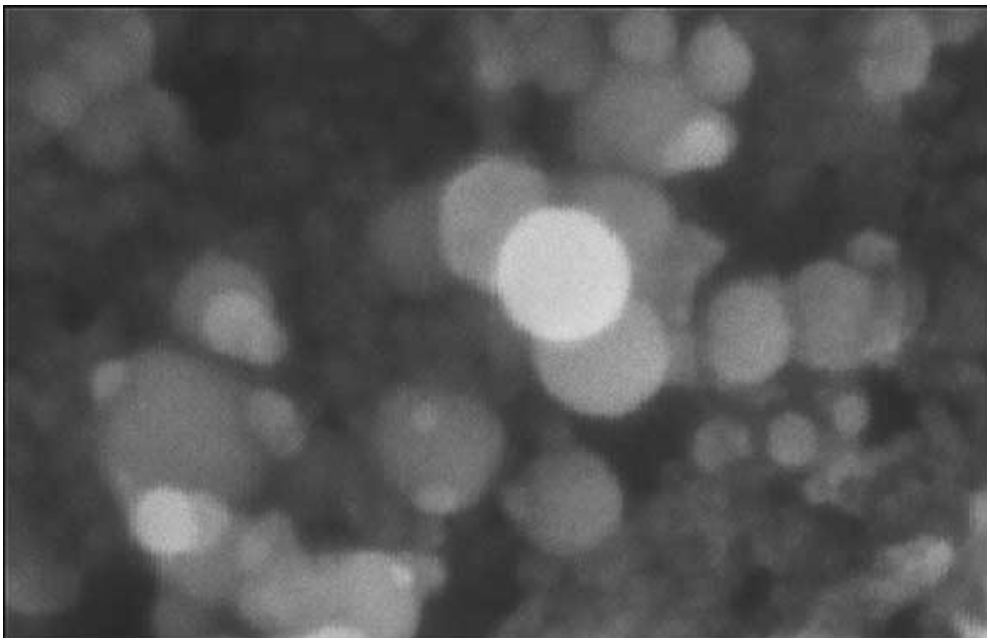


Figure 1.9. SEM image of dispersed Al2O3 nanoparticle in water [60].

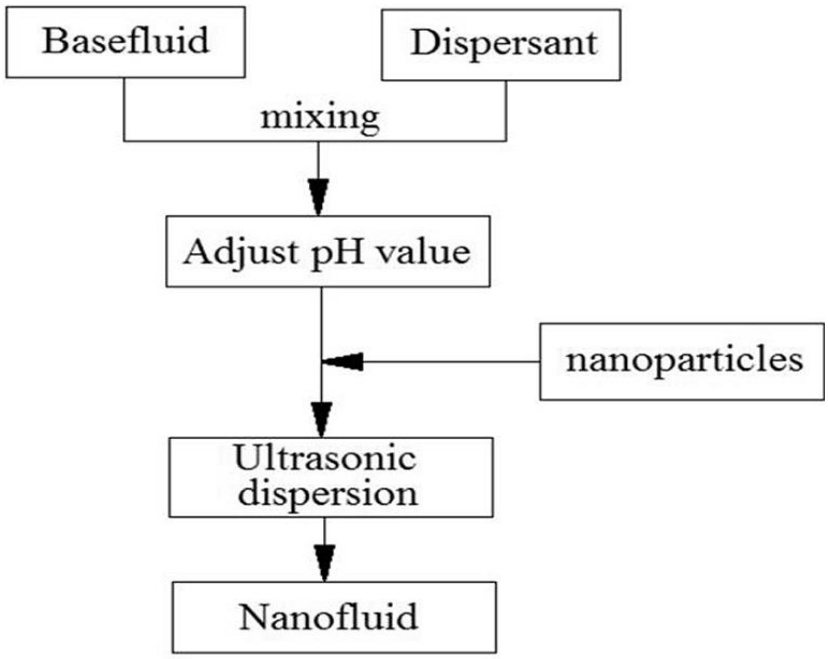


Figure 1.10. Typical procedure of two-step method of preparation of nanofluids [23]

Table 1.2. Nanofluids systems reported in literature. [21, 22]

System conductivity	Synthesis process Ref	Particle loading (Vol %)	Particle size (nm)	Increase in thermal (%)	
Cu/EG	Single-step	0.3	10	4	[24]
Cu/H2O	Single-step	0.1	75~100	23.8	[25]
Cu/H2O	Two-step	7.5	100	78	[26]
Fe/EG	Single-step	0.55	10	18	[27]
Ag/toluene	Two-step	0.001	60~80	16.5 (60 °C)	[28]
Au/toluene	Two-step	0.00026	10~20	21 (60 °C)	[29]
Au/ethanol	Two-step	0.6	4	1.3±0.8	[29]
Fe3O4/H2O	Single-step	4	10	38	[30]
TiO2/H2O	Two-step	5	15	30–33	[31]
Al2O3/H2O	Two-step	5	20	20	[32]
Al2O3/EG	Two-step	0.05	60	29	[32]
CuO/H2O	Two-step	5	33	11.5	[33]
SiC/H2O	Two-step	4.2	25	15.9	[34]
NCTs/engine oil	Two-step	2.0	20~50 nm	30	[35]
NCTs/poly oil	Two-step	1.0	25 nm×50 μm	160	[36]
NCTs/EG	Two-step	1.0	15×30 μm	19.6	[37]
NCTs/H2O	Two-step	1.0	15×30 μm	7.0	[37]
NCTs/decene	Two-step	1.0	15×30 μm	12.7	[37]
H2O/FC-72	Two-step	12	9.8 nm	52	[38]

1.6. IMPORTANCE OF NANOFLUIDS

The main purpose of nanofluids is to raise the thermal conductivity of base liquid as we have observed that in Table1.1. To illustrate, the thermal conductivity of copper at room temperature is about 700 times bigger than that of water and about 3000 times greater than that of engine oil. The thermal conductivity of metallic liquids is highly greater than that of nonmetallic liquids. As noted above, the basic concept of dispersing solids in liquids to improve the thermal conductivity is not recent; it dates back to Maxwell [12]. The reason why solid granules are included is that they transmit heat quite better than the fluids. The pivot concern with using wide granules is the quick settling of them in liquids. Other concerns consist of corrosion and clogging. These concerns are rather undesirable for a number of practical cooling practices. Nanofluids have led the way in handling these concerns by levelly suspending in liquids with nanometer-sized granules rather than millimeter- or micrometer-sized granules. The comparison was made between micro granules and nanoparticles in table 1.3. Researchers in the field of nanofluids make use of the unique features of these little nanoparticles to render stable and high-thermal-conductivity heat transfer liquids. Constant suspension of a few little granules renders traditional heat transfer in which liquids cool more rapidly and thermal management systems are smaller and less heavy.

Table 1.3. The comparison between the micro particles and nanoparticles [15].

	Micro particles	**Nanoparticles**
Stability	Settle	Stable (indefinitely remain suspended almost)
Surface/volume ratio	1	Nanoparticles are greater than that of the microparticles to 1,000 times
Conductivity	Low	High
Clog in microchannel	Yes	No
Erosion	Yes	No
Pumping power	Large	Small
Nanoscale phenomena	No	Yes

It should be specified that in today's world, size is of importance. Size is also a significant physical variable in nanofluids as it is exploited to modify nanofluid thermal features in addition to the suspension fixity of nanoparticles. Maxwell's concept is outdated, yet what is novel and innovative with it is the idea of exploiting nanometer-sized granules (which have only recently become available to researchers) to form constant and quite conductive suspensions, mainly for suspension fixity (gravity is trivial) and for dynamic thermal interactions. Nanotechnology provides perfect prospects for creating a new type of heat transfer liquid that has flawless thermal features and cooling capacity, thanks to new nano scale phenomena that overturns our feeling of familiarity. Hence, the pcasetters of nanofluids have transformed the solid–liquid suspension concept to a completely novel dimension [15].

1.7. APPLICTION OF NANOFLUIDS

Nanofluids can be utilized to improve the heat transfer and energy efficiency in a variety of thermal systems. Many studies based on nanofluids are being conducted in national laboratories and academia and is beyond discovery research. Recently, the number of companies that foresee the potential of nanofluid technology and are in active development work for specific industrial applications have produced some examples of actual and potential applications [13, 39]. And they can be juxtaposed in the following areas:

- ***Transportation*** (Automotive coolant, greased, fan clutches, engine coil, lube oils, power steering fluid, brake fluid).
- ***Electronics Cooling*** (Chips, servers, high power lasers, cooling of high performance computers).
- ***Defense*** (Military vehicles, submarines, directed energy weapons and high-power laser diodes).
- ***Space*** (Due to their low fluid inventory, it needs simplifying and lighter cooling systems which are feasible with nanofluid).
- ***Nuclear Systems Cooling*** (Emergency safety systems and major coolant in pressurized water reactors (PWR) and economic performance of nuclear systems).

- ***Biomedicine*** (Biomedical industry, for example, traditional cancer treatment method, killing cancers cells, drugs radiation without harming, cool the brain, safer surgery).
- ***HAVC*** (Air conditioning ventilation, heating of buildings without increased pumping power in heating and Energy efficient cooling).
- ***Other Applications*** (Power transmission and generation, Production, Fabrication and Renewable energy).

1.8. THE OBJECTIVES OF THE PRESENT STUDY

Most researchers have acknowledged that usage of a nanofluid rather than a base fluid facilitates increasing the heat transfer coefficient. Although a consensus about nanofluids is reached, there is a significant discrepancy in the results of nanofluid researches as the amount of heat transfer enhancement could not be forecasted well. In fact, the primary aim of this study is to design a numerical investigation tool so as to analyze both the flow and the heat transfer behavior of metal oxide nanofluids (TiO2/water), in a horizontal circular tube along with the different inserted nozzles at three pitch lengths (126,180 and 315 mm) under fully developed turbulent flow with a uniform wall heat flux condition. Some models which represent individual or similar ideas are tested and compared. And we hope to be of great contribution to the understanding of the absolute benefit of the nanofluid heat transfer. It is aimed to obtain reasonable results and observe the heat transfer betterment for nanofluids by considering variable thermal conductivity (including Brownian motion effect which will be discussed later) and single phase approach and evaluation of heat transfer performance of nanofluids in terms of heat transfer and flow which is not an extensively debated issue in the literature. The heat transfer enhancement definition cannot be sufficient to explain the heat transfer performance as it fails to inform about increased pumping power of flow by replacing the base fluid with the nanofluid. That’s why, a study about this topic is to be of great help for understanding the certain advantage of the nanofluid heat transfer. A novel study on this issue is developed, proposed, and related analyses are carried out.

1.9. BENEFITS OF THE STUDY

Nanofluid possesses the advantages below in comparison with the traditional liquids, which renders them appropriate for a variety of practices including heat exchange. The heat transfer liquids or other components related with the heat transfer were invented and improved with thriving technology. Usage of more compact, larger heat transfer areas and heat transfer devices are widespread in today's industry.

1.9.1. Scientific Benefits

Heat transfer improvement with enhancement techniques has a notably large place in scientific research. It has become a topic of interest to researchers because of its high values of self-made improvements both in terms of ease of access to implementation and improvement rates. This study will be of great contribution to the heat transfer improvement with enhancement techniques as it contains inner elements with a rare designing structure similar to the literature. There may be examples of researchers working on this subject and will take on new studies in their work.

1.9.2. Technological Benefits

During the production stage of the nanofluid, the setup of the experiment is carried out in every area of the technology as long as it is established. In automobile sector, nanofluids have probable application as engine coolant, automatic transmission liquid, brake liquid, gear lubrication, transmission liquid, engine oil and greases. While braking, the heat formedleads the brake liquid to reach its boiling limit, a vapor lock is formed which sets back the hydraulic system by dispersing the heat formed by braking. It will cause a brake malfunction and bears a safety risk in vehicles. Nanofluids with improved features augment the performance in heat transfer as well as solving any safety concerns.

1.9.3. Environmental Benefits

Nanofluid has a positive effect on the environment and there is a big body of analysis on the role of nano materials in environmental remediation and monitoring. Nano materials can be utilized to clean up toxins and bacteria from natural waters, waste waters and the air. For instance, silver nano granuleshave been found to be effective antimicrobial agents and can treat wastewater with bacteria, viruses and fungi. Nano scale titanium dioxide can kill bacteria and disinfect water when activated by light as well. In addition to solving pollution, nanoparticles can be employed as sensors to monitor toxins, heavy metals and organic pollutants in soil, air and water and have proved more sensitive and selective than conventional sensors

1.9.4. Industrial Benefits

The effect of this new heat transfer technology is hoped to be immense, regarding that heat exchangers are prevalent in all sorts of industrial applications and that heat transfer performance is vital in various multibillion-dollar industries. Currently, there is a great industrial interest in nanofluids. Some researchers argue that removal of cooling and heating water with nanofluids is likely to save about 300 million kWh of energy for industries. Regarding the electric power industry, nanofluids can save about 3000-9000 million kWh of energy annually which is equal to the yearly energy consumption of about 50,000-150,000 households. [40].

1.9.5. Economical Benefits

Successful application of nanofluids will yield remarkable energy and cost savings as heat exchange systems can be rendered smaller and lighter. For instance, in heat exchangers with conventional liquids, the heat transfer parameter can be significantly raised only by increasing the speed of the liquid in the heat transfer equipment. However, the requited pumping power rises considerably with the increasing speed. For a nanofluid flowing in the same heat transfer equipment at a stable speed, the enhancement of heat transfer as a result of the increased thermal conductivity can be foreseen. To illustrate, pumping power must be raised by a factor of about 10 in order to enhance the heat transfer of a conventional liquid by a factor of 2.

2. LITERATURE REVIEW

The purpose of this literature review is to go through the main topics of interest and address number of experimental studies, which focused on the nanofluids and turbulator performance in a tube and conducted in order to cover the enhancements in the heat transfer by using the nanofluids and turbulator in all applications and the effect of volume concentration, Reynolds number, type of nanofluid, and diameter of nanoparticle and other parameters.

2.1. INVESTIGATIONS ON USING TURBULATORS

The enhancement of energy transport has been observed extensively in the passive techniques which usually utilize facet or geometrical modifications to the current channel by incorporating inserts or additional devices. They render higher heat transfer parameters by disturbing or shifting the available current act except for extended facet. They don’t necessitate any direct input of external power; it is obtained from the system itself which eventually results in an increase in the liquid pressure drop.

Jiinkhan and Bergles [41] examining three popular "turbulator" inserts for fire tube boilers developed an electrically heated current facility to transfer the hot air to a water-cooled steel tube employed to attain sectional average heat transfer parameters for four areas of the tube displayed 135 and 175 % rise in heat transfer parameter at a Reynolds number of 10,000. Consisting of narrow, thin metal strips bent and twisted in a zig-zag style to permit periodic contact with the tube wall, displaying increase in the wall in heat transfer parameter turbulator, the results indicate that the commercial turbulator inserts tested supply significant enhancement of gas-side tube boilers. Despite the fact that it is possible to diminish the fuel consumption through the use of tabulators, gas-side convection parameters improve in boiler sufficiency. The friction factor rises accompanying these heat transfer parameter increases were 1110, 1000, and 160%, respectively, for the same Reynolds number. Moreover, enhancement of gas side parameters is stemmed from one sole factor among many elements such as fuel/air proportion adjustment, tube cleanliness, and air/gas system current resistance that result in lower fuel consumption and enhanced boiler sufficiency. The calculation of boiler sufficiency with turbulators should also take into account the changes in the water side current distribution and heat transfer parameter.

Manglik and Bergles [41] and [42] outlined experimental correlations between pressure drop and the heat transfer coefficient of many types of flow regions such as laminar flow, transition flow, and turbulent flow in isothermal-wall tubes and all of which were with the twisted tape inserts. The increase in the heat transfer coefficients and the concomitant pressure drops with twisted-tape inserts is found to be considerably influenced by tape-induced vortex motion and higher flow velocity due to the tube blockage that they avoid the need of identifying the flow regime and readily comply with off-design performance ratings and the optimization of thermal-hydraulic characteristics of twisted-tape inserts.

Al-Fahed and Chakroun [43] carried out a series of experiments in order to examine the effect of the fitting between both tape and the pipe wallon the heat transfer parameter under fully developed turbulent current with isothermal tube-wall boundary case and tests were run on 15 distinct tapes using a water as the teat liquid and a smooth copper tube. The results revealed that the heat transfer was risen by the tape width. However, for low values of the twist ratio, the tight-fit tape (width equal to the tube diameter) was found to cater almost the same rate of heat transfer as the loose-fit tape, which is a sign of probable existence of an optimum tape width.

Saha and Dutta [44] investigated the Laminar swirl current of a large Prandtl number (205<Pr<518) Viscous liquid was regarded. The swirl was produced by short-length twisted-tape inserts; neatly spaced twisted-tape elements with multiple twists in the tape module and linked by thin radial rods; and smoothly shifting (gradually lowering) pitch twisted-tapes. A PVC tube was used as test section and water as the teat liquid and Reynolds Number range (205<Pr<518). The heat transfer test section was heated electrically imposing axially and circumferentially stable wall heat flux. According to the results, Thermohydraulic performance indicates that twisted-tapes with multiple twists in the tape module is not quite variant from the one with single twist in the tape module. Friction factor and Nusselt number are roughly 15% lower for twisted-tapes with smooth swirl with the average pitch identical to that of the regular pitch along twisted-tape and the twisted-tapes with fractionally lowering pitch perform worse than their regular-pitch counterparts.

Yakut et al. [45] investigated fully developed turbulent current for Reynolds number ranging from 5000 to 20,000. The conical-rings with 10, 20 and 30 mm pitches are infixed in a model pipe-line through which air is passed as the working liquid. The pipes and orifice meter were made of aluminum which provided a constant heat flux. The results suggest that as the pitch increases, vortex shedding frequencies increase as well and the maximum amplitudes of the vortices produced by conical-ring turbulators take place with small pitches. Besides, the impacts of the promoters on the heat transfer and friction factor are examined for all the arrangements. It was discovered that the Nusselt number goes up with the increasing Reynolds number and the maximum heat transfer is attained for the smallest pitch arrangement.

Promvonge et al.'s [46] experiment on heat transfer and current friction with a twisted-tape elements used water as the working liquid in a double copper pipe heat exchanger placed in two different cases: (1) full-length typical twisted tape at different twisted proportion and (2) twisted tape with various free space proportions, and the twisted tape were made of the stainless steel through the Reynolds number range from 2000 to 12000. The results refer that the heat transfer parameter increased with twisted proportion despite the rise in the free space proportion and friction factor and getting a new correlation between forecasting the heat transfer and friction factor for radial tubes with twisted taped insert.

Promvonge and Eiamsa [8] and [47] studied the augmentation of heat transfer and turbulent current with different nozzles (conical-nozzle & V-nozzle and snail entry) and various cases. The turbulators are completely embedded inside the tube with varying pitch proportions with Reynolds number ranging from 8000 to 18,000. Air was used as working liquid at regular heat flux. The turbulator was made of aluminum inside the copper test tube. The results of the experiment denote that raising Reynolds number at a specific pitch proportion of the turbulators causes a considerable rise in Nusselt number emphasizing enhanced heat transfer parameter caused by raising the convection as the current rises. Yet, the friction factor at a specific Reynolds number remarkably rises by diminishing the pitch proportion and Reynolds number. And compared with be higher than that from the plain tube in two cases based on Reynolds number and the turbulator arrangements. Besides, correlations between Nusselt number and friction factor are also proposed.

Ozceyhan et al [48] analyzed the heat transfer enhancement in a tube with the radial cross sectional rings. The rings were embedded near the tube wall. Five different spacings among the rings were regarded as regular heat flux which was employed to the external facet of the tube, and air was opted as the working liquid in the range of Reynolds number of 4475–43725. Quantitative calculations were carried out with FLUENT 6.1.22 code. The results obtained from a smooth tube were compared with those of previous studies so as to validate the technique. The Nusselt number increases and friction factor decreases with increasing Reynolds number.

Yadav [49] explored the impacts of the half-length twisted tape insertion on heat transfer and pressure drop features in a U-bend double pipe heat exchanger. The swirling current was included by utilizing half-length twisted tape fitted inside the inner test tube. Twisted tapes were produced from stainless steel strip and isothermal condition with oil which was selected as the working liquid. The results outlined that the rise in heat transfer rate of the twisted-tape inserts appear to be significantly affected by tape-induced swirl or vortex motion. The heat transfer parameter seems to rise by 40% with half-length twisted tape inserts compared to the simple heat exchanger. It was discovered that in terms of equal mass current rate, half-length twisted tape is of a better heat transfer performance than plain heat exchanger, and with regard to the unit pressure drop, the heat transfer performance of smooth tube is better than half-length twisted tape. Moreover, it is seen that the thermal performance of plain heat exchanger is 1.3-1.5 times better than half-length twisted tape.

Gunes et al. [7] conducted an experiment on heat transfer and pressure drop in a tube with coiled current regime at five varying pitch proportions with regular heat flux deployed to the external facet of the tube and Reynolds numbers varied from 4105 to 26400 and the steel test tube. Air was opted as the working liquid in the experiments. The results indicate that the use of coiled wire inserts results in a significant rise in heat transfer and pressure drop over the smooth tube. The Nusselt number and friction factor rise with the decreasing pitch proportion and distance for coiled wire inserts. The highest overall enhancement sufficiency of 50% was achieved for the coiled wire with low Reynolds number As a result, the experimental results unveil that using these coiled wire inserts are thermodynamically beneficial at all Reynolds numbers.

The current visualization was administered using dye injection technique and the experiment heat transfer and friction factor in tube with twisted tape including alternate axis with water selected as working liquid by Seemawute and Eiamsa [50]. The heat transfer experiment was run under a regular heat flux and test tube which was made of Copper with twisted aluminum tape. The impacts of the twist proportions on heat transfer and liquid friction were also investigated in detail. The visualization results provide better liquid mixing and thus higher heat transfer rate than typical twisted tape at similar conditions. Furthermore, swirl number and residence time of a liquid current are promoted as tape twist proportion decreases, which is compatible to the superior heat transfer at smaller twist ratio. The tape with smaller twist proportion supplies more swirl number and thus longer residence time which help to extend the heat transfer between tube wall and liquid.

Bai and Liu [51] investigated the numerical investigation on helical vortices impelled by a short twisted tape placedin a radial pipe. The simulations are the same as the parameters in the experiment with iso-thermal turbulent current, and the working liquid in the model is water at room temperature. The stable state current is obtained using the software FLUENT. The solver is (3D), pressured based and coupled. The pressure and speed pairing is handled by using the SIMPLE and the Reynolds number hinges on the pipe diameter. The results are calculated by RNG k-ε turbulence model. The results demonstrate that two symmetrical stable helical vortices are present in the downstream of the twisted tape. The vortices form in the twisted tape and stay in the structure downstream of the twisted tape. Torsion fosters the formation of helical vortices. The intensities of helical vortices decrease along the stream wise direction. As Reynolds numbers increase, the intensities of helical vortices decay slowly compared to the intensities of swirling current.

Roslim et al. [52] examined the effects of porous twisted plate as insert to improve heat transfer performance and current characteristic for a single fitted tube. The porous twisted plate was designed with various numbers of holes with hot gas emitted from the boiler which was used as working liquid of the experiment. The twisted tap was made of copper, and the heat transfer was carried out in constant heat flux at Reynolds number ranging from 3000 to 18,000. The results point out that the creation of holes shifted the current profile by generating secondary current and approaching turbulence current.

Furthermore, the speed of the current was increased which allows more liquid mixing inside the tube, thus provides more heat transfer across the tube. Porous twisted plate with larger numbers of holes render better heat transfer rate compared to the plain tube and plain twisted plate.

Eiamsa et al. [53] explored the augmentation by dual-helical twisted tapes D-HTTs and triple-helical twisted tapes T-HTTs which is presented in comparison with that by single-helical twisted tape (S-HTT). Air was selected as the working liquid for Reynolds number between 6000 and 20,000 with a permanent heat flux condition during the entire test section. The results regarding the use of D-HTTs and T-HTTs lead to the rise of Nusselt number and the increase of friction factor respectively and the decrease of thermal performance factor compared to those obtained from the results as the width proportion augments, However, as a result of the poorer trade-off between the rises of Nusselt number and friction factor, lower thermal performance factor is consistently obtained at the conditions involving higher Nusselt number and the maximum thermal performance factors given by S-HTTs at Reynolds number of 6000. Besides, the foreseen data from the empirical correlations for Nusselt number, friction, and thermal performance developed diverge from the experimental data.

Dagdevir et al. [54] conducted a quantitative investigation so as to analyze heat transfer, friction characteristic and thermo-hydraulic performance by using two-dimensional axisymmetric geometry. The impact of the formed sinusoidal conical-nozzle turbulators which are located in a radial tube on a regular heat-flux applied and (k-ε RNG) turbulence model was fixed on to simulate turbulent aircurrent throughout the tube fitted formed sinusoidal conical-nozzles with a constant heat flux condition for nine different Reynolds numbers ranging from 8000 to 24000. CFD (Computational Liquid Dynamics) simulations have been commonly employed to predict at “Semi Implicit Technique for Pressure Linked Equations” (SIMPLE). In addition, the test-tube section was made of copper and conical-nozzle was aluminum. The results reveal that amplitude and period values have rather effects on increasing turbulent near the nozzles, and that results in both increasing of heat transfer and the friction factor. As a result, the highest thermo-hydraulic performance is attained.

Boonloi and Jedsadaratanachai [55] investigated the heat transfer, pressure loss and thermal performance evaluation in a radial tube heat exchanger with modified-twisted tapes. The influences of the hole sizes for the mono and dual twisted tapes with Reynolds numbers varying from 3000 to 10,000. The finite volume technique and the SIMPLE algorithm and the realizable (k-ε) turbulent model is performed with a stable heat flux. Air is opted as the working liquid. The results regarding current design and heat transfer act and comparison between the smooth tube and the regular twisted tape revealed that the modified-twisted tape supplies higher heat transfer rate than the smooth tube as a result of the longitudinal vortex currents created by the twisted tape. The longitudinal vortex currents raise the liquid mixing. The rectangular punched holes of the twisted tape can diminish the pressure loss of the heating system. Furthermore, the top thermal enhancement factor is obtained in the dual twisted tape and mono twisted tape at Re = 3000.

Rao et al [56] studied the augmentation techniques' role in the enhancement of heat transfer radial tube fitted with conical-ring turbulators and a twisted-tape swirl generator placed in a plain tube at different pitches. The air is used as working liquid in Reynolds number ranging from 7696 to 15410. A copper plain tube and the conical-ring was made of aluminum, and the twisted-tapes made of steel strip. The results show that the smaller the twist proportion is, the larger the heat transfer is for all Reynolds numbers. The highest heat transfer rates by employing both the conical ring and twisted tape are discovered to be 325% and 312% over the plain tube. Yet, the friction factor stemmed from using both devices also significantly augments and the correlations for Nusselt number and Friction factor evaluation criteria to evaluate the real advantages in using the turbulator and swirl generator of the enhanced tube are detected.

2.2. INVESTIGATIONS ABOUT USING NANOFLUID

Pak and Cho [57] investigated the heat transfer and friction nature of TiO2/water and γ-Al2O3/water nanofluids with mean diameters of 27 and 13 nm, respectively**,** and the currents in a turbulent current regime over a Reynolds number ranging between 10000 and 100000 and Prandtl numbers ranging between 6.5 and 12.3. It was stated that Nusselt number rises with volume concentration and Reynolds number. The heat transfer section were produced using a seamless, stainless steel tube (type 304), and

constant-heat-flux boundary condition. These results were considerably larger than the estimates from the conventional theory of suspension rheology. Darcy friction factors for the dispersed liquids of the volume density range from 1% to 3% .The Nusselt number of the dispersed liquids for completely enhanced turbulent current rose with increasing volume consummation and the Reynolds number. Yet, it was discovered that the convective heat transfer parameter of the dispersed liquid at a volume density of 3% was 12% smaller than that of pure water compared to under stable average speed. Thus, better choosing of granules with higher thermal conductivity and larger dimensions is offered so as to make use of the dispersed liquids as a working medium to foster heat transfer performance. A novel interaction for the turbulent connective heat transfer is obtained for dilute dispersed liquids with submicron metallic oxide granules.

Li and Xuan [58] explored the convective heat transfer and current features of the nanofluid in a tube. Both the convective heat transfer parameter and friction factor of Cu-water nanofluid for the laminar and turbulent current are gauged. The test section is a straight brass tube to obtain a permanent heat-flux boundary condition in which 0.3%, 0.5%, 0.8%, 1.0%, 1.2%, 1.5% and 2.0% volume fraction Cu-water nanofluids are included. The Reynolds number (*Re*) ranges between 800 and 25000. The results reveal that the suspended nanoparticles considerably raise the heat transfer performance of the base liquid and the nanofluid has larger heat transfer parameter than pure water under the same Reynolds number. The heat transfer feature of a nanofluid escalates with the volume fraction of nanoparticles. The friction factors of the nanofluids corresponds well to those of the water in the pressure drop test as the nanoparticles are so little that a suspension with nanoparticles acts like a pure liquid. The nanofluid with the low volume fraction creates almost no augmentation of pressure drop.

In a similar vein, Xuan and Li [59] studied the convective heat transfer and current features of the nanofluid in a tube under the same conditions with Li and Xuan [58]. By considering the micro convection and micro diffusion impacts of the suspended nanoparticles. This correlation correctly regards the main elements influencing the heat transfer of the nanofluid. In other respects, the friction factor for the dilute nanofluids including water and Cu-nanoparticles is nearly the same as that of water. The nanofluid with the low volume fraction of the suspended nanoparticles leads to nearly no extra penalty of pump power.

Ding and Wen [60] examined the convective heat transfer of nanofluids made of γ-Al2O3 nanoparticles and de-ionized water flowing through a copper tube in the laminar current regime. With thermal isolating tier encircling the heater to attain a stable heat flux condition along the test section with Reynolds number of 500–2100 and granule densities less than 2%. The results are considerable in terms of the enhancement of convective heat transfer using the nanofluids. The enhancement was especially remarkable in the entrance area, and was quite higher than that caused merely by the enhancement on thermal conduction. It was also suggested that the classical Shah equation failed to estimate the heat transfer act of nanofluids. Migration of nanoparticles and the resulting disturbance of the boundary tier were claimed to be the major reasons.

Ding et al. [61] conducted an experiment on the heat transfer act of aqueous suspensions of multi-walled carbon nanotubes (CNT nanofluids) flowing through a horizontal tube. With a stable heat flux condition along the test section, a straight copper tube, the density of gum Arabic was 0.25 wt. % to 0.5% regarding water, which was found to render excellent fixity to the CNT nanofluids under Reynolds number of 800–1200. The results argued that the enhancement is based on the current condition, CNT density and the pH level Also, the effect of pH is found to be small. For nanofluids containing 0.5 wt. % CNTs, the maximum enhancement is over 350% at Re = 800, and the maximum enhancement takes place at an axial distance of almost 110 times of the tube diameter. Granule re-arrangement, shear induced thermal conduction enhancement, reduction of thermal limit tier thickness because of the existence of nanoparticles.

He et al. [62] explored the forced convective heat transfer of aqueous suspensions of titanium dioxide nanoparticles (TiO2 nanofluids). Then, the nanofluids are gauged for their heat transfer and current act while flowing upward via a vertical pipe in both the laminar and turbulent current regimes. The test section is made of copper and nanofluids containing 1.0%, 2.5%, and 4.9% TiO2 granules. There was a stable condition of heat flux along the test section. The results suggest that the inclusion of nanoparticles into the base liquid improves the thermal conduction, and the enhancement increases with rising granule density and decreasing granule (agglomerate) size. The convective heat transfer parameter is not vulnerable to the average granule dimensions under the conditions of this study. The results also demonstrate that the pressure drop of the

nanofluid currents is quite similar to that of the base liquid currents for a specific Reynolds number.

Santra et al. [63] examined a cooling medium to simulate the heat transfer act in a two-dimensional (infinite depth) horizontal rectangular duct for cuo/water nanofluid, for a laminar current through the SIMPLER algorithm. For a wide range of Reynolds number (*Re* = 5 to 1500) and solid volume fraction ($0.00 \leq \varphi \leq 0.050$), the results outline that the heat transfer increase is possible by using nanofluid compared to the conventional liquids for both cases. The rate of heat transfer rises with the increase in current as well as the increase in solid volume fraction of the nanofluid. In contrast to the natural convection, the increase in heat transfer is almost same for both the cases. At Re = 1500, the wall shear stress diminishes with φ, which indicates that less pumping power than Newtonian liquid is essential with non-Newtonian liquid. Local shear distribution at wall suggests that at lower Re non-Newtonian liquid creates more shear than Newtonian liquid. However, as Re increases, the difference decreases and at higher Re it becomes less than Newtonian liquid.

Duangthongsuk and Wongwises [64] studied the heat transfer parameter and friction factor of the TiO2-water nanofluids current which flows in a horizontal dual tube counter- current heat exchanger under conditions of turbulent current with TiO2 nanoparticles dispersed in water with volume densities of 0.2–2 vol. % which are exploited as the test liquid and the tube is made of smooth copper and the Reynolds number of the nanofluid ranges between 3000 and 18,000. The results reveal that the heat transfer parameter of nanofluid is bigger than that of the base liquid and increase with rising Reynolds number and granule densities. The heat transfer parameter of nanofluids was nearly 26% greater than that of pure. Furthermore, the results outline that the heat transfer parameter of the nanofluids at a volume density of 2.0 % was about 14% less than that of the base liquids for the available conditions. Regarding the pressure decrease, the results suggest that the pressure decrease of nanofluids was a bit higher than the base liquid and goes up with rising volume densities. Lastly, they proposed new parameters for estimating the Nusselt number and friction factor of the nanofluids.

Mansour et al. [65] conducted an investigation on mixed convection of Al2O3/water nanofluid inside an inclined copper tube fixed to a constant wall heat flux at its outer facet with granule volume density from 0 to 4% and Reynolds number from 350 to 900 and from 5 $^{x}10^{5}$ to 9.6 ^{x} 10^{5} and Grashof numbers (Gr = 4.50 $^{x}10^{4}$). The results indicate that the experimental heat transfer parameter diminishes vaguely with an increase in granule volume density from 0 to 4%. Two new correlations are proposed to reckon the Nusselt number in the fully developed area for horizontal and vertical tubes, for Reynolds number and granule volume densities up to 4%. And to compute the asymptotic Nusselt number for a horizontal and a vertical tube, the explicit contradictory act was observed between the experimental data and analytical/numerical results with regard to the heat transfer enhancement of nanofluids under buoyant forces. This has raised serious concerns with the applicability of utilizing the single stage and homogeneous liquid model for nanofluids under natural convection effect.

Albadr et al. [66] studying the forced convective heat transfer and current features of a nanofluid including water and various volume densities of Al2O3 nanofluid (0.3–2%) which currents in a horizontal shell and tube heat exchanger counter current under turbulent current conditions discovered that the convective heat transfer parameter of nanofluid is a little higher than that of the base liquid at same mass current rate and inlet temperature. The heat transfer parameter of the nanofluid rises with an increase in the mass current rate, so does the heat transfer parameter with the rise of the volume density of the Al2O3 nanofluid. However, increasing the volume density results in a rise in the viscosity of the nanofluid leading to increase in friction factor.

Abdolbaqi et al. [67] quantitatively explored the heat transfer enhancement of nanofluids under turbulent current through a straight square channel under permanent heat flux conditions. The nanofluids are prepared as solid nanoparticles of CuO, TiO2 and Al2O3 which are suspended in water (CFD) and analyzed by FLUENT software using the conducted and Reynolds numbers from 10^{4} to 10^{6} and constant volume density of 1–4% with the SIMPLE scheme adopted a turbulent viscous (k–ε) model. According to the results, the heat transfer enhancement stemmed from various parameters such as the nanoparticle density of volume and the Reynolds number is reported. Finite volume techniques are employed to sort out the governing equations with certain assumptions which are obtained through the numerical simulation. The

enhancement of the friction factor and the Nusselt number 2 %, 21 %, respectively, the 4% volume density of nanofluid has the highest friction factor values, followed by 3%, 2% and 1%. The Nusselt number of CuO precedes TiO2 and Al2O3.

Azmi et al. [68] investigated the heat transfer parameter and friction factor of TiO2 and SiO2 water based nanofluids which flow in a radial tube under turbulent current in stable heat flux boundary condition. TiO2 and SiO2 nanofluids with an average granule size of 50 nm and 22 nm are included in the working liquid for volume densities up to 3.0% and the Reynolds number ranging from 5000 to 25000 and the copper tube test section. The results of enhancements in viscosity and thermal conductivity of TiO2 are greater than SiO2 nanofluid. Yet, a maximum enhancement of 26% in heat transfer parameters is attained with TiO2 nanofluid at 1.0% density whereas SiO2 nanofluid provided 33% enhancement at 3.0% density. The heat transfer parameters are lower at all other densities. The granule density at which the nanofluids supply the maximum heat transfer has been determined and validated with property enhancement ratio. It is discovered that the pressure drop is directly proportional to the density of the nanoparticle.

Manca et al. [69] examined the laminar mixed convection in triangular ducts filled with nanofluids so as to assess the liquid dynamic and thermal properties of the regarded geometry by taking into account Al2O3/water based nanofluids. The system is heated by a stable and regular heat flux also along the perimeter of the triangular duct section with FLUENT (Computational Liquid Dynamic) Code Version (6.3) User Guide to sort out the stationary equations and a second-order upwind scheme by using SIMPLE and a Reynolds number value of 100. The results depicted various nanoparticle volume densities and Richardson number values of 0% to 5% and from 0 to 5, sequentially. The improvement of average convective heat transfer parameters regards the increasing values of Richardson number and granule pieces. Nevertheless, wall shear stress and essential pumping power profiles rise as expected. The PEC analysis revealed that using nanofluids in mixed convection seems a bit appropriate. It must be emphasized that, for the present time, experimental data do not exist to compare the quantitative model proposed for the mixed convection in horizontal triangular ducts with nanofluids.

Li et al. [70] investigated the mass transfer and energy transmission between liquid stage and steam stage, a mixture model for boiling heat transfer of nanofluid of TiO2–water nanofluid. The material of the boiling cavity is copper and the mass fraction is wt.1%, wt. 2%, and wt. 3% with numerical solution in the FLUENT 6.3. The results proposed that the boiling bubble dimensions in TiO2–water nanofluid is just one-third of the one in de-ionized water. It is also discovered that there is a crucial nanoparticle mass fraction (wt. % = 2%) between enhancement and degradation of TiO2–water nanofluid. In comparison with water, nanofluid improves the boiling heat transfer parameter by 77.7% when the nanoparticle mass fraction is less than 2%, although it decreases the boiling heat transfer by 30.3% when the nanoparticle mass fraction is more than 2%. The boiling heat transfer parameters augment with the superheat for water and nanofluid. A mathematical relationship was obtained between heat flux and superheat.

Dagdevir and Ozceyhan [71] conducted a study on a horizontal straight tube's fraction effect of hybrid water based CuO-TiO2 nanofluid on thermal performance. A CFD modeling was employed in order to ensure fully developed current, the tested tube was adjusted, and regular heat flux was implemented on outer facet of the test tube. Different turbulence models were studies and (k-ω) Shear Stress Transport (SST) turbulent model was opted to simulate turbulent current for Reynolds number ranging from 10,000 to 50,000. Besides, nanofluid volume fractions (φ) in water were applied as 5, 4, 3, and 2% in which each density has varying volume fractions of CuO and TiO2. The results revealed that the highest effective Nusselt number is obtained for which volume fraction of CuO and TiO2 is similar to each other. On the other hand, hydraulic performance of hybrid nanofluid current was examined. Adding nanoparticle, especially CuO rises the pressure drop in comparison with the distilled water. However, the highest effective Nusselt number of 1.145 is received at volume fraction of CuO and TiO2 of 0.02 and 0.03, respectively at Reynolds number of 50,000.

Bajestan et al. [72] focused on enhancing the heat transfer features of heat exchangers in solar practices by exploiting nanofluids as the heat transfer tool for laminar convective heat transfer of water-based TiO2 nanofluid flowing with straight copper tube with a stable and regularregular heat flux condition along the test stage. The constant suspensions were supplied at different nanoparticles' volume densities of 1, 1.5, 1.6, 2,

and 2.3% and numerical in (CFD) with Grid-independence (1460) computational cells are essential for the radial cross section of the tube. The results related to the top enhancement of 21% in average heat transfer parameter have been attained by TiO2/water nanofluids. As for the quantitative stage, the single-stage model was compared with the common two-stage numerical approaches. The numerical investigation showed that the predicted heat transfer parameters using single-stage and common two-stage approaches, even based on experimental thermophysical properties of nanofluids, underestimate and overestimate the experimental data. Hence, some modifications are carried out to the common two-stage model to attain sound predictions of the heat transfer properties of nanofluids. This revised model explored the impacts of granule density, granule diameter, and granule and base liquid material on the heat transfer rate at varying Reynolds numbers. The results suggest that the convective heat transfer parameter rises with a rise in nanoparticle density and current Reynolds number whereas granule dimensions have an adverse impact. The attained results can be of great benefit for the investigation of the probable applications of nanofluid-based solar collectors.

2.3. INVESTIGATIONS ON USING BOTH TURBULATOR AND NANOFLUID

Sundar et al. [73] evaluate the heat transfer parameter and friction factor for current in a copper tube and with twisted tape inserts made from aluminum in the transition range of current with Al2O3 nanofluid which is conducted under constant heat flux and Reynolds number ranging from 3000 to 9000 with a nanofluid of less than 3% volume density. The results of the heat transfer parameter of nanofluid flowing in a tube with 0.1% volume density is found to be 23.7% higher than water at number of 9000. Heat transfer parameter and pressure drop with nanofluid have been experimentally specified with tapes of various twist proportions and found to diverge with the values obtained from equations developed for single-stage current. A regression equation was developed to estimate the Nusselt number validity for both water and nanofluid flowing in the transition current within Reynolds number range in radial plain tube and with tape inserts. The maximum friction factor with twisted tape at 0.1% nanofluid volume density is 1.21 times that of water flowing in a plain tube.

Sundar and Sharma [74] also studied the turbulent convective heat transfer and friction factor act of Al2O3 nanofluid in a radial tube with various aspect proportions of longitudinal strip inserts which are with the Reynolds number range (3000 < Re < 22,000), granule volume density (0 < u < 0.5%) and longitudinal strip aspect proportions (0 < AR < 18) with a permanent heat flux boundary condition. The nanofluid currents through a copper tube and insert, and the longitudinal strips are made of aluminum. The results outline that heat transfer parameters increase with the nanofluid volume density and decrease with the aspect ratio. The friction factor of 0.5% volume density nanofluid with longitudinal strip insert having AR = 1 is 5.5 times greater at 3000 Reynolds number and 3.6 times greater at 22,000 Reynolds number compared to water or nanofluid flowing in a tube. The use of longitudinal strip inserts is beneficial at higher Reynolds number based on the values of friction factor and the heat transfer compared to either water's or nanofluid's current in a tube. The use of nanofluid improves the heat transfer parameter without any significant enhancement in pressure drop compared to water in the range tested.

Eiamsa and Wongcharee [75] analyzed the heat transfer, friction and thermal performance characteristics of CuO/water nanofluid which have been utilized in a radial tube equipped with modified twisted tape with alternate axis (TA) with the density of nanofluid varying from 0.3 to 0.7%)by volume and the Reynolds number range (830≤Re≤1990). In addition, the test tube was made of copper and twisted tapes were made of an acrylic sheet at regular heat flux. According to the results, Nusselt number rises with increasing Reynolds number and nanofluid density. Through the individual uses of 9TA and TT), Nusselt numbers increase up to 12.8 and 7.2 times of the plain tube, respectively. The simultaneous use of nanofluid and TA improve Nusselt number up to 13.8 times of the plain tube. Over the range studied, the maximum thermal performance factor is found to be 5.53 by the simultaneous employment of the CuO/water nanofluid at 0.7% volume and TA at Reynolds number of 1990. Furthermore, the empirical correlations for heat transfer parameter, friction factor and thermal performance factor were also developed and reported. The predicted data obtained from the empirical correlations developed are in line with the experimental data.

Suresh et al. [76] made a comparison of thermal performance of helical screw tape inserts in laminar current of Al2O3/water and CuO/water nanofluids via a straight radial duct with stable heat flux boundary condition. To that end, 0.1% volume density Al2O3/water and CuO/water nanofluids and different the helical screw tape inserts with twist proportions which were made by winding regularly a copper and test sections are made of straight copper tube and Reynolds number (Re < 2300) were used. The results show that the insertion of helical screw tape inserts leads to very significant convective heat transfer enhancement in the laminar current of both nanofluids. The higher turbulence intensity of the liquid which is close to the tube wall associated with the helical screw tape insert is responsible for an excellent liquid mixture and an efficient redevelopment of the thermal/hydrodynamic boundary tier which consequently evokes the improvement of convective heat transfer. The friction factors of both nanofluids also rise significantly when coupled with helical screw tape inserts and Thermal performance factor of helical screw tape inserts. Using CuO/water nanofluid is higher than the akin value using Al2O3/ water. Thus, the helical screw tape inserts render better thermal performance when matched with CuO/water nanofluid than with Al2O3/water nanofluid.

Suresh et al. [77] conducted an experimental investigation on the heat transfer and friction factor characteristics in a radial tube fitted with wire coil inserts by using Al2O3/water nanofluid as the working liquid under isothermal current conditions. Also, section of straight copper tube with a volume density of (0.1%) was prepared and the Reynolds number ranged from 2500 to 5000 Wire coil inserts were also carried out with distilled water as the working liquid for experimental setup validation and comparison. The analysis of experimental data suggest that the use of nanofluids raises the heat transfer rate with negligible increase in friction factor in the plain tube and the tube fitted with wire coil inserts. In addition, empirical correlations are proposed based on the experimental results of the present study, which seem to be quite accurate for the prediction of the heat transfer and friction factor features.

In another experimental study, Behabadi et al. [78] examined the heat transfer and pressure drop properties of CuO/Base oil nanofluid laminar current in a smooth tube with varied wire coil inserts under stable heat flux. The nanofluid is prepared through the dispersion of CuO nanoparticles in base oil. Granules' volume fraction is ranging

from 0.07% to 0.3%, and five coiled wires having pitches with a copper tube are used as test section and wire coil inserts are manufactured from stainless steel wire. The results show that for a specific nanoparticle density, inserting coil wires increases both heat transfer and pressure drop. On average, 45% increase in heat transfer parameter and 63% penalty in pressure drop was observed at the highest Reynolds number inside the wire coil embedded into the tube with the highest wire diameter. As the applied heat transfer enhancement techniques are accompanied by an increase in current pressure drop, two empirical correlations are developed in order to predict the Nusselt number and friction factor of the nanofluid current within the coiled wires embedded tubes.

Kahani et al. [79] investigated the influence of curvature ratio and coil pitch for Al2O3/water nanofluid laminar flow on heat transfer behavior and pressure drop on helical coils via different coils with curvature ratio and coil pitch. Moreover, the volume fractions of nanoparticles were 0.25, 0.5, 0.75 and 1.0 vol% and the helical coils and a straight pipe were employed in test sections which were made of copper all tests were done at Re<4500 under constant heat flux boundary condition. The results suggest that the increase in nanofluid concentration will improve both the Nusselt number and pressure drop of working fluid through helical coils. According to the empirical data, reducing the curvature ratio or increasing the pitch coil result in increment in the heat transfer rate and pressure drop although the pitch effect is weaker than the curvature effect.

Azmi et al. [80] compared the convective heat transfer parameter and friction factor of TiO2 nanofluid current in a tube with twisted tape inserts with nanofluid up to 3.0% volume density and the Reynolds number range of 8000 to 30,000 for current in tubes and with tapes of varying twist proportions with a tube of the test section made of copper with heaters and the twisted tapes produced with aluminum strips. The results indicate a significant enhancement (23.2%) in the heat transfer parameters at 1.0% density for current in a tube. Through exploiting twisted tapes, the heat transfer parameter rose with the drop in the twist proportion for water and nanofluid. The heat transfer parameter and friction factor are 9981.1% and 1.5 times greater at Re = 23,558 with 1.0% density and twist proportion of 5 compared to values with current of water in a tube. A rise in the nanofluid density to 3.0% reduced the heat transfer parameters to values less than water for current in a tube and with tape inserts. A thermal system with

tape insert of twist proportions (15 and 1.0%) TiO2 density provides the top advantage proportion, if pressure decrease is regarded along with the betterment in heat transfer parameter.

Sharma et al [81] studied on SiO2/water nanofluid to develop the turbulent current of nanofluids in a tube with twisted tape inserts with the volume density range of 0.5 to 4.0% at various Reynolds number range (3000 < Re < 100,000) and the generalized equation for the estimation of nanofluid friction factor. In addition, Nusselt number is proposed with the experimental data for twisted tapes. The parameter and the Prandtl index in the eddy diffusivity equation of momentum and heat are attained from the numerical values as a function of Reynolds number, density and twist ratio. An enhancement (94.1%) in heat transfer parameter and higher friction factor (160%) at Re = 19,046 are observed at a twist proportion of five with volumetric density (3.0%) compared to the current of water in a tube. The study aligns with the limited experimental data of other investigators regarding Al2O3 and Fe3O4 nanofluids which indicates the validity of the numerical model to use with twisted tape inserts.

Naik and Sundar [82] conducted an experiment on the convective heat transfer and friction factor characteristics of water/propylene glycol-based CuO nanofluids flowing in a horizontal radial tube fitted with and without the helical inserts with volume densities of CuO nanofluids (0.025%, 0.1%, and 0.5%). Also, the Reynolds number was ranging from 2500 to 10,000 with a constant heat flux throughout the test section, and test section was made of a copper tube. According to the results, the Nusselt number obtained with 0.5% density of CuO nanofluids is around 28% higher in a plain tube and is rather increased up to 5.4 times over the base liquid when the helical insert with twist proportion 3 is employed. In the plain tube, the friction factor increased by 10% and further improved to 140% through the usage of helical insert compared to the friction factor obtained with the base liquid alone. The friction factor penalty is fairly much less compared to the benefit of the heat transfer enhancement. Correlations for predicting Nusselt number and friction factor are developed by using the experimental data regarding CuO nanofluids in a plain tube with and without the helical inserts. Moreover, the use of helical inserts in liquid current renders significant enhancement in heat transfer parameter of liquids accompanied by a pressure drop. Compared to the conventional base liquid, CuO nanofluids provide better heat transfer performance.

Adding some new variables, Prasad et al. [83] investigated the turbulent forced convection heat transfer and friction of Al2O3 – water nanofluid current via a concentric tube U-bend heat exchanger with and without helical tape inserts in the inner tube at Reynolds number ranging from 3000 to 30000In addition, volume densities (0.01%, 0.03%) and helical tape inserts (p/d = 5, 10, 15 and 20) were specified with the inner tube made of Copper and the helical tape inserts made by aluminum. The results suggest that increasing Reynolds number and Prandtl number increase the average Nusselt number, and rise of thermal conductivity in the nanofluid contributes to heat transfer enhancement. The Nusselt number of all pipes for 0.03% densities of nanofluid with helical tape inserts of p/d = 5 points an enhancement of 32.91% compared to water. The friction factor for the entire inner tube for 0.03% density of nanofluid with helical tape inserts (p/d = 5) rises (1.38 times) compared to water. Generally and in line with the theory, the pressure decrease in the inner tube goes up by increasing the nanoparticle volume density and aspect proportion of the inserts. The empirical correlations for the Nusselt number and friction factor are obtained as functions of the Reynolds number, Prandtl number, volume density and aspect ratio. Furthermore, the whole enhancement proportion for nanofluids with helical tape inserts is more than combination of all current rates.

Eiamsa et al. [84] examined the heat transfer enhancement for (TiO2) in water as nanofluid with overlapped dual twisted tapes (O-DTs) with Reynolds numbers ranging from 5400 to 15,200 and overlapped twist proportions (yo/y) of 1.5, 2.0 and 2.5 and nanofluids with TiO2 volume densities (0.07%, 0.14% and 0.21%) with test tube which was measured with manometer under an isothermal condition. In addition, numerical assumptions were implemented for the conventional current momentum and energy equations to simulate the heat transfer process in a constant heat flux tube with O-DTs. The central assumptions are; (1) the current is stable and incompressible, (2) the current through the O-DTs is turbulent, (3) natural convection and thermal radiation are disregarded and (4) the thermo-physical features of the liquid are temperature independence and solution by CFD in the pressure speed coupling algorithm (SIMPLE). The sustainability, accelaration and energy equations for the three dimensional models were utilized. For steady state current, incompressible. The results when using O-DTs at the smallest overlapped twist proportion (1.5) improved the heat transfer rates up to

89%, friction factor by 5.43 times and thermal performance up to 1.13 times compared to those of plain tube. Besides, the heat transfer increased as TiO2 volume density of nanofluid increased due to the increases of contact facet and thermal conductivity. The simultaneous use of the O-DTs having twist proportions (1.5) with the nanofluid with TiO2 volume density of 0.21% formed heat transfer enhancement around 9.9-11.2% and thermal performance improvement up to 4.5% compared to the use of O-DTs alone. The empirical correlations of the heat transfer rate (Nu), friction factor (f) and thermal performance (h) in a permanent wall heat flux tube equipped with O-DTs at different overlapped twist proportions (yo/y) and volume densities of TiO2 nanoparticles (f) are also reported for the heat transfer applications.

Similar to aforementioned studies, Mali et al. [85] explored the heat transfer enhancement of Al2O3 qater based nanofluid with centrally hollow twisted tape under laminar current condition at constant wall heat flux boundary condition with variations of Reynolds numbers (600-1600) and with 0.25% and 0.5% volume densities inside a copper tube. The results outline that centrally hollow twisted tape improves the heat transfer parameter (1.27-22.4 %) compared to the plain twisted tape of same pitch. In addition, Nanoparticle with 0.25-0.5 % volume density increases the heat transfer (6.84-12.8 %) compared to centrally hollow twisted tape of 8 mm hollow width. Furthermore, friction factor of centrally hollow twisted tape at central width 8 mm has (33.7-40.6 %) friction factor of plain twisted tape.Nanoparticle with 0.25-0.5 % density increases friction factor by 8.23-25 % with respect to friction factor obtained from water.

Safikhani et al. [86] also investigated the Al2O3-water nanofluid current in laminar and turbulent currents inside the tubes fitted with diamond-shaped turbulators by CFD by practicing a two-stage mixture technique and applying the constant heat flux boundary condition at tube walls and different geometrical parameters such as TR and θ and Reynolds number from laminar and turbulent range (1000 to 10000) with the k-ε model. Also, a second order upwind technique is employed for the convective and diffusive terms and SIMPLE. According to the results, the heat transfer parameter increase as well as the wall shear stress. In a similar vein, with the reduction of TR and increase of θ, the amount of secondary currents, vortices and the turbulent kinetic energy increase. Moreover, the increase in the volume fraction of nanoparticles and the reduction of

nanoparticles diameter result in the increase of the heat transfer parameter and wall shear stress.

In a similar trend with their counterparts, Pavan et al. [87] explored the enhancement of heat transfer in the heat exchangers using plain tube, tube with twisted tape inserts and also the tube with regularly punched twisted tapes with a twisting proportion of (2.37) and the water. Then, Al2O3 nanofluid is passed through the test section separately at varying current rate (4, 6, 8 LPM). The thermal features of both liquids are noted and the nanofluid is included into the test section at a steady state facet temperature with the range of Reynolds number (2000<Re<10000). It is suggested that the rise of the heat transfer parameter in plain twisted tape was 30% higher than TT tube without insert and the rise of heat transfer in punched twisted tape was 56% higher than the plain tube of heat exchanger. Moreover, the friction factor in plain twisted tape inserts was 33% lower than twisted tape without inserts in tube, and for punched twisted tape inserts 38% lower than plain tube without inserts. This rise was observed as a result of the turbulence formed by the change in the geometrical shape of the twisted tape inserts on the plain tube of heat exchanger.

Sundar et al. [88] also investigated the convective heat transfer, friction factor, effectiveness and number of transfer units (NTU) of Fe3O4/water nanofluids current in a dual pipe U-bend heat exchanger with or without wire coil inserts under turbulent current conditions which includes Reynolds numbers (16,000–30,000), different granule densities (0.005–0.06%) and different wire coil inserts of coil pitch to tube inside diameter (p/d) proportions (1, 1.34 and 1.79) with double pipe with a stainless steel. The rod of spring steel (EN 42J) material was wire coil. According to the results, Nusselt number rises with increasing Reynolds number and granule densities, and lowering p/d proportion of wire coil inserts. The Nusselt number betterment for (0.06%) volume density of nanofluid is (14.7%) and it rather increases to 32.03% for the same nanofluid (0.06%) with wire coil inserts of (p/d = 1) with a friction penalty (1.162-times) at Reynolds number of 28,954 compared to related water data. The experimental data was fitted using regression analysis to predict the Nusselt number and friction factor of nanofluid as a function of the Reynolds number, Prandtl number, volume density, and wire coil helix ratio. The effectiveness of heat exchanger is formulated in terms of amount of transfer units (NTU) for the base liquid and nanofluids.

Avval et al. [89] studied the convective heat transfer with nanofluids in helically coiled tubes in the laminar area. Two boundary conditions are implemented to the coil walls; constant temperature and constant heat flux. In (CFD), heat transfer in nanofluids are essentially investigated using either the homogeneous model or the two-stage model and also the four-equation model is applied, with Water/CuO with a (0.2%) volume fraction and water/Ag with a (0.03%) volume fraction. Furthermore, a second order of finite difference technique is applied at different Reynolds numbers and different curvature proportions. The results pointed out that higher Reynolds numbers and higher curvature proportions augment the secondary currents in the coil, thus raising the heat transfer rate, especially in the outer radius area of the coil. The results were also compared to the ones received from the experimental investigations. Water/CuO, with 0.2% volume fraction and water/Ag with 0.03% volume fraction were regarded in the constant temperature and constant heat flux boundary conditions, respectively. It was discovered that the four-equation model renders closer results to the experimental data compared to the homogeneous model stating that the solution technique is less complicated.

Tavakoli et al. [90] investigated the forced convection heat transfer and pressure drop in helically coiled pipes using TiO2/water nanofluid. The experiments were carried out in the range of Reynolds number from 3000 to 18000 and in the nanoparticle densities of 0.1, 0.2, and 0.5% for five different curvature proportions. In quantitative simulations, the thermophysical features of the working liquid were regarded to be a function of the nanofluid temperature and density. As for the turbulent regime, the standard model was applied to simulate the turbulent current characteristics (k-ε).At constant wall temperature condition and (SIMPLE) algorithm was employed to pair pressure and momentum and the second-order upwind scheme. The quantitative results were in line with the experimental data. The results outlined that utilization of nanofluid rather than distilled water leads to an enhancement in the Nusselt number up to 30%. Besides, four formulas were introduced to attain the average Nusselt number and friction factor in helically coiled tubes under constant wall temperature condition for both laminar and turbulent current regimes.

CHAPTER 2

METHODOLOGY

In many cases, only an approximate solution is sought. Some of the mathematical techniques needed for the Thermo-hydrodynamic concern regarding the design of the heat exchanger structures are analytical while many are nominal in nature. While the evolution of computers has made the numerical techniques more advantageous over the classical analytical in order to analyze the current and thermal fields in a pipe under the heat flux including or not including a different nozzle insert, a solution of (Navier-Stokes) equations with the energy equation, continuity equation and momentum equations are required. The complexity of nozzles configurations precludes to obtain an analytical solution of the governing equations for practical configuration. Quantitative simulations allow the analysis of the complex geometry of the current domain. Thus, limited volume numerical techniques by CFD have been applied to sort out the equations. The used liquid medium in the analysis is the mixture of some most commonly utilized nanoparticles and distilled water, and it is assumed as a single stage to simplify the concern. The main aim upon which the present work is based is to give an extensive review on different CFD approaches employed in quantitative simulation of nanofluid current.

2.1. INFLUENTIAL PARAMETERS IN THE INVESTIGATION

2.1.1. Boundary Layer (Hydraulic)

The interface between a liquid and a facet in relative motion, a condition known as “no slip” dictates an equivalence between liquid and facet velocities. A way from the facet to the liquid speed rapidly increases, the zone in which this takes place is called as boundary tier and symbolized with (δ) and in accordance with the Newton Liquid the shear stresses effect on facet is direct function of the speed gradient at the facet at

external and internal current in equation (2) and we can show that current the liquid over flat plate in Figure 2.1. The speed of the granules in the first liquid tier next to the plate becomes zero due to the no-slip condition. This motionless tier slows down the granules of the adjacent liquid tier as a result of friction between the granules of these two contiguous liquid tiers at varying speeds. This liquid tier then decelerates the molecules of the next tier [91, 92]. The current regime in the first case is of laminar manner identified by smooth streamlines and highly-ordered motion, and turbulent in the second case, where it is formed by the speed fluctuations and highly-disordered act. The transition from laminar to turbulent current does not happen suddenly; instead, it takes place over some areas in which the current undulates between laminar and turbulent currents before it becomes completely turbulent. [91, 92].

$$\tau = \mu \frac{du}{dy} \tag{2}$$

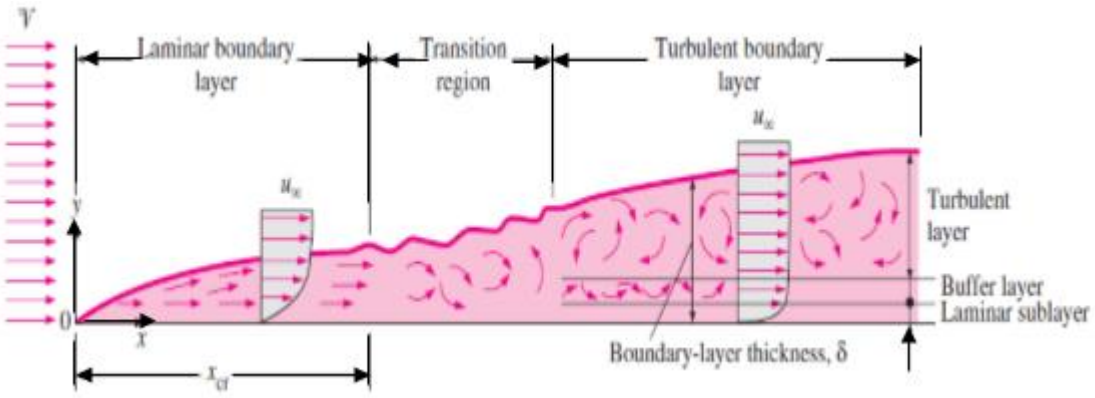


Figure 2.1. The development of the boundary layer for flow over a flat plate, and the different flow regimes. [91].

If the liquid enters a radial tube at a regular speed, the area from the tube inlet to the point at which the boundary tier combines at the centerline is called the hydrodynamic entrance area, and the length of this area is called the hydrodynamic entry length. (L_h) current in the entrance area is called hydrodynamically developing current as this is the area where the speed profile develops. [91, 92]. The area beyond the entrance area in which the speed profile is fully formed and remains unchanged is called the hydrodynamically fully developed area. As shown the Figure 2.2, the speed profile in

the fully developed area is parabolic in laminar current and somewhat flatter in turbulent current due to the eddy motion in circular direction.

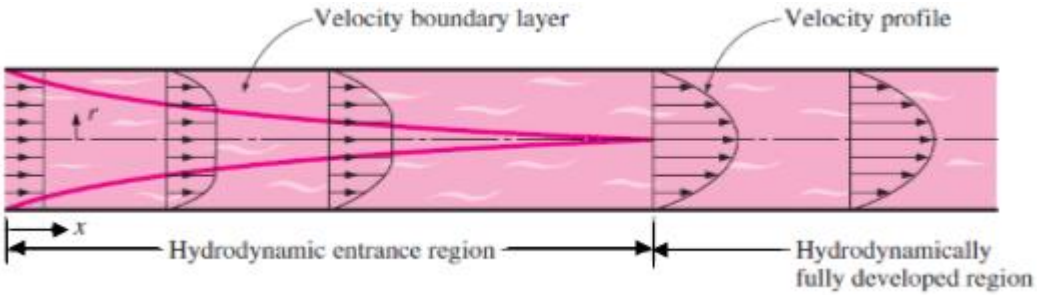


Figure 2.2. The development of the velocity boundary layer in a tube. (The developed mean velocity profile will be parabolic in laminar flow, as shown, but somewhat blunt in turbulent flow). [91].

2.1.2. Thermal Boundary layer

Now regard a liquid at a regular temperature entering a radial tube facet of which is sustained at a variant temperature. This time, the liquid granules in the tier in contact with the facet of the tube will assume the facet temperature. This will launch the convection heat transfer in the tube and the development of a thermal boundary tier along the tube. The thickness of this boundary tier also augments in the current direction until the boundary tier reaches the tube core and thus fills the whole tube, as illustrated in Figure 2.3. [93].

As defined by some researchers, the area of current over which the thermal boundary tier develops and reaches the tube center is termed as the thermal entrance area, and the length of this area is called the thermal entry length. [94] Current in the thermal entrance area is termed as thermally developing current as this is the area where the temperature profile develops. The area beyond the thermal entrance area in which the nondimensional temperature profile stays same is termed as the thermally fully developed area. The area in which the current is both hydrodynamically and thermally formed and thus both the speed and nondimensional temperature profiles stay same is called Fully Developed Flow [94].

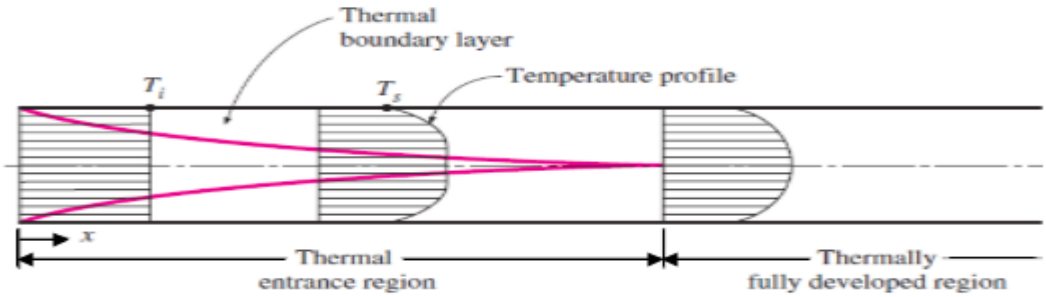


Figure 2.3. The development of the thermal boundary layer in a tube. (The fluid in the tube is being cooled.) [94].

In addition, as Cengel and Cimbala [91] put, the hydrodynamic entry length is usually admitted as the distance from the tube entrance where the friction parameter reaches in the range about 2 % of the fully developed value and when it can be calculated through equations 3 and 4. That temperature profile in the thermally completely developed area may vary with x in the current direction. In other words, contrary to the speed profile, the temperature profile can vary at other cross sections of the tube in the developed area.

For laminar flow $L_h \approx 0.05ReD$ (3)

For turbulent flow $L_h \approx 10D$ (4)

2.1.3. Pressure Drop (ΔP)

A body of interest in the analysis of the tube current is directed to the *pressure drop (ΔP)* which is the variance between the pressures at the entry and the exit of the tube bank. It is a measurement of the resistance the tubes provide to current over them, we note (dP/dx= stable), and include it from (x = 0) in which P_1 represents the pressure with (x =L) where P_2 refers to the pressure is. That is expressed as:

$$\frac{dP}{dx} = \frac{P_2 - P_1}{X_2 - X_1} = -\frac{\Delta P}{L} \quad (5)$$

Some researchers note that in liquid mechanics, the pressure drop ΔP is a positive value, and is identified as $\Delta P = P1 - P2$. In practice, it is seen convenient to express the pressure drop for all types of internal currents (laminar or turbulent currents, radial or nonradial tubes, smooth or rough face) as shown in Figure 2.4. [93, 94].

The *pressure drop* can be calculated as:

$$\Delta P = f\frac{L\,\rho\,V^2}{2\,D} \quad (6)$$

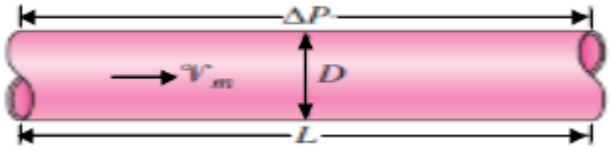


Figure 2.4. The sketch show pressure drop is one of the most general relations in fluid mechanics [94].

The power necessitated to move a liquid via a tube bank is commensurate with the pressure decrease, and when the pressure decrease is available. [93, 94]. The pumping power required for the favor of enhancing the heat transfer in a tube bank via rearrangement should be weighed against the cost of extra power requirements which can be determined through:

$$\dot{W} = V\,\dot{\Delta}P \quad (7)$$

2.1.4. Thermal Conductivity (K)

The thermal conductivity of a material is defined as the rate of the heat transfer via a unit thickness of the material per unit area per unit temperature variance. The thermal conductivity of a material is an estimate of the capability of the material to transmit heat. A high rate for thermal conductivity refers that the material is a successful heat transmitter, and a low rate means that the material is a bad heat transmitter or insulator and that units of *k* are in watts per meter per Celsius degree. The thermal transmission of a material is normally the highest in the solid stage and the least in the gas stage. For instance, (k = 0.608 W/m ·°C) for water and (k = 80.2 W/m · °C) for iron at room temperature [93]. Also, it is conveniently identified by Fourier's law of heat conduction in equation. (8) and (9).

$$\dot{Q} = -kA\frac{dT}{dX} \quad (8)$$

$$k = \frac{\dot{Q}\,dx}{A(T_1 - T_2)} \quad (9)$$

2.1.5. Heat Transfer Coefficient (h)

Heat transfer processes involving change of stage of a liquid are also regarded to be convection due to the liquid motion induced during the process such as the rise of the vapor bubbles during boiling or the fall of the liquid droplets during condensation. The heat transfer parameter is observed to be comparative with the temperature difference as outlined by Holman [93], and is conveniently expressed by Newton's law of cooling as:

$$\dot{Q} = h\,A(T_s - T_\infty) \tag{10}$$

$$h = \frac{\dot{Q}}{A\,(T_S - T_\infty)} \tag{11}$$

The convection heat transfer parameter (h) is not a characteristic of the liquid. It is an experimentally determined coefficient, the value of which relies on all the variables affecting the convection such as the facet geometry, [93], the nature of liquid act, the features of the liquid, and the bulk liquid speed and those units of *h* are in watts per square meter per Celsius degree when the heat current is in watts.

2.1.6. Non-Dimensional Number

2.1.6.1. Reynolds Number (Re)

The Reynolds number is the ratio of inertial forces to viscous forces. Acritical Reynolds number differentiates among the current regimes. The passage from laminar to turbulent current relies on the facet geometry, facet roughness, free-stream speed, facet temperature, and type of liquid among other factors such as laminar or turbulent current in the boundary tier or around immersed objects and the nondimensional [95].

$$Re = \frac{V\,\rho\,D}{\mu} \tag{12}$$

In which *V* is the upstream speed (equivalent to the free-stream speed (u_∞) for a pipe), *D* is the characteristic diameter of the pipe and ρ is the density of liquid. In addition, current type can be determined by gauging the Reynolds number in internal current e.g. at small Reynolds numbers, the current is laminar which means the viscous forces are large enough to deal with the inertia powers and to keep the liquid, and at large

Reynolds numbers the current is turbulent which means the inertia drives, which are commensurate with the density and the speed of the liquid, are large compared to the viscous powers, and so the viscous drives cannot prohibit the random and rapid fluctuations of the liquid [93].

For laminar flow $\mathrm{Re} \leq 2300$ (13)

For turbulent flow $\mathrm{Re} \geq 4000$ (14)

The rate of the critical Reynolds number varies for various geometries in internal current.

$\mathrm{Re} = 2300$ (15)

2.1.6.2. Prandtl Number (Pr)

The relative thickness of the speed and the thermal boundary tiers are described by the nondimensional coefficient of Prandtl number**,** which is identified as:

$$\mathrm{Pr}=\frac{\nu}{\alpha}=\frac{\mu\, C_P}{K} \quad (16)$$

It is termed after Ludwig Prandtl, who found the concept of boundary tier and remarkably contributed to the boundary layer theory. The Prandtl numbers of liquids range from less than 0.01 for liquid metals to more than 100,000 for heavy oils. Researchers note that the Prandtl number is in the order of 10 for water. The Prandtl numbers of gases are about 1, which implies that both acceleration and heat disperse through the liquid at about the same rate. Heat diffuses very quickly in liquid metals ($\mathrm{Pr} \ll 1$) and very slowly in oils ($\mathrm{Pr} \gg 1$) relative to momentum. As a result, the thermal boundary tier is quite thicker for liquid metals and much thinner for oils compared to the speed boundary tier. [94].

2.1.6.3. Nusselt Number (Nu)

The Nusselt number refers to the improvement of heat transfer via a liquid tier as a result of the convection compared to the conduction across the same liquid tier. In convection studies, it is the governing equations are common nondimensionalized and merge with the variables, which group together into nondimensional numbers so as to

diminish the sum of the variables. It is also a widespread application to render the heat transfer parameter (*h*) nondimensionalized with the Nusseltnumber [94], which is depicted as:

$$\text{Nu} = \frac{h\,D}{K} \tag{17}$$

In which *k* is the thermal conductivity of the liquid and *D* is the property diameter. The bigger the Nusselt number is, the more effective the convection becomes. A Nusseltnumber of *Nu = 1* for a liquid tier represents the heat transfer across the tier by pure conduction. There exist many equations related with the smooth radial tube in turbulent current thermohydrolic, some of which are outlined in the table 2.1.

Table 2.1. The equations that pertain for smooth circular tube in turbulent flow thermohydrolic.

Name of equation	Relation	Re-range	No. of eq.
Petukhov [96]	$Nu_D = \frac{\left(f/8\right) Re_D\, Pr}{1.07 + 12.7\left(f/8\right)^{1/2}\left(Pr^{2/3} - 1\right)}$	$0.5 \le Pr \le 2000$ $10^4 \le Re_D \le 5 \times 10^6$	(18)
Colburn [97]	$Nu_D = 0.023 {Re_D}^{0.8} Pr^{1/3}$	$0.5 \le Pr \le 3$ $10^4 < Re_d < 5 \times 10^6$	(19)
Dittus & Boelter [98]	$Nu_D = 0.023 {Re_D}^{0.8} Pr^{n}$	$0.7 < Pr < 120$ $2500 \le Re_D \le 10000$ n = 0.4 for heating n = 0.3 for cooling	(20)
Kays & Crawford [99]	$Nu_D = 0.023 {Re_D}^{0.8} Pr^{0,5}$	$0.5 < Pr \le 1$ $10^5 < Re_D < 5 \times 10^6$	(21)
Webb [2]	$Nu_D = \frac{\left(f/8\right) Re_D\, Pr}{1.07 + 9\left(f/8\right)^{1/2}(Pr - 1)Pr^{-1/4}}$	$0.5 < Pr \le 100$ $10^4 \le Re_D \le 5 \times 10^6$	(22)
Gnielinski [100]	$Nu_D = \frac{\left(f/8\right)(Re_D - 1000)\, Pr}{1.07 + 12.7\left(f/8\right)^{1/2}\left(Pr^{2/3} - 1\right)}$	$0.5 \le Pr \le 2000$ $2300 \le Re_D \le 5 \times 10^6$	(23)
Prandtl [101]	$Nu_D = \frac{\left(f/8\right) Re_D\, Pr}{1.07 + 8.7\left(f/8\right)^{1/2}\left(Pr^{2/3} - 1\right)}$	$0.5 < Pr$	(24)
Nusselt [102]	$Nu_D = 0.023 {Re_D}^{0.786} Pr^{0,45}$	$1 > Pr$ $10^3 \le Re_D \le 10^6$	(25)

2.1.6.4 Friction Factor (*f*)

Pipe current under pressure is utilized for a lot of purposes. Energy input to the gas or liquid is required in order to help it current through the pipe or conduit. This energy input is essential because there is frictional energy loss (also called Frictional Head Loss or Frictional Pressure Drop) due to the friction among the liquid and the pipe wall and internal friction within the liquid. As suggested by Cengel and Cimbala [94]. Moreover, it is the nondimensional quantity of the pressure drop which can be calculated as:

$$ƒ = \frac{2\,D\,\Delta P}{L\rho\,V^2} \tag{26}$$

For the solution of (*f*) gives the friction factor for the completely developed laminar current in a radial tube to be as:

$$ƒ = \frac{64\,\mu}{\rho\,D\,V} = \frac{64}{Re} \tag{27}$$

The friction factor in completely developed turbulent current pivots the Reynolds number and the proportional roughness (ε/D). In addition, there are a lot of equations for friction factor in smooth radial tube in turbulent current hydrodynamic some of which are presented in Table 2.2.

$$\frac{1}{\sqrt{ƒ}} = -\,2.0\log\left(\frac{\varepsilon/D}{3.7} + \frac{2.51}{Re\sqrt{ƒ}}\right) \tag{28}$$

The physical explanation for dimensionless number has been summarized in table 2.3.

Table 2.2. The equations of friction factor for smooth circular tube in turbulent flow

Name of equation	Relation	Re- range	No. of eq.
Moody [103]	$ƒ = (0.79\ln Re - 1.64)^{-2}$	$Re \le 20000$	(29)
Moody [103]	$ƒ = 0.18Re^{\frac{-1}{5}}$	$Re \ge 20000$	(30)
Petukhov [96]	$ƒ = (0.79\ln Re - 1.64)^{-2}$	$3000 \le Re \le 5\times10^6$	(31)
Gnielinski [100]	$ƒ = \frac{1}{1.82(\log(Re) - 1.64)^2}$	$2300 \le Re \le 5\times10^4$	(32)
Mc Adams [104]	$ƒ = 0.046xRe^{-0.2}$	$3\times10^4 \le \mathrm{Re} \le 10^6$	(33)
Blasius [105]	$ƒ = 0.0791Re^{-0.25}$	$4000 \le Re \le 10^5$	(34)
Nikuradse [106]	$ƒ = 0.0008 + 0.0533Re^{-0.237}$	$10^5 \le Re \le 10^7$	(35)

Table 2.3. The physical explanation for dimensionless number

Dimensionless number	Physical meaning
Nu (Nusselt number)	Dimensionless temperature distribution on the surface
Re (Reynolds number)	Ratio of inertia forces to friction forces
Pr (Prandtl number)	The ratio of momentum to heat dissipation coefficients
ƒ (Friction factor)	Dimensionless pressure drop for internal flow

2.2. Computational Domain

In this study, thermal performance of the nozzles embedded in a horizontal straight tube under stable heat flux is quantitatively investigated through a CFD program which is composed to describe nanofluid current properties in a straight radial tube in which nozzles with three pitch length (126,180 and 315 mm) are embedded and two cases as depicted in Figure 2.5. (a and b) and Figure 2.6.

The model is opted as diameter (D) and an entrance section (L1) which is considered as a 10D to provide completely developed current at the inlet of the test area. Test part (L2) is regarded as L2 and an exit section (L3) from the test section is chosen as 5D to prevent the reverse current. Boundary condition types and dimensions of the computational domain are summarized in Table 2.4 and shown in Figure 2.7

(a) The nozzles without hole. The length of the nozzle is (40 mm) and big diameter is (38 mm) and small diameter is (28mm).

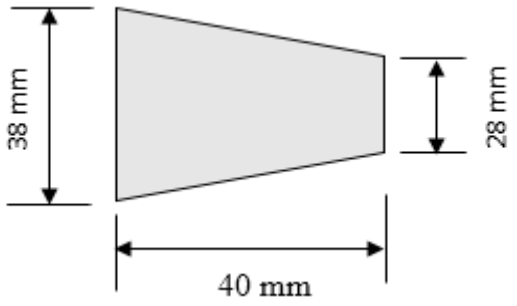


Figure 2.5. (a) Boundary condition and definition of solution domain for nozzle without hole

(b) The nozzles with circle hole. The length of the nozzle is (40 mm) and big diameter is (38 mm) and small diameter is (28mm) and diameter of circle hole is (5 mm).

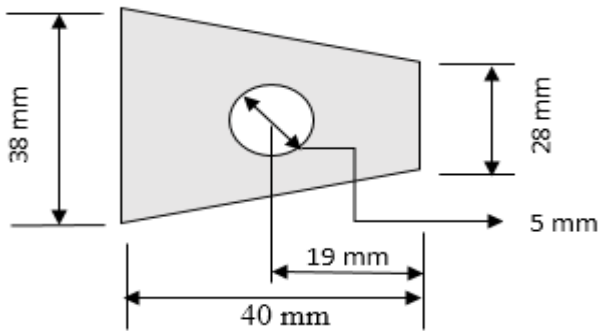


Figure 2.5. (b) Boundary condition and definition of solution domain for nozzle with circle hole

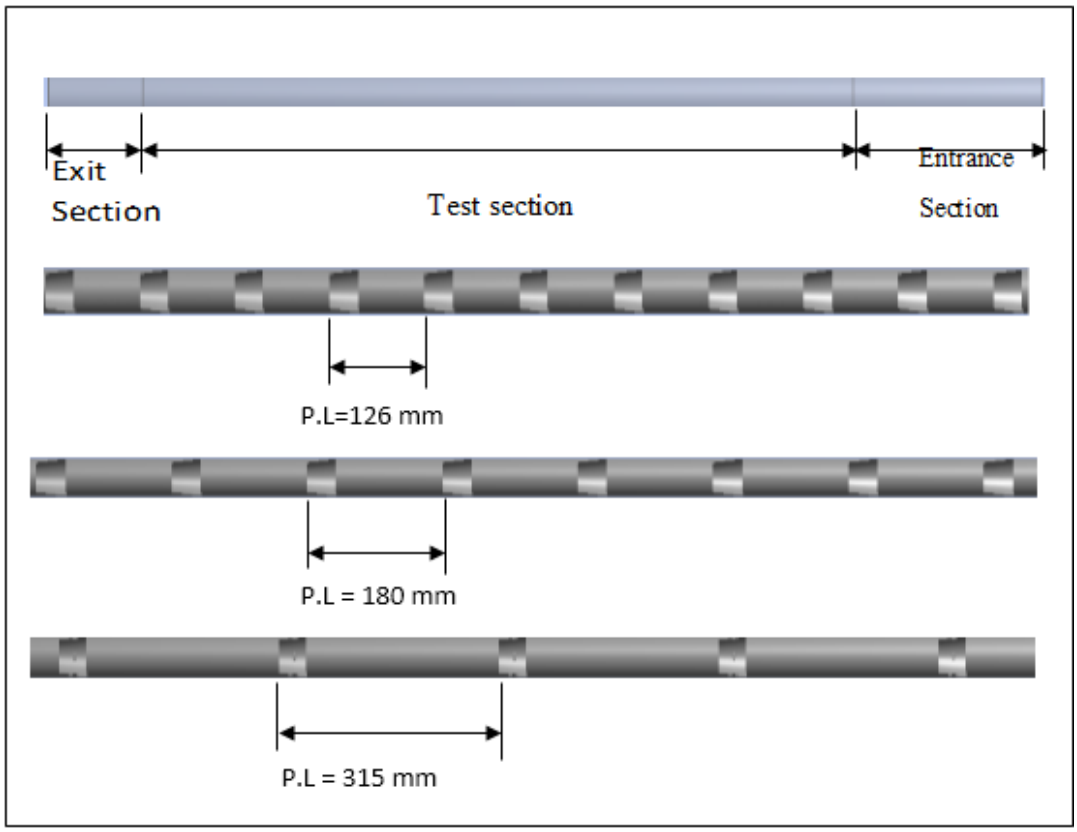


Figure 2.6. Boundary condition and definition of solution domain for nozzle inserted tube

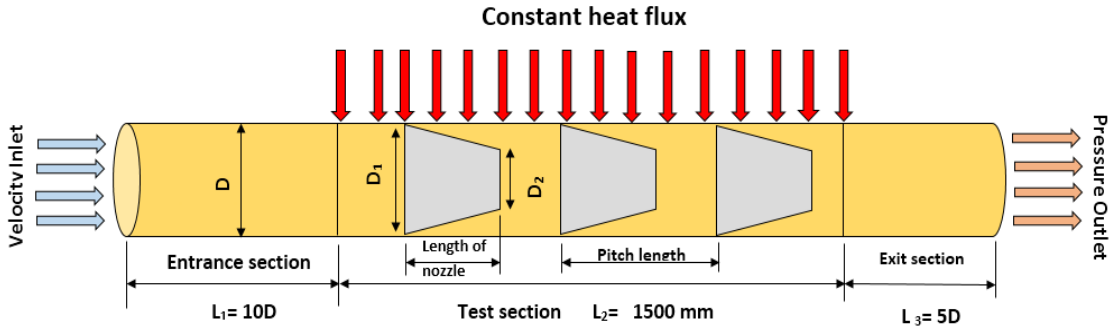


Figure 2.7. Boundary condition and definition of solution domain for nozzle inserted tube

Table 2.4. Definitions, symbols and magnitudes of the solution geometry and boundary conditions

Definition	*Symbol*	*Magnitude*
Diameter of the tube	*D*	*40 mm*
Entrance diameter of the nozzle	*D1*	*38 mm*
Exit diameter of the nozzle	*D2*	*28 mm*
Entrance Section Length	*L1*	*10 D*
Test Section Length	*L2*	*1500 mm*
Exit Section Length	*L3*	*5D*
Nozzle Length	*Ln*	*40 mm*
Diameter of circle hole	*d*	*5 mm*
Pitch Length	*P.L*	*126 – 180 – 315 mm*
Constant Heat Flux	-	50 kW/m2
Inlet Temperature	-	293 K
Inlet Velocity	-	Calculated depends on Reynolds number
Pressure Outlet	-	0 Pa

2.3. Method and Governing Equation

2.3.1. Governing Equation

The CFD program employs differential conservation equations for mass, momentum, energy and turbulent model which are utilized to solve the liquid current under the heat flux. Also, speed inlet (m/s) relies on the Reynolds numbers in a turbulent current regime. Material property data values are obtained from the online materials

information resource (ANSYS FLUENT (v14.5)). The liquid current concern is handled with the fundamental assumption given below:

1. Steady state.
2. Incompressible liquid.
3. Newtonian liquid.
4. Turbulent current.
5. Three dimensional

2.3.1.1. Conservation of mass equation [107]:

This can be expressed mathematically for an incompressible fluid as follows:

$$\frac{\partial \rho}{\partial t} + \nabla.(\rho u) = 0 \quad (36)$$

2.3.1.2. Conservation of momentum equation [107]:

The momentum equations that run the flow of incompressible fluid take the form:

$$\frac{\partial}{\partial t}(\rho \vec{v}) + \nabla(\rho \vec{v}\vec{v}) = -\nabla P + \nabla(\bar{\bar{\tau}}) + \rho \vec{g} + \vec{F} \quad (37)$$

2.3.1.3. Energy equation [107]:

The equation below refers to the transport of heat within the flow field:

$$\frac{\partial}{\partial t}(\rho E) + \nabla\big(\vec{v}(\rho E + p)\big) = \nabla\big(k_{eff}\nabla T - \sum_j h_j \vec{J}_i + (\bar{\bar{\tau}}_{eff}.\vec{v})\big) + S_h \quad (38)$$

2.3.2. Determining of the Numerical Methodology

In order to assure the validation of the quantitative techniqueology, especially including the liquid mechanics, concerns of the turbulence model should be determined, and experimental results or empirical correlations can be utilized for the comparison of quantitative results. In this context, varied turbulence models are tested with reference results for the validation of the quantitative study for smooth tube and water of Nusselt number and friction factor, respectively as well as the mesh independence for smooth tube and nozzle and property of nanofluid.

2.3.2.1. Determining of the Water Analyses

2.3.2.1.1. Turbulence Models (smooth tube)

Turbulence models are computational procedures to close the system of mean current equations and employed in Computational Liquid Dynamics to involve the effect of turbulence and simulate the mean current characteristics. The closed mean current equations are used to estimate the turbulent transport of mass, momentum, and heat between the tiers. The prediction of the eddy viscosity distribution along the current field is a fundamental in order to measure the parameters of momentum and heat diffusion in the closed mean current equations.

As the exact prediction of reverse pressure gradient boundary tier currents is crucial for a turbulence model. The κ–w standard model was chosen in the present study as can be seen in Figure 2.8 (a and b). The model provides superior performance for complex currents including recirculation, rotation, separation, boundary tiers under strong adverse pressure gradients, and strong streamline curvature. Also, a second-order upwind scheme was employed for energy and momentum equations. Pressure and speed were paired by using SIMPLEC coupling scheme. Simulations were considered as converged by assuming the convergence criteria of 10^{-7} for energy residual and 10^{-4} for other residual criteria. The turbulent current was limited in 4000 to 14,000 range of Reynolds number.

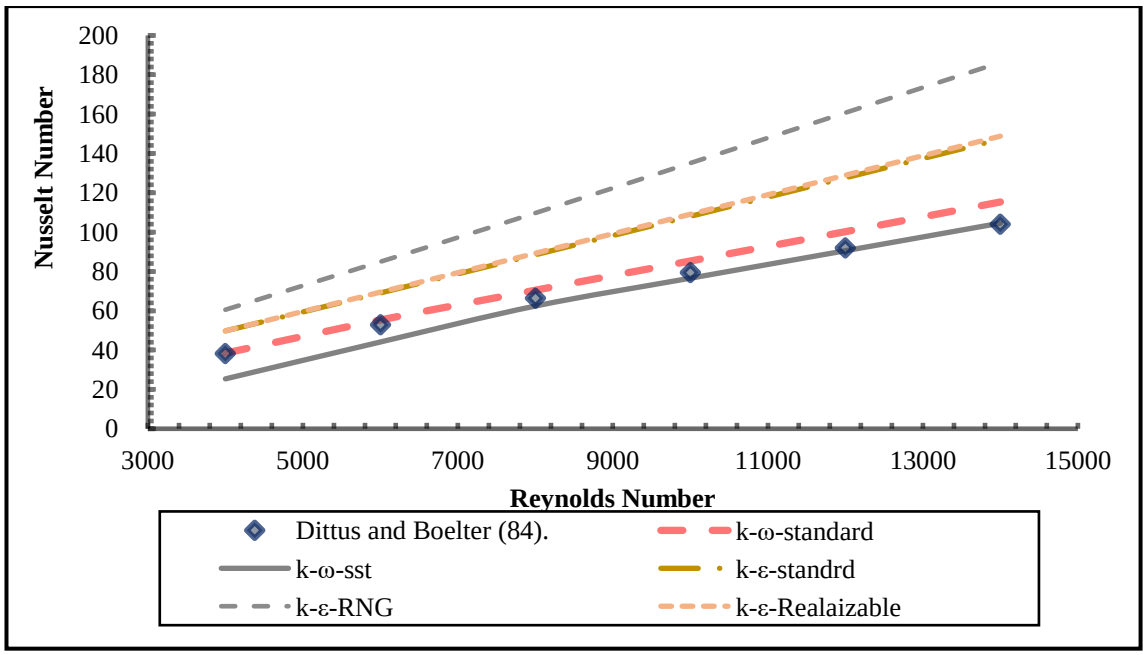


Figure 2.8. (a) Comparison of a turbulence model with the effect of Reynolds number and Nusselt number.

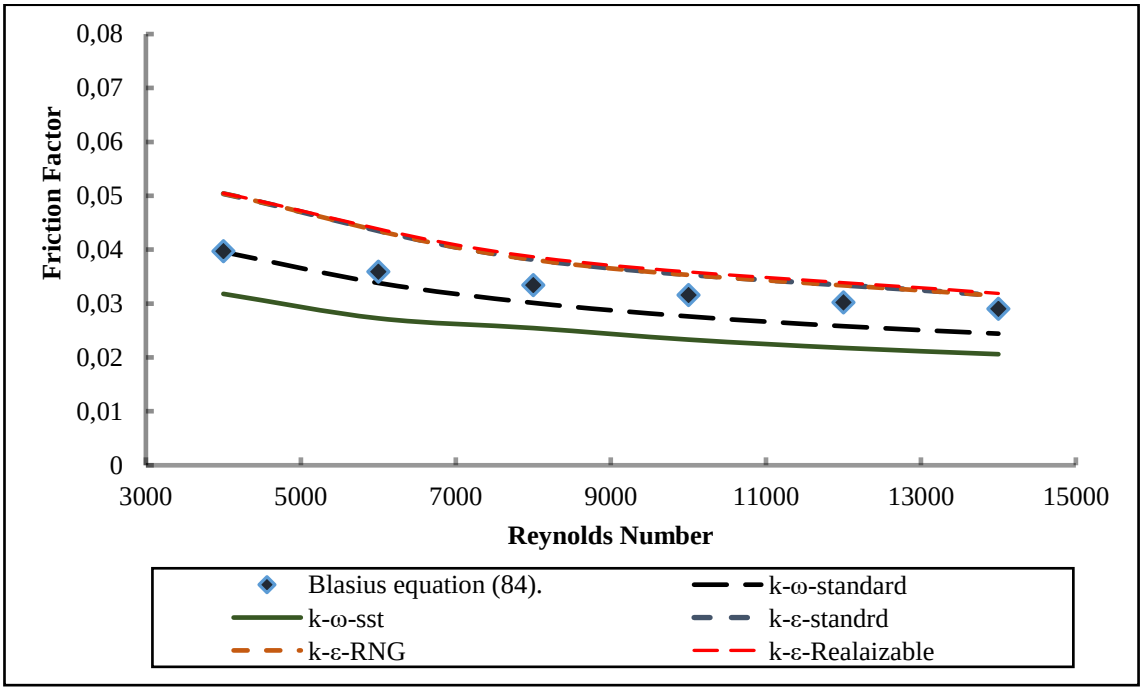


Figure 2.8. (b) Comparison of a turbulence model with the effect of Reynolds number and fraction factor.

2.3.2.1.2. Mesh Independence

That generated mesh fits the limits of the computational domain being studied. It is impractical to find a single general mesh generation technique that fits the whole range of concerns. Thus, it is rather favored to employ an appropriate technique that is best adjusted to the type of engineering application in mind.

There are two sorts of volume meshing approaches commonly used in CFD: structured and unstructured. The structured mesh is exorbitantly inefficient and spends more time producing the mesh compared to unstructured mesh for complex geometries. Hence, it has been eliminated from this research as the geometry being considered complex and contains many details.

As for the unstructured approach, automated grid generation allows much less effort by the user to define the mesh and in general effective for complex geometries. However, the tetrahedral elements of these grids do not twist or stretch well for complex shapes, and this will have serious impacts on the accuracy of the results. Moreover, post processing requires a bigger amount of operation power to obtain the results.

There are several kinds of mesh one of which is an automatic cell agglomeration algorithm in (Ansys) Fluent Software as seen in Figure 2.9 (a and b) and the other one is also converted in Figure 2.9 (c). which is opted in the present study, Polyhedral cells generally allow rapid convergence with less iteration, sound convergence with lower residual values, and faster solution runtimes than other mesh types by providing the equivalent accuracy of computational results.

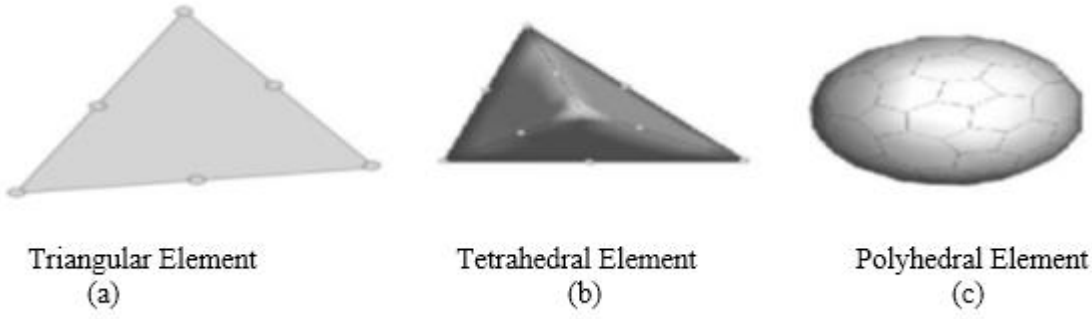


Figure 2.9. Element types (a) Triangular, (b) Tetrahedral, and (c) Polyhedral [108].

The mesh generation can be categorized into following steps including two major issues for further controlling of the mesh:

1. Facet mesh generation.

2. Volume mesh generation.

The mesh structure near the wall was designed finer than the rest of the tube. Application of the boundary tier mesh is significant for boundary tier current analysis as there is a necessity of a thin and intense mesh in areas adjacent to the wall facet. It is mainly utilized to regulate the mesh size distribution and, thereby, to manage the amount of computational information received from the computing areas of interest.

As there are speed, pressure and temperature fluctuations near the walls and the fine mesh distribution for smooth tube and nozzle, it is vital to assess this mesh for quality and dependency before running to assure that solid results can be successfully obtained. There are some general guidelines to form a robust mesh such as quality, resolution, and total count of the cells. A robust mesh should be strong enough with high quality and good distribution. Furthermore, the mesh should not contain more cells than the

available computer resources can deal with. Similar boundary conditions and mesh strategy have been adopted for all the models nozzle embedded and nanofluid types in this study as illustrated in Figure 2.10.

Grid independence was checked by six different grid structures with cell numbers of 2.9, 3.2, 3.7, 4.1, 4.7 and 5.3 million respectively. Each grid case with the pitch length of 126 mm was designed with the same mesh topology as outlined in Figure 2.11. The study revealed that the solution is grid-independent case with over 4.1 million grid cells, where the predicted Nusselt number is almost the same as the predicted value from the 4.7 million grid cells.

Regarding the pitch length of 180 mm, grid independence was also checked by using six different grid structures with cell numbers of 2.5, 2.8, 3.5, 3.8, 4.2 and 4.6 million. The predicted Nusselt number is also almost the same as the predicted value from 4.2 million. In addition, grid independence of pitch length 315 mm was checked by using six different grid structures with cell numbers of (2.5, 2.8, 3.5, 3.8, 4.2 and 4.6) million as well. The predicted Nusselt number is nearly to the same as the predicted value from 4.2 million.

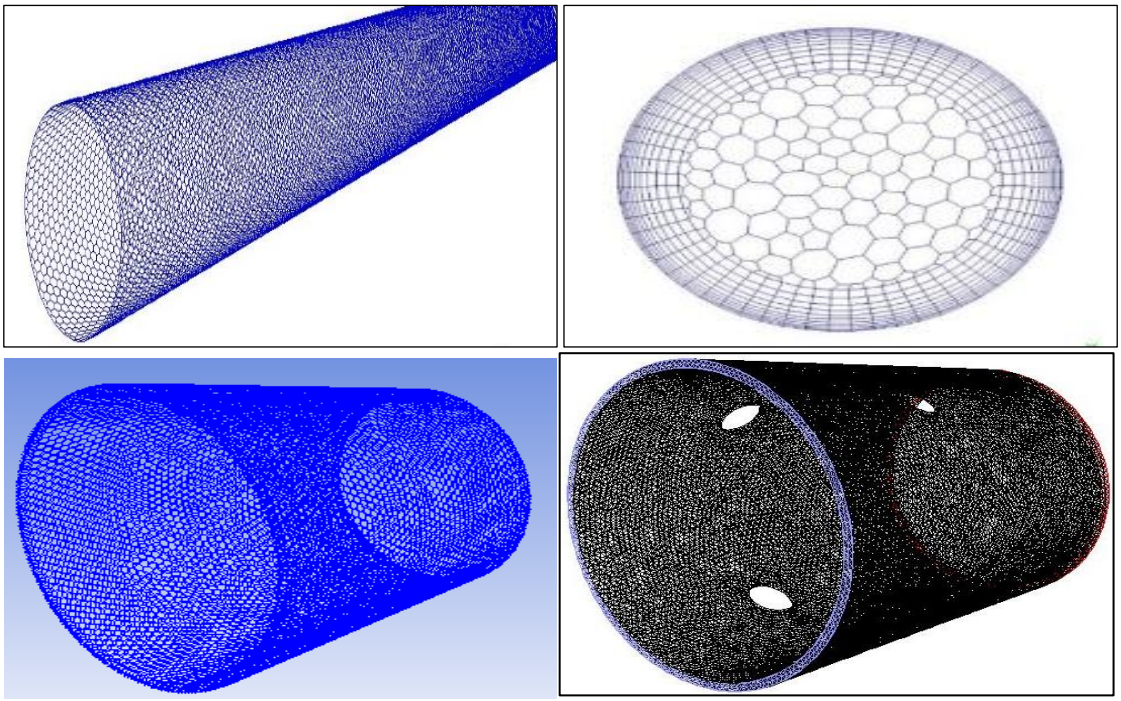


Figure 2.10. Mesh sizes for the grid independence study of the tube and inserted nozzle.

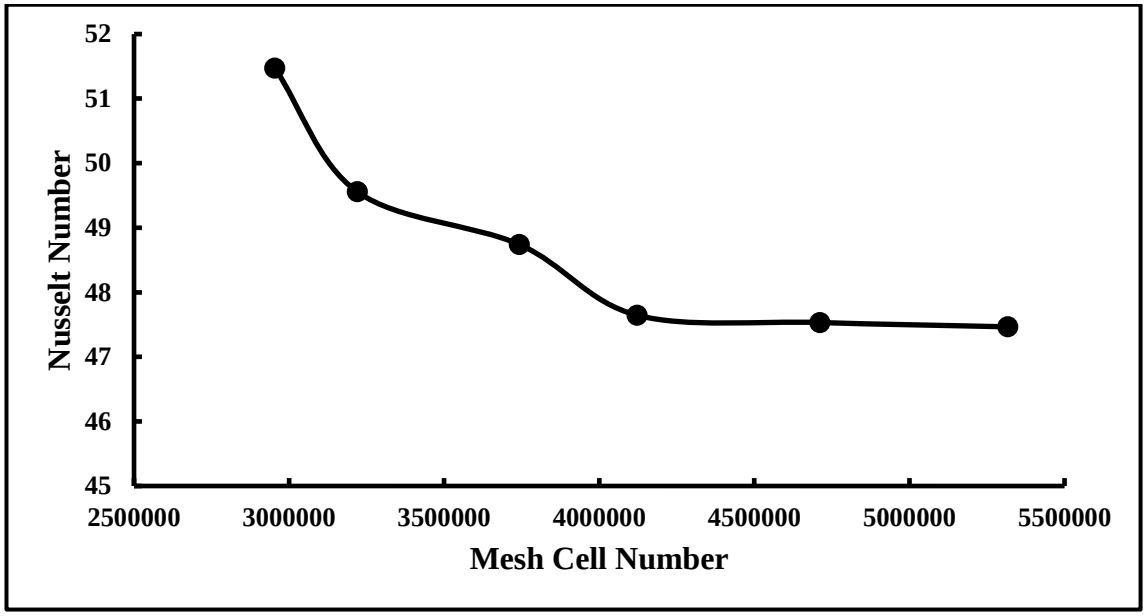


Figure 2.11. Grid independence study for the simulation of nozzle inserted tube

2.3.2.2 Validation of Nanofluid Analyses

2.3.2.2.1. Property of Nanofluid (Thermo- physical properties)

In the present study, the thermos-physical characteristics (density, specific heat, viscosity and thermal conductivity) of nanofluid are considered as a function of nanoparticles' volume density (φ) and two-stage models considering the granules and base liquid. For all the cases, nanoparticles and base liquid are regarded as incompressible liquids.

2.3.2.2.1.1. Density

Density prediction does not necessitate complex correlations or models as it's the effect on the heat transfer performance of nanofluids. It can be calculated by general formula for mixing theory [109] presented below:

$$\rho_{nf} = (1-\varphi)\rho_{water} + \varphi\rho_{np} \quad (39)$$

In which ρ represents the density,φ represents the volumetric fraction of the nanoparticles in nanofluid.

2.3.2.2.1.2. Specific Heat

Specific heat is a dioristic marker for heat transfer applications because effective heat transfer requires high heat carrying capacity. The same weighted fraction technique is commonly used in the calculation of specific heat of nanofluids as proposed by Bock et al. [57], as with density, yet there is an ongoing debate on this technique:

$$Cp_{nf} = \varphi Cp_{np} + (1-\varphi)Cp_{water} \quad (40)$$

However, that Equation (40) is the unit of the specific heat considered (e.g. J/kg·K). This feature is on per unit mass and must be calculated based on this consideration. A mass-based weighted fraction technique (thermal equilibrium model) gives another equation as (41) which is more consistent with the experimental results [110].

$$C_{nf} = \frac{\varphi(\rho c)_p + (1-\varphi)(\rho c)_f}{\rho_{nf}} \quad (41)$$

2.3.2.2.1.3. Viscosity

Most current applications need low viscosity liquids as low viscosity means low pumping power to move the liquid. In heat transfer applications, transportation of liquid also needs an additional pumping power for active systems. During nanofluid heat transfer in convective systems, viscosity of nanofluids may raise the need for pumping power of the system while increasing the heat transfer. In nanofluid current, viscosity relies on several factors such as nanoparticle density, type, size, shape, base liquid type, and pH value of the nanofluid. The viscosity of nanofluid can be measured by Einstein's equation. Drew and Passman [111] suggested the following equation.

$$\mu_{nf} = (1 + 2.5\varphi)\mu_{water} \quad (42)$$

2.3.2.2.1.4. Thermal Conductivity

Nanofluid heat transfer enhancement idea emerges from their higher thermal conductivity. Thus, thermos-physical properties and especially the thermal conductivity is a crucial issue in nanofluid heat transfer phenomena. The goal is to keep it as high as possible while providing a practical, long term heat transfer capability. In fact, the first issue is to attain a sound heat transfer liquid which has a high thermal conductivity. The

second concern is to estimate the conductivity accurately. In general, the previous researches focused on determining the influential parameters first and then obtaining a theoretical or an empirical model for nanofluid heat transfer.

Maxwell [21] introduced a thermal conductivity model for conventional suspensions with spherical non-nano sized granules. The interaction between the granules is ignored; hence, the importance of the shape of the granules is not taken into consideration. The model is described below:

$$\frac{k_{nf}}{k_w} = \frac{k_{np}+2k_w+2\varphi(k_{np}-k_w)}{k_{np}+2k_w-\varphi(k_{np}-k_w)} \quad (43)$$

Timofeeva et al. [112] introduced the influential medium theory for calculating the thermal transmission of nanofluids, which is identified as follows:

$$K_{nf} = (1+3\varphi)K_{water} \quad (44)$$

Table 2.5. Thermo-physical properties of water –TiO_2nanofluid

Φ	ρ_{nf}[kg/m^3]	k_{nf}[W/mK]	Cp_{nf} [j/kg/K]	μ_{nf} [kg/ms] x (10^{-3})
0 %	998.20	0.598	4182.00	1.002
0.2 %	1004.34	0.601	4175.02	1.008
0.6 %	1017.03	0.608	4161.05	1.018
1.0 %	1029.72	0.615	4147.08	1.028
1.5 %	1045.58	0.624	4129.62	1.040
2.0 %	1061.44	0.633	4112.16	1.053

2.3.2.3. Thermal Performance Factor

A beneficial comparison between reverse and straight currents can be made by comparing heat transfer parameters at equal pumping power, as this is relevant to the operation expense. For constant pumping power, Eiamsa et al. [84] suggested the following equation:

$$(\dot{V}\Delta P)_P = (\dot{V}\Delta P)_t \quad (45)$$

And the relation between friction factor and Reynolds number can be put as:

$$(f\,Re^3)_P = (fRe^3)_t \quad (46)$$

The enhancement sufficiency (η_e) at constant pumping power is the proportion of the convective heat transfer parameter of the tube with nozzles turbulators to the plain tube which can be formulated as follows:

$$\eta_e = \frac{h_t}{h_p}\Big|_{pp} \quad (47)$$

CHAPTER 3

RESULTS AND DISCUSSION

In this chapter, computational results obtained by Ansys.14.5 Fluent software are presented and discussed. It includes the tests' results of distilled water, the nanofluid mixture and distilled water with nanofluid densities (0.2%, 0.6%, 1%, 1.5% and 2%) for TiO_2–water nanofluid percent by volume in a plain tube. Two cases are used as well as the plain tube one is a nozzle embedded tube without hole and the second is a nozzle embedded tube with circle hole with pitch length of 126mm, 180mm and 315mm. All the above tests' results were obtained under fully developed turbulent conditions with ranging Reynolds numbers (4000-14000) and regular heat flux (50 kw/m^2). The current was investigated to observe the heat transfer performance and the pressure drop characteristics of these configurations.

3.1. Validation

3.1.1. Validation of Water flow:

Firstly, the convective heat transfer and friction factor results of the present plain tube (the tube without nozzle inserts) for water are validated by comparing the present convective heat transfer and friction with those obtained from the standard correlations. The convective heat transfer and the friction factor are utilized to validate the quantitative study by comparing the correlations in the literature in terms of thermal and hydraulic, respectively.

3.1.1.1. Convective Heat Transfer

The Nusselt number results of the quantitative analyses are compared with the Dittus-Boelter equation (48), which is presented below:

$$Nu = 0.023 Re^{0.8} Pr^{0.4} \quad (48)$$

The comparison of the present study (smooth tube through water flow) with Dittus-Boelter equation in terms of the Nusselt number is illustrated in Figure 3.1. As can be seen in this figure, a neat agreement is reached with the literature for the present study which is smooth tube through water flow. The Nusselt number is close to the references with maximum ±2 errors.

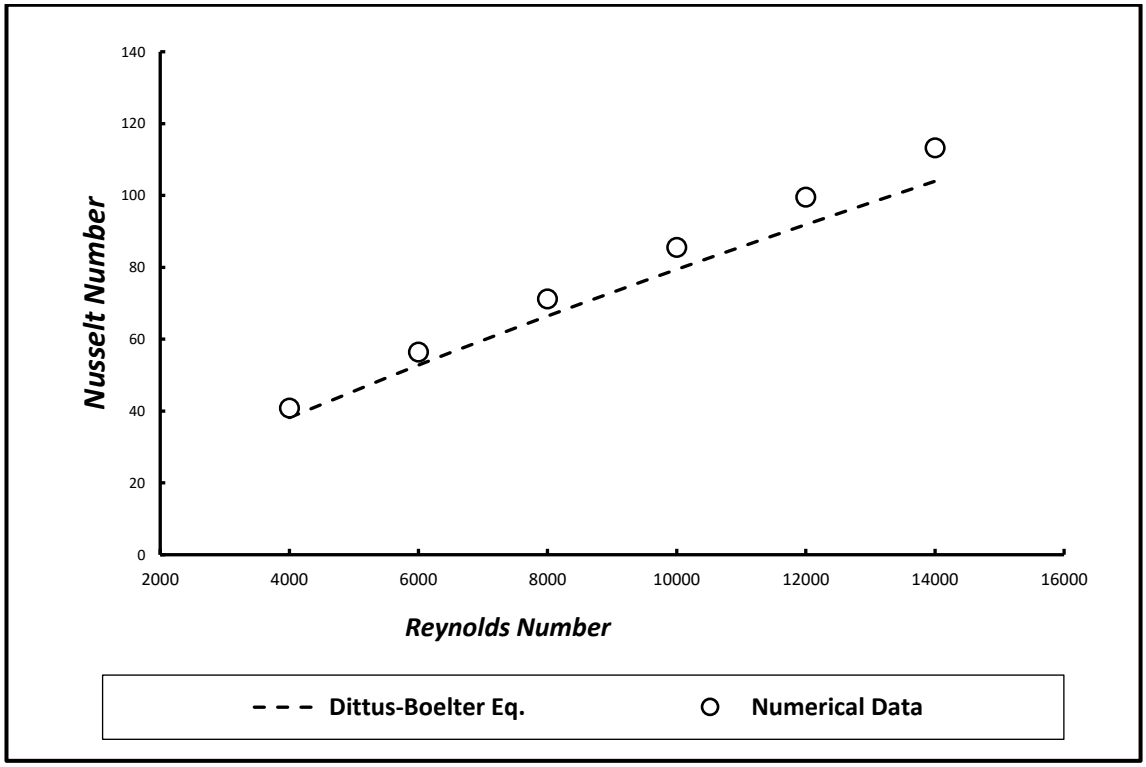


Figure 3.1. Comparison of quantitative results with Dittus-Boelter Equation in terms of Nusselt number versus Reynolds number

3.1.1.2. Friction Factor

The friction factor results of the present study is compared with Blasius equation (49) given in Figure 3.2. As can be clearly seen in the figure, there is a neat consensus between the literature and this study regarding smooth tube through water flow. The friction factor results are close to the references with maximum ±4 errors.

$$f = 0.316Re^{-0.25} \tag{49}$$

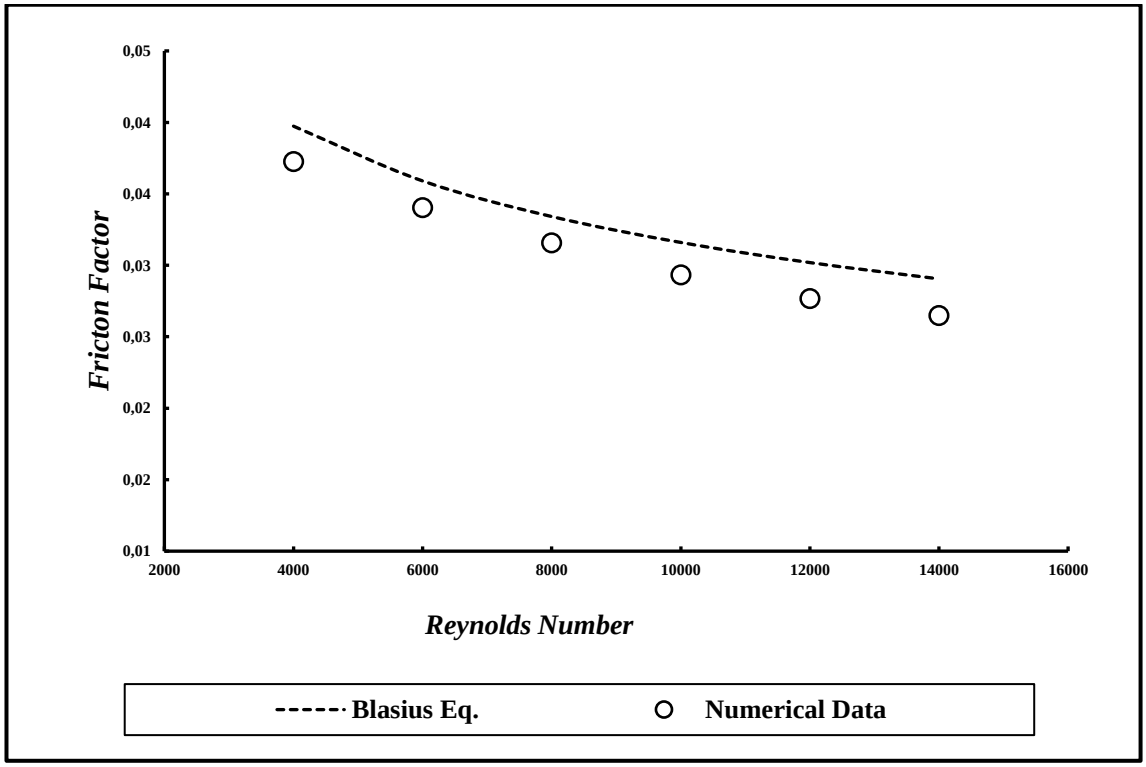


Figure 3.2. Comparison of quantitative results with Blasius Equation in terms of Friction factor versus Reynolds number

3.1.2. Validation of nanofluid flow

The flow changes as nanofluid in the study, it has to ensure the nanofluid flow agreement in literature. Figures from 3.3 to 3.8 depict the agreement between nanofluid flow and the studies by Pak and Cho equation (50), Duangthongsuk and Wongwises equation (51), Sajadi & Kazemi (52) and Duangthongsuk and Wongwises (54) with regard to the Nusselt number and the friction factor. The Nusselt number and the friction factor results are close to the references with maximum ±2 and ±5 errors.

$$Nu_{nf} = 0.021 Re_{nf}^{0.8} Pr_{nf}^{0.5} \quad (50)$$

$$Nu_{nf} = 0.074 Re_{nf}^{0.707} Pr_{nf}^{0.385} \varphi^{0.074} \quad (51)$$

$$Nu_{nf} = 0.067 Re_{nf}^{0.71} Pr_{nf}^{0.35} + 0.0005 Re \quad (52)$$

$$f = 0.961 \varphi^{0.052} Re^{-0.375} \quad (53)$$

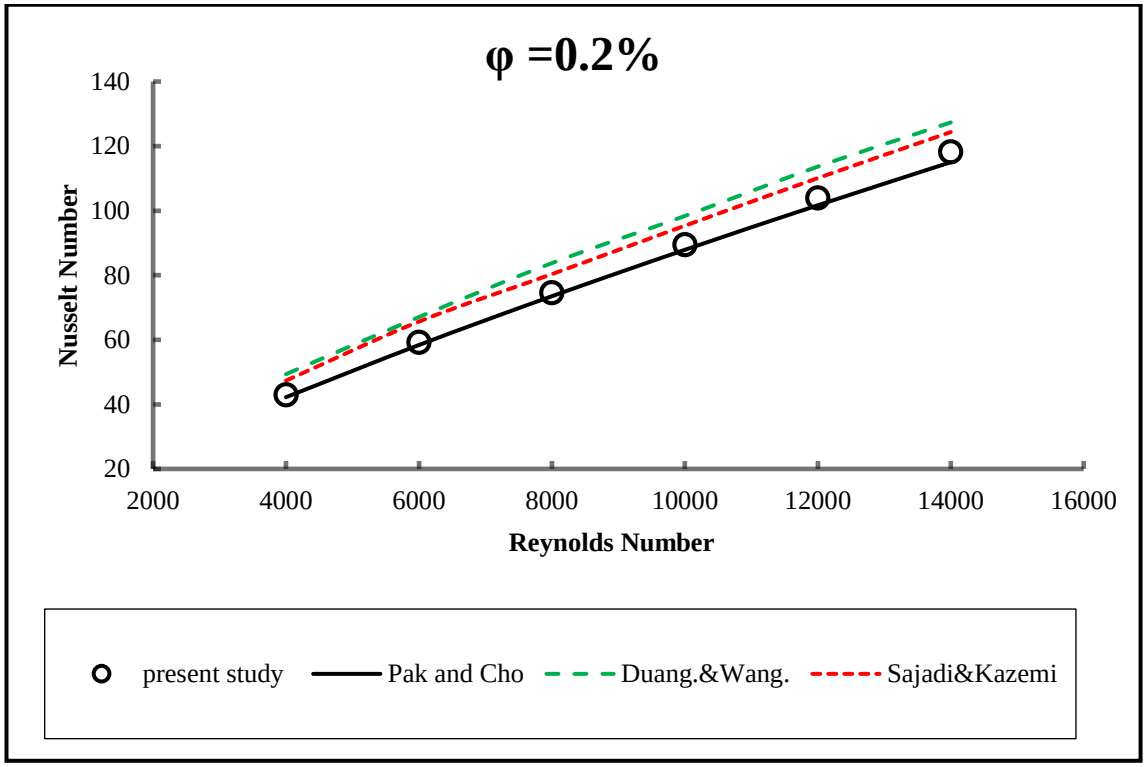


Figure 3.3. Validation of nanofluid study in terms of Nusselt number versus Reynolds number in correlation with Pak and Cho, Duangthongsuk & Wongwises and Sajadi & Kazemi at 0.2% TiO2/water nanofluid.

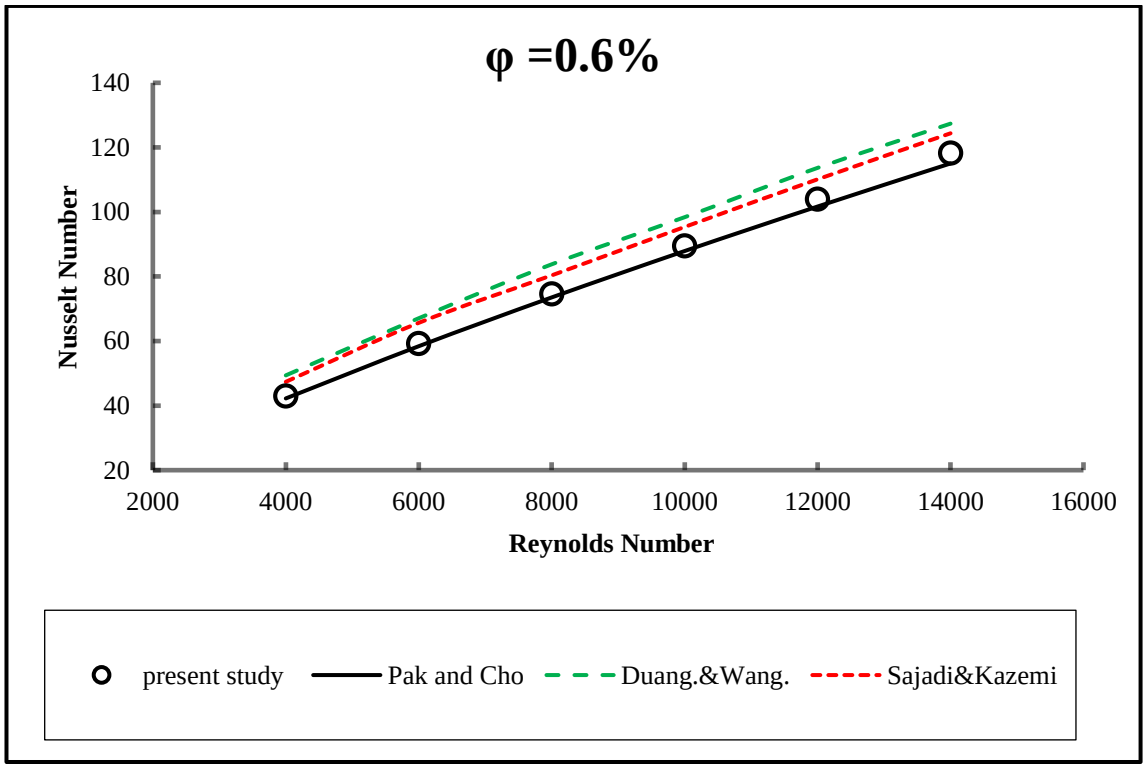


Figure 3.4. Validation of nanofluid study in terms of Nusselt number versus Reynolds number in correlation with Pak and Cho, Duangthongsuk & Wongwises and Sajadi & Kazemi at 0.6% TiO2/water nanofluid.

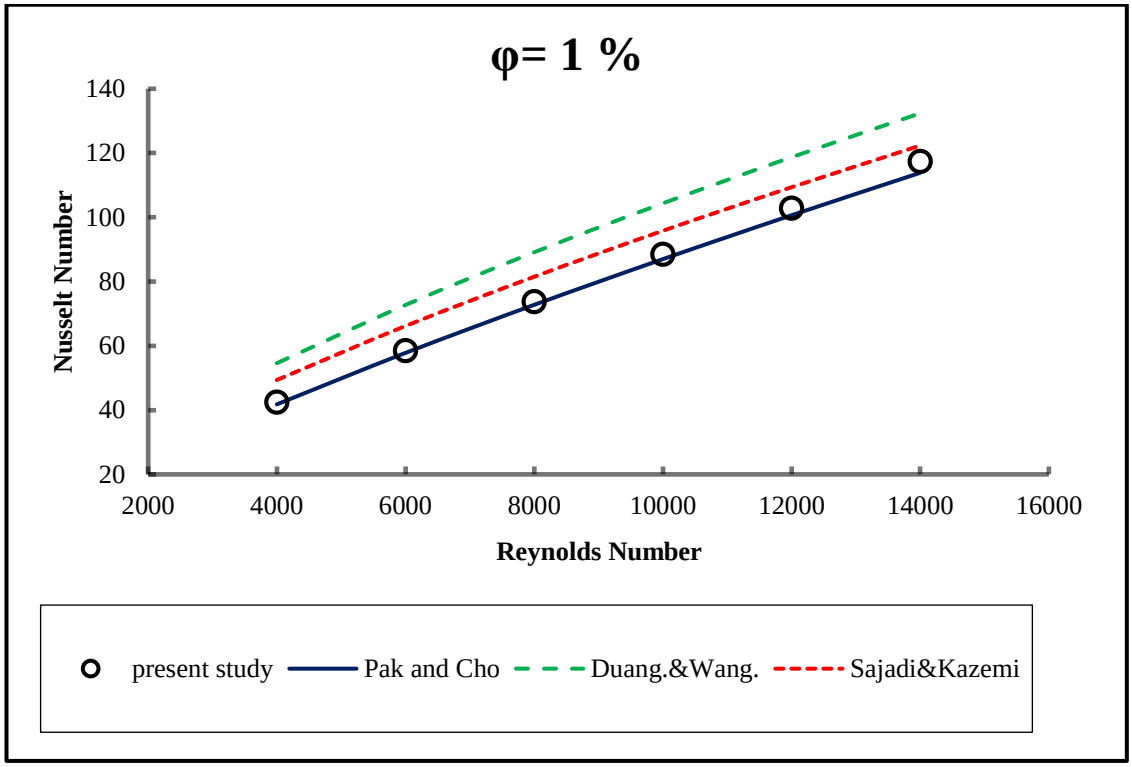


Figure 3.5. Validation of nanofluid study in terms of Nusselt number versus Reynolds number in correlation with Pak and Cho, Duangthongsuk & Wongwises and Sajadi & Kazemi at 1 % TiO2/water nanofluid.

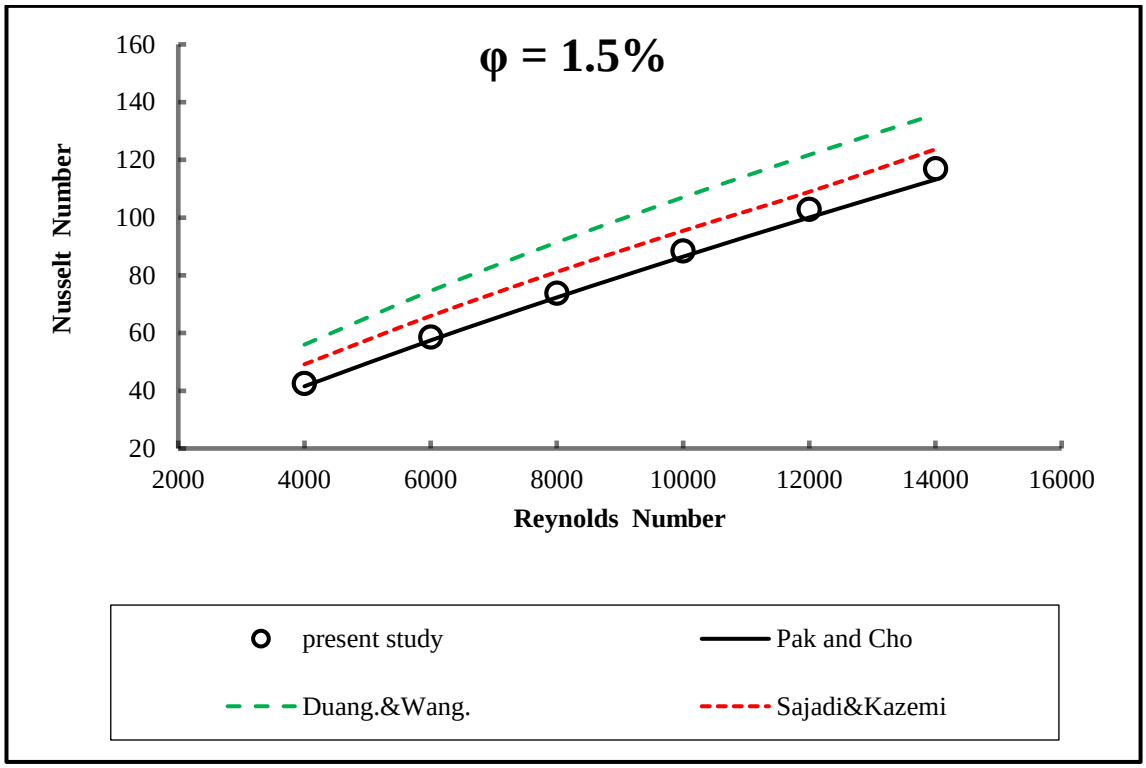


Figure 3.6. Validation of nanofluid study in terms of Nusselt number versus Reynolds number in correlation with Pak and Cho, Duangthongsuk & Wongwises and Sajadi & Kazemi at 1.5 % TiO2/water nanofluid.

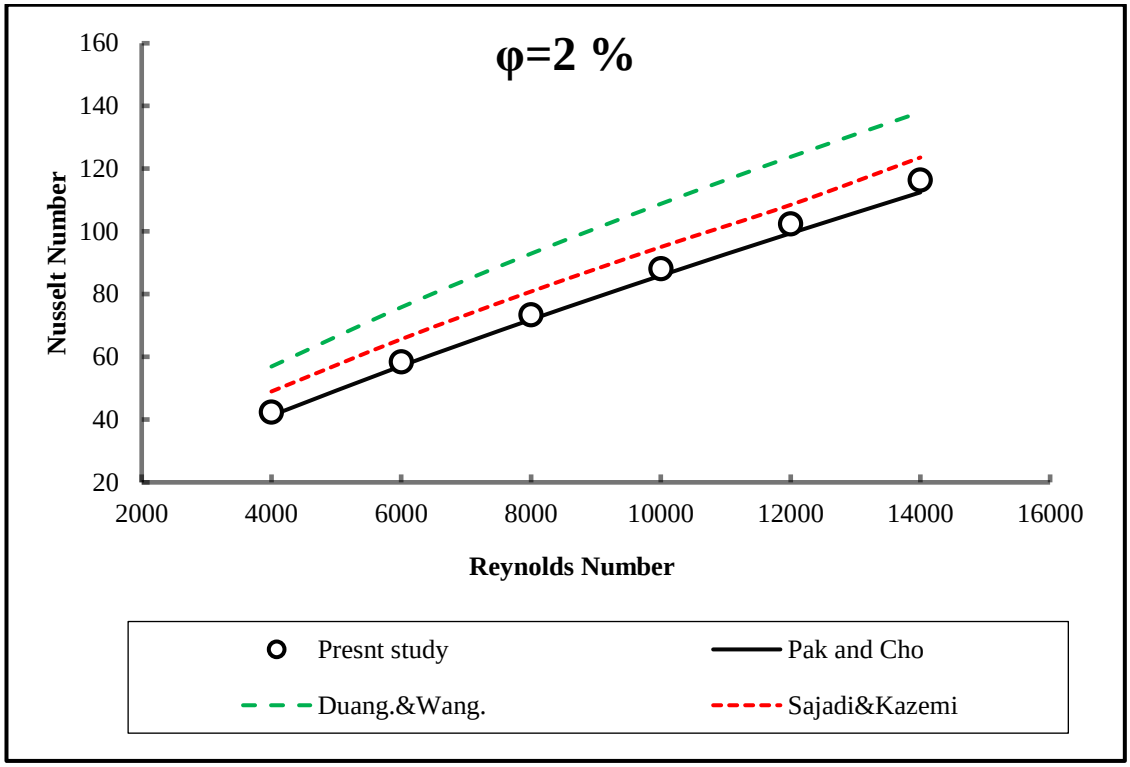


Figure 3.7. Validation of nanofluid study in terms of Nusselt number versus Reynolds number in correlation with Pak and Cho, Duangthongsuk & Wongwises and Sajadi & Kazemi at 2 % TiO2/water nanofluid.

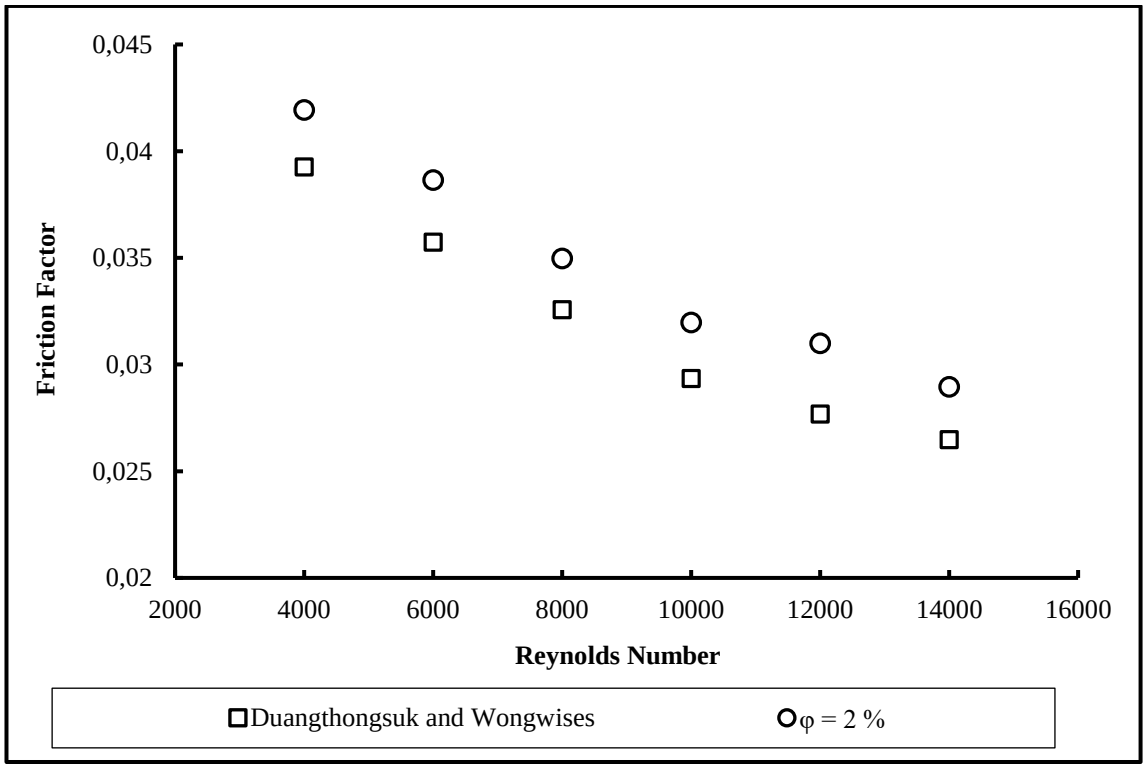


Figure 3.8. Comparison of friction factor between the quantitative data and the reckoned values from correlation and Duangthongsuk and Wongwises.

3.1.3. Comparison between water and nanofluid flow in smooth tube

3.1.3.1. Convective Heat Transfer

The connective heat transfer in terms of Nusselt number of the nanofluid is higher than those of the base liquid, and they rise with increasing Reynolds number and decreasing with rising volume density of TiO2/ water nanofluid. As shown in Figure 3.9, this act may be stemmed from the fact that the nanoparticles presented in the base liquid raise the thermal conductivity and the viscosity of the base liquid at the same time, and rise with the increasing granule densities. The rise of the thermal conductivity renders a rise in the heat transfer performance whereas the rise of the viscosity of the liquid raises the boundary tier thickness. In addition, the Nusselt number decreases with the increase in the volume friction because the conduction heat transfer gather than convection heat transfer.

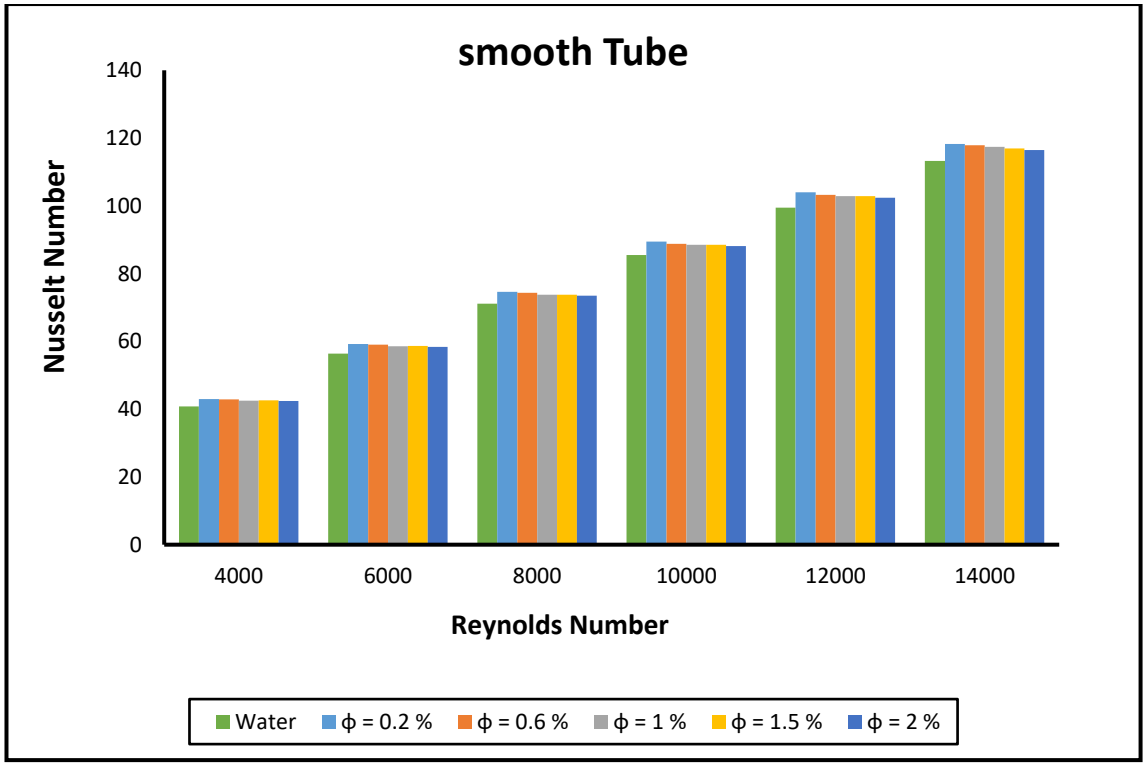


Figure 3.9. Comparison of Nusselt Number and Reynolds Number for the nanofluid and water for smooth tube

3.1.3.2. Friction Factor

In order to employ the nanofluids in practical applications well as the heat transfer activity of the nanofluids, it is essential to investigate their current characteristics. This study exploited nanofluid with 0.2, 0.6, 1.0, 1.5 and 2.0 vol. % suspended nanoparticles in the pressure decrease test under the turbulent current condition corresponding to the convective heat transfer parameter of nanofluids. As shown in Figure 3.10, the results indicate that the pressure drop and friction factor of the nanofluids rise with the increasing Reynolds number and that there is a minor rise with the increasing granule densities. Increment of volume fraction of TiO_2 in water increases the pressure drop penalty, main reason of which is that rise of the density and viscosity of the nanofluid.

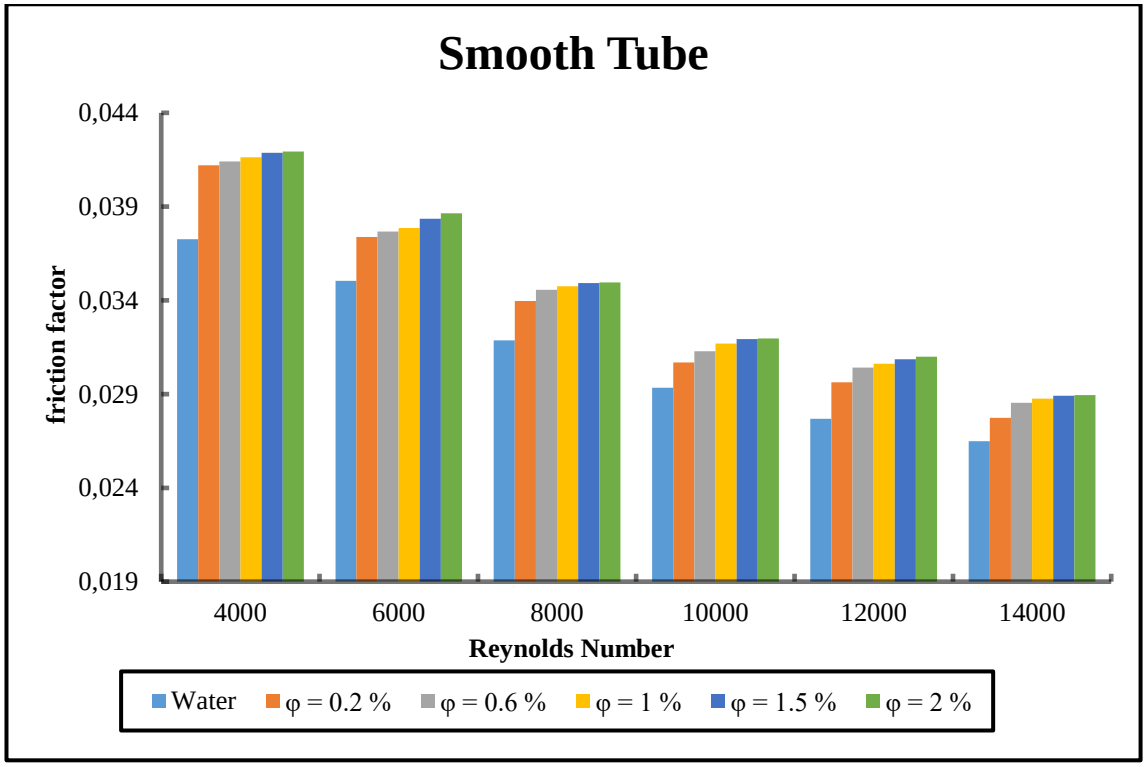


Figure 3.10. Comparison of Friction Factor and Reynolds Number for nanofluid and water

3.1.3.3. Performance Enhancement Factor

A third parameter should be regarded which can relate heat transfer to pressure drop and provide the conditions for the comparison of these two parameters. To this end, the performance enhancement factor and the effect of TiO2/water concentration on thermal performance factor of nanofluid with the volume friction (0.2%, 0.6%, 1%, 1.5% and 2%) were higher than that of the base fluid and increase the thermal performance factor with rises in the volume friction .The maximum thermal performance factor of the nanofluid in the volume friction (2%) is 1.089 at Reynolds Number (14000) which is presented in Figure 3.11 below.

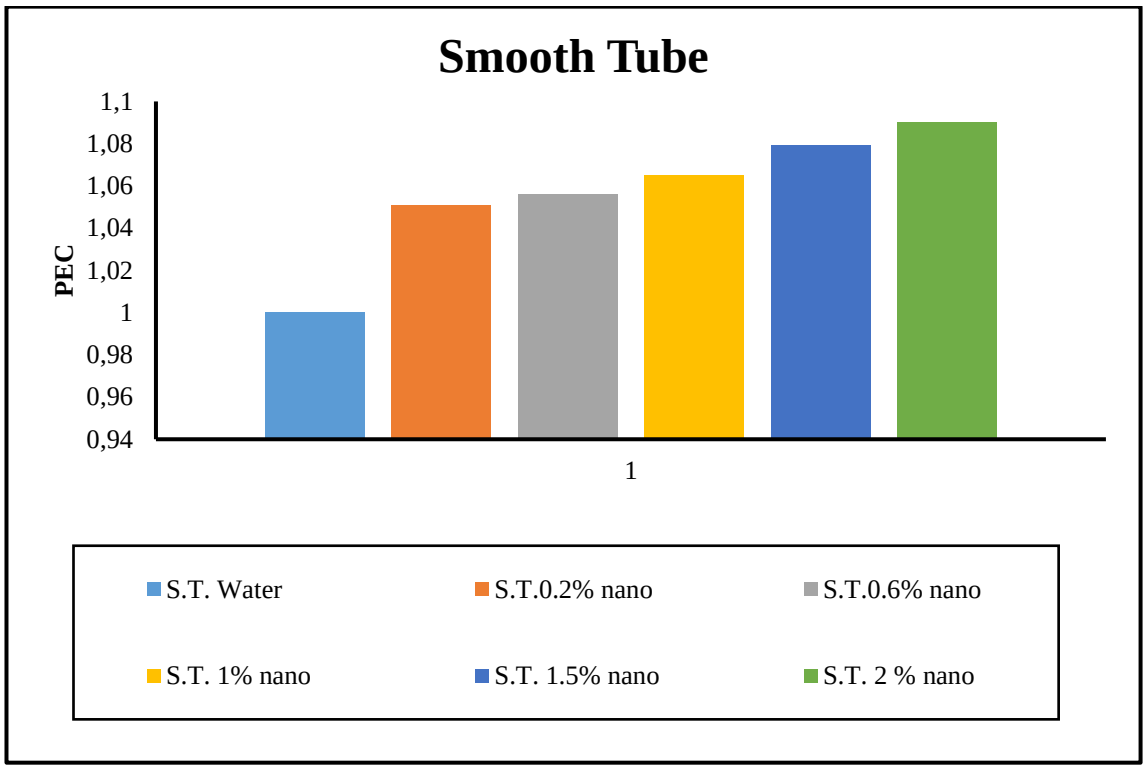


Figure 3.11. Effect of nanofluid on smooth tube on thermal performance factor

3.2. Non drilled nozzle inserted-Smooth tube

3.2.1. Water flow

3.2.1.1. Convective Heat Transfer

The results revealed that water flow in the tube and inserting non-drilled nozzle in tube and comparison with smooth tube increase the convective heat transfer coefficient with the rises in Reynolds number and decrease with the increases of pitch length as shown in Figure 3.12 and outlined by the results in an improvement of the heat transfer rate over the smooth tube for water flow. Therefore, in all cases of nozzle inserts, the reverse flow renders higher values of the heat transfer coefficient than that of fully developed axial flow as depicted in Figure 3.12. The rise in the heat transfer rate with diminishing pitch ratio is resulted from the higher turbulent intensity imparted to the flow between the non-drilled nozzles.

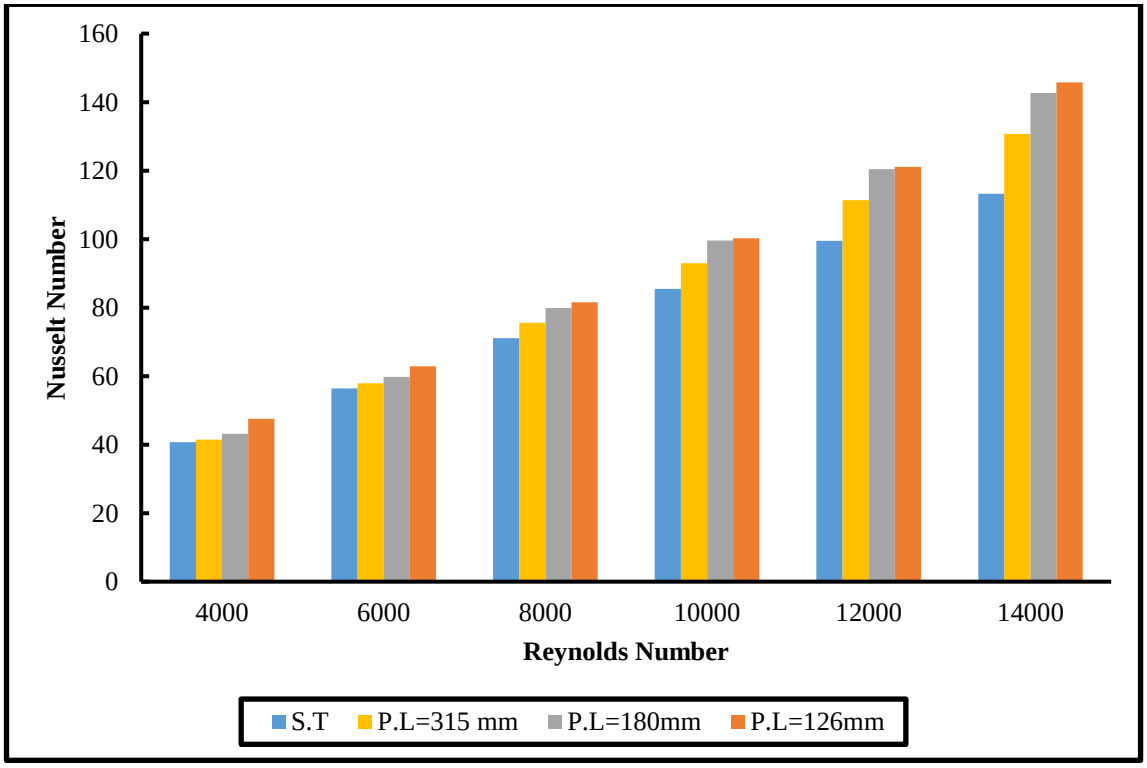


Figure 3.12. Comparison of convective heat transfer coefficient and Reynolds Number for the water between smooth tube and inserted nozzle at varying pitch lengths (126mm, 180mm and 315mm)

3.2.1.2. Friction factor

The variation of the friction factor in across the test section as a function of Reynolds number is summarized in Figure 3.13. It can be understood that the friction factor obtained from three different pitch lengths and comparison go hand in hand and rise with the increasing Reynolds number and decreases with increasing pitch length of non-drilled nozzle with reverse/turbulent current for three different pitch lengths. In general, it is much higher than that with axial current. This is stemmed from the dissipation of dynamic pressure of the liquid due to the higher facet area and the act caused by the reverse current. Moreover, the friction factor is quite likely to occur by the interaction of the pressure drives with inertial drives in the boundary tier.

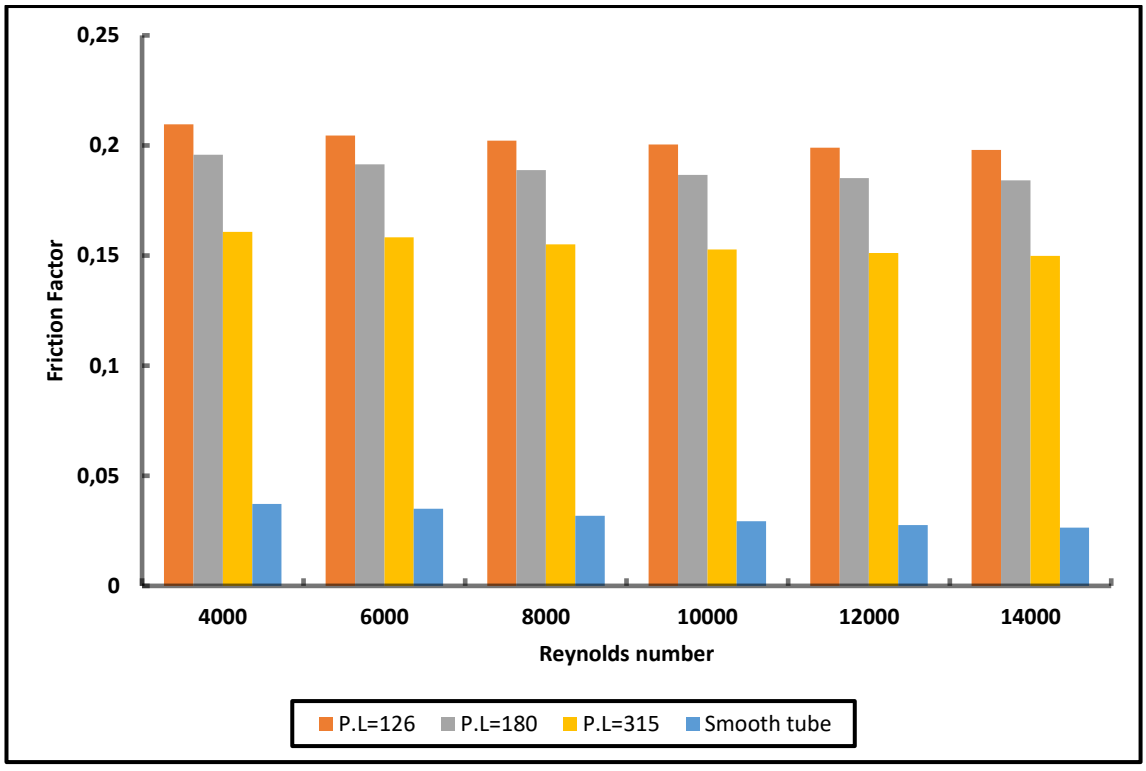


Figure 3.13. Comparison of friction factor and Reynolds Number for water between smooth tube and varying pitch lengths (126mm, 180mm and 315 mm) for non-drilled nozzle

3.2.1.3. Performance Enhancement Factor

The performance enhancement factor result associated with the use of the non-drilled nozzle inserted and water based on the same pumping power criteria is outlined in Figure 3.14. Evidently, thermal performance factor increased as the pitch length of nozzle decreased and is higher than smooth tube. Enhancement efficiencies at Re=14000 is 1.28, 1.24 and 1.15, for pitch lengths of 126 mm, 180 mm, and 315 mm, respectively. This refers that nozzle turbulators are feasible regarding the energy saving at higher Reynolds numbers.

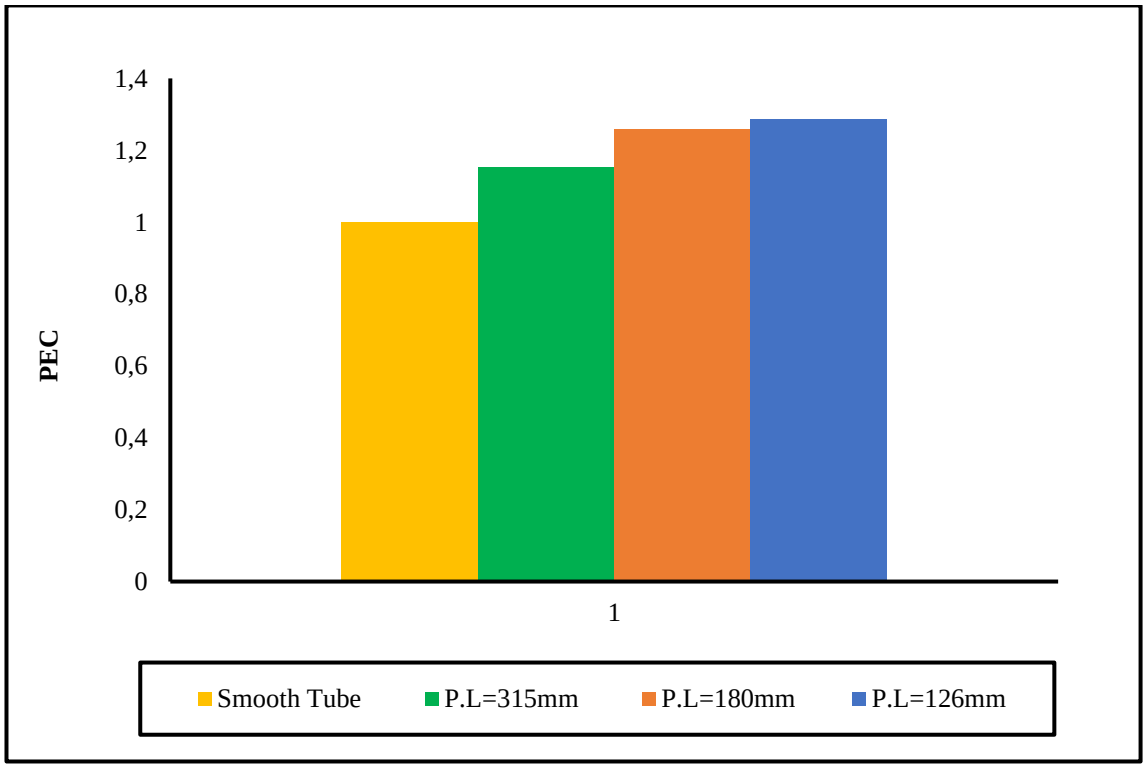


Figure 3.14. Effect and comparison of inserted non-drilled nozzle on tube and smooth tube on thermal performance factor for water flow

3.2.2. Nanofluid flow

3.2.2.1. Convective Heat Transfer

The effect of density of TiO2/water nanofluid over “convective heat transfer coefficient” of the tube with the non-drilled nozzle embedded is compared with the smooth tube. For the studied range, the convective heat transfer parameter augmented with the increasing TiO2 density and all TiO2/water nanofluids provided higher

convective heat transfer parameter than smooth tube. The higher heat transfer by nanofluids is stemmed from: (a) the ability of suspended nanoparticles enhancing the thermal conductivity; (b) the movement of the nanoparticles delivering energy exchange. The higher volume density of nanoparticles would increase the thermal conductivity and contact facet, thus increase the heat transfer rate which is presented in Figure 3.15 by comparing the pitch length of the embedded non-drilled nozzles and smooth tube through volume fraction of 2.0% nanofluid current.

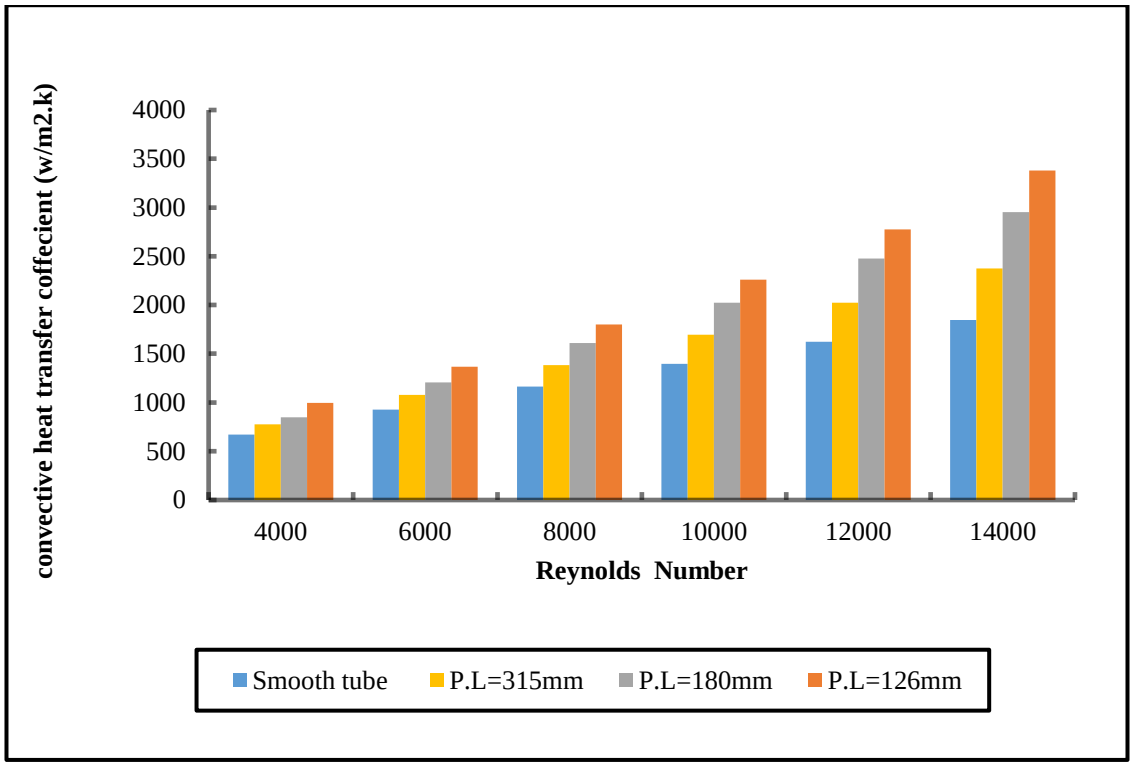


Figure 3.15. Effect of inserted non-drilled nozzles upon the tube with considered pitch length at constant volume fraction of 2.0% in terms of convective heat transfer versus Reynolds number

3.2.2.2. Pressure Drop

When the results are investigated in terms of hydraulic characteristic, it is beneficial to use pressure drop property of the considered configurations. Increment of volume fraction of TiO_2 in water increases the pressure drop penalty. On the other hand, a comparison of a smooth tube results with inserting non-drilled nozzle and decreasing the pitch length of the nozzles increase the pressure drop penalty similarly and it is higher than smooth tube. It is likely to expect this result, as any inserts into the tube become an obstacle to the flow. Thus, friction increases and outlet pressure decreases

much more than the inlet pressure. These results are plotted in Figure 3-16 by comparing the pitch length of the inserted nozzles through volume fraction of 2.0% nanofluid flow.

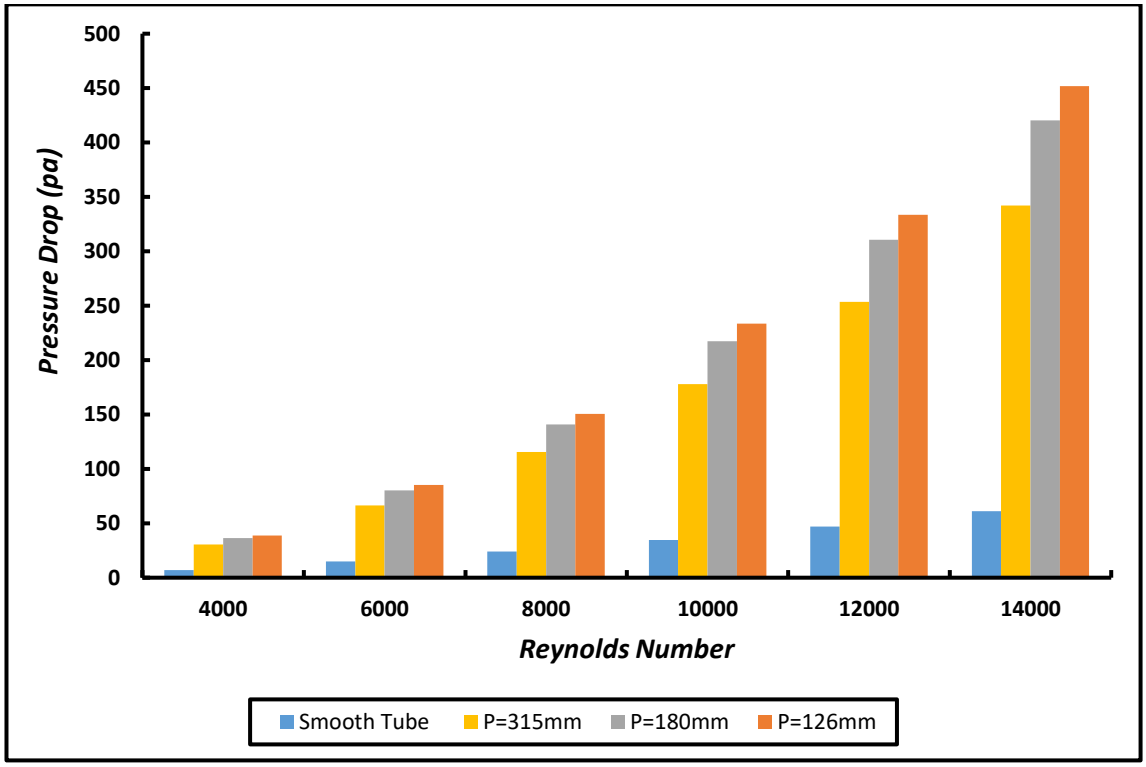


Figure 3.16. Effect of inserted non-drilled nozzles into the tube with considered pitch length at constant volume fraction of 2.0% in terms of pressure drop versus Reynolds number.

3.2.2.3. Performance Enhancement Factor

Thermal performance factor results for pitch length of 126, 180 and 315 mm and volume fraction of TiO_2 in water of 0.2%, 0.6%, 1%, 1.5% and 2% are presented in figures 3.17, 3.18. and 3.19. The results indicate that the thermal performance rises with decreasing pitch length and increasing volume fraction. Performance enhancement efficiencies ranges are 1.5-1.9, 1.3-1.7 and 1.2-1.4, for pitch length of 126 mm, 180 mm, and 315 mm, respectively and all volume frictions.

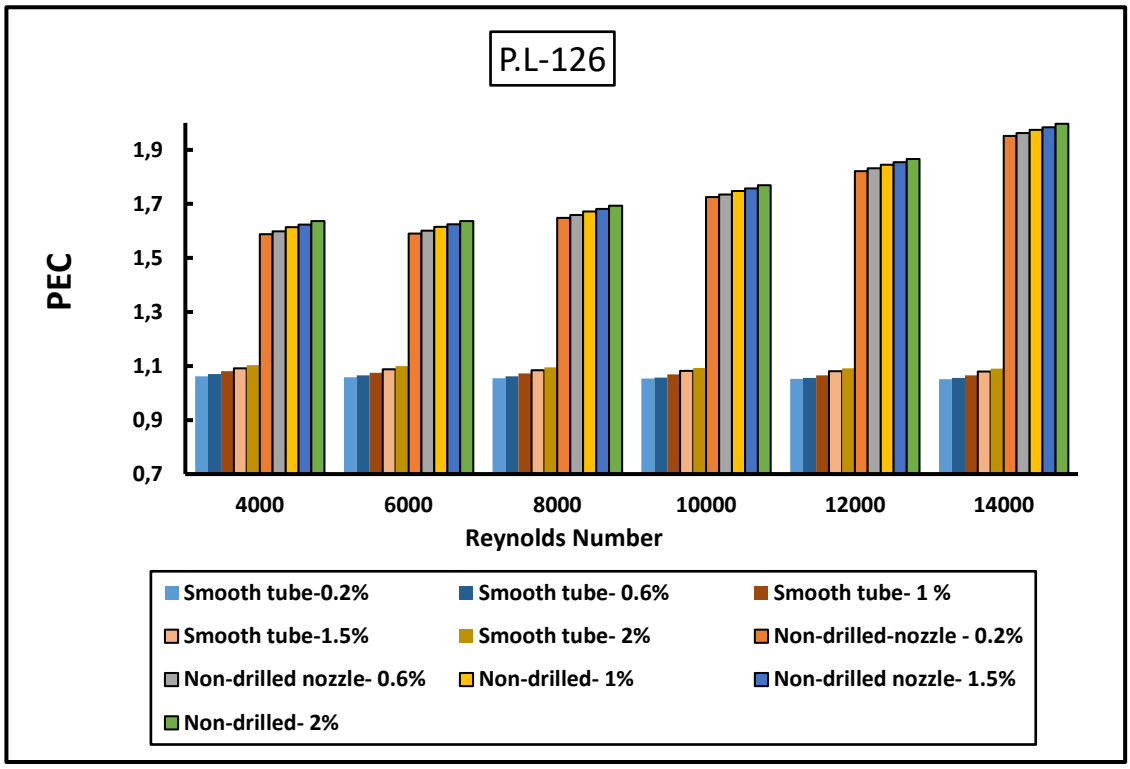


Figure 3.17. Effect of inserting non-drilled nozzles inside the pipe and volume friction on thermal performance factor for the pitch length of 126 mm and comparison with smooth tube

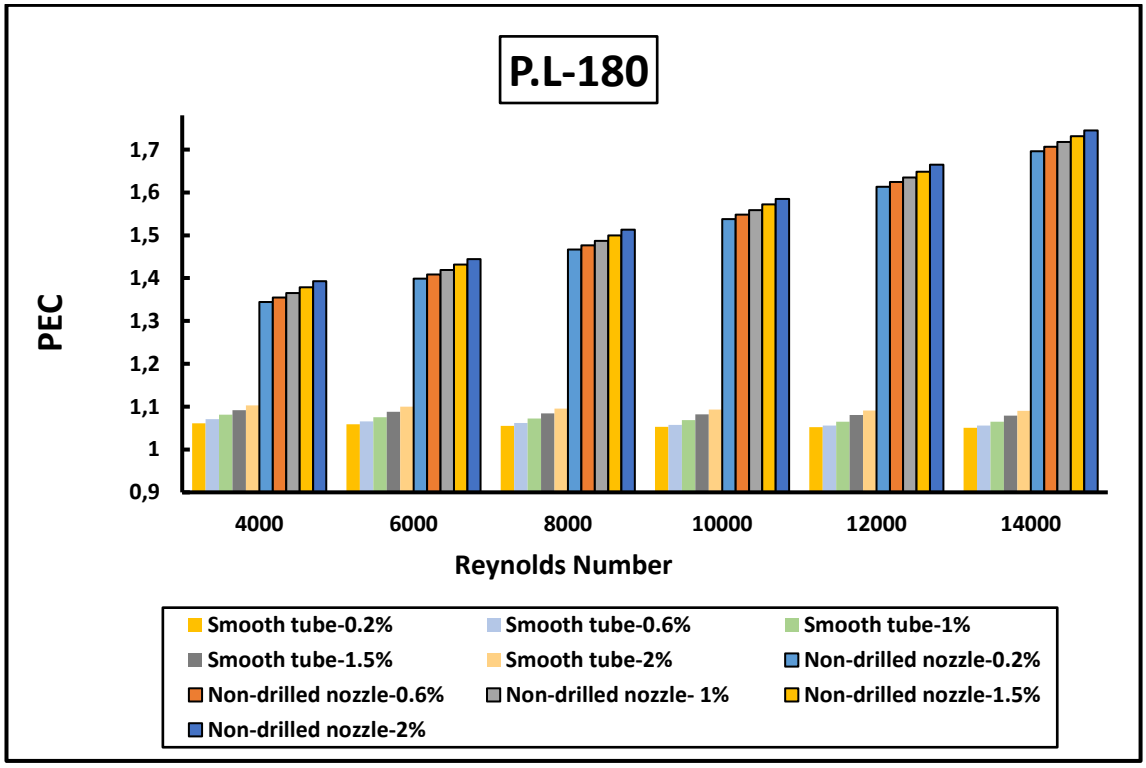


Figure 3.18. Effect of inserting non-drilled nozzles inside the pipe and volume friction on thermal performance factor for the pitch length of 180 mm and comparison with smooth tube

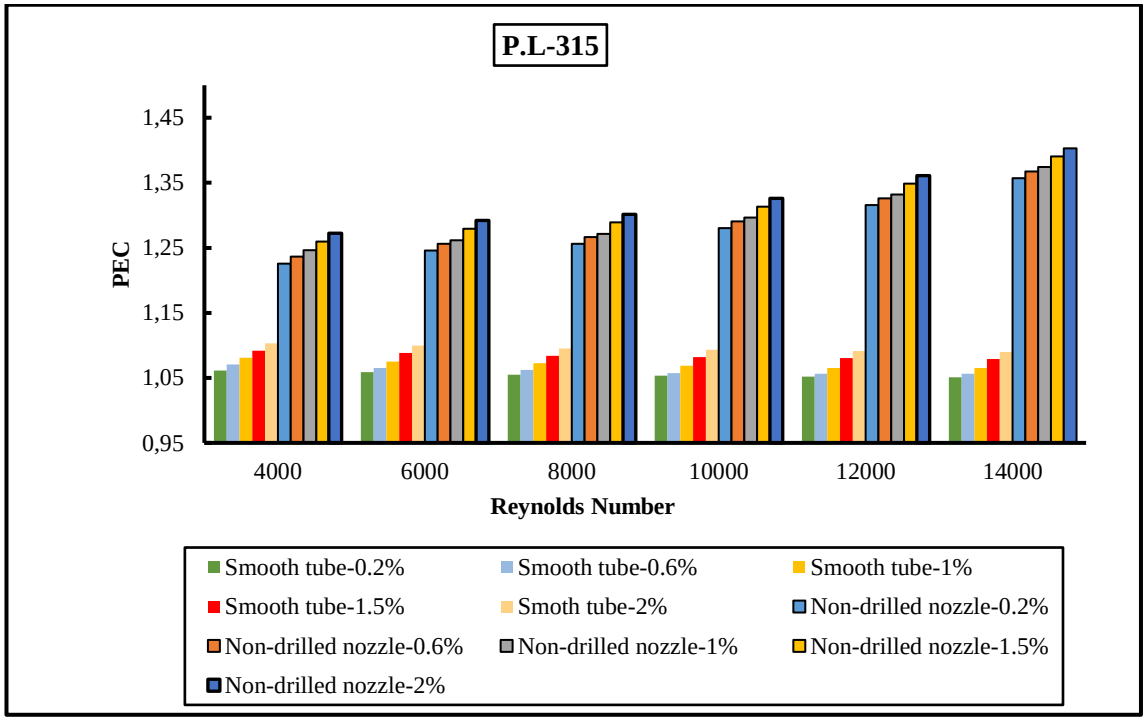


Figure 3.19. Effect of inserting non-drilled nozzles inside the pipe and volume friction on thermal performance factor for the pitch length of 315 mm and comparison with smooth tube

In order to easily comprehend the effect of the nanofluid in the smooth tube on heat transfer and hydraulic performance and comparison with non-drilled nozzle inserted, figures 3.20 and 3.21 can be examined visually. Total pressure contour of the considered cases is illustrated in Figure 3.22 when using nanofluid flow in the tube leads to decrease in outlet pressure. As a result, pressure drop penalty increases, so in order to supply same flow conditions, more pumping power is required.

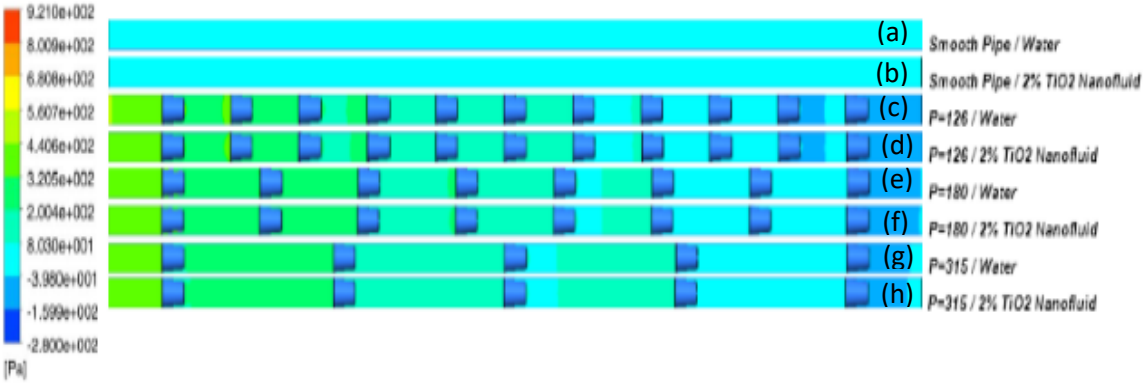


Figure 3.20. Pressure contours of considered configurations for total pressure (a) smooth tube / water. (b) smooth tube /2% TiO2-water. (c) P.L=126mm / water, (d) P.L=126mm / 2% TiO-water, (e) P.L=180 mm / water, (f) P.L=180mm 2% TiO-water, (g) P.L=315mm / water and (h) P.L=315mm / 2% TiO-water.

The total temperature contours of the considered cases are illustrated in Figure 3.21. As can be interpreted from this figure, due to using nanofluid flow inside the tube, temperature distribution adjacent the wall decreases and influences the heat transfer performance positively.

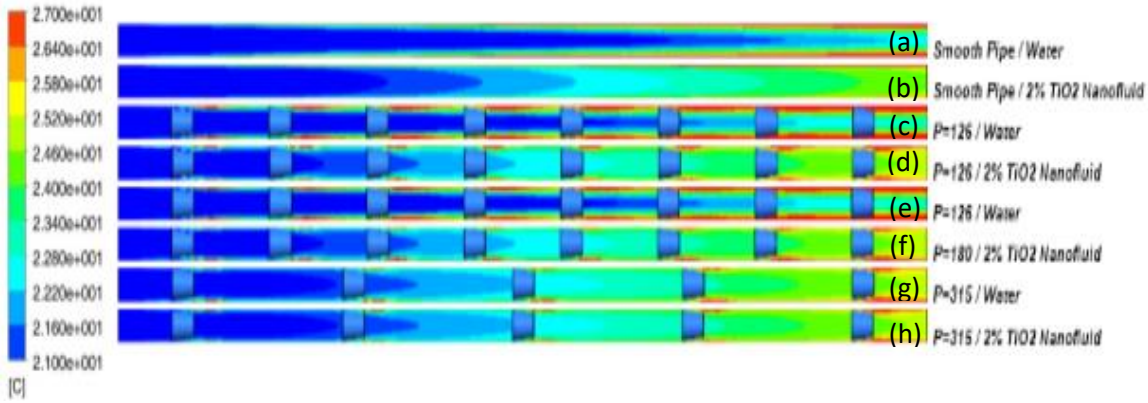


Figure 3.21. Temperature contours of considered configurations for total pressure (a).smooth tube / water. (b).smooth tube /2% TiO2-water. (c).P.L=126mm / water, (d).P.L=126mm / 2% TiO-water, (e). P.L=180 mm / water, (f) P.L=180mm 2% TiO-water, (g). P.L=315mm / water and (h). P.L=315mm / 2% TiO-water.

3.3. Drilled – non drilled nozzle

3.3.1. Water flow

3.3.1.1. Convective Heat Transfer

The results indicated that water flow in the tube and inserting drilled nozzle into the tube rise Nusslet number coefficient with increases in Reynolds number and decreases with rises of pitch length. In addition, drilled nozzle is greater than non-drilled nozzle. As depicted in Figure 3.22, the results indicate an enhancement of the heat transfer rate over the smooth tube for water flow. Hence, in all cases of nozzle inserts, the reverse flow renders higher values of the heat transfer coefficient than that for completely developed axial flow. The rise in heat transfer rate with diminishing pitch ratio is stemmed from the higher turbulent intensity distributed to the flow between the drilled nozzles.

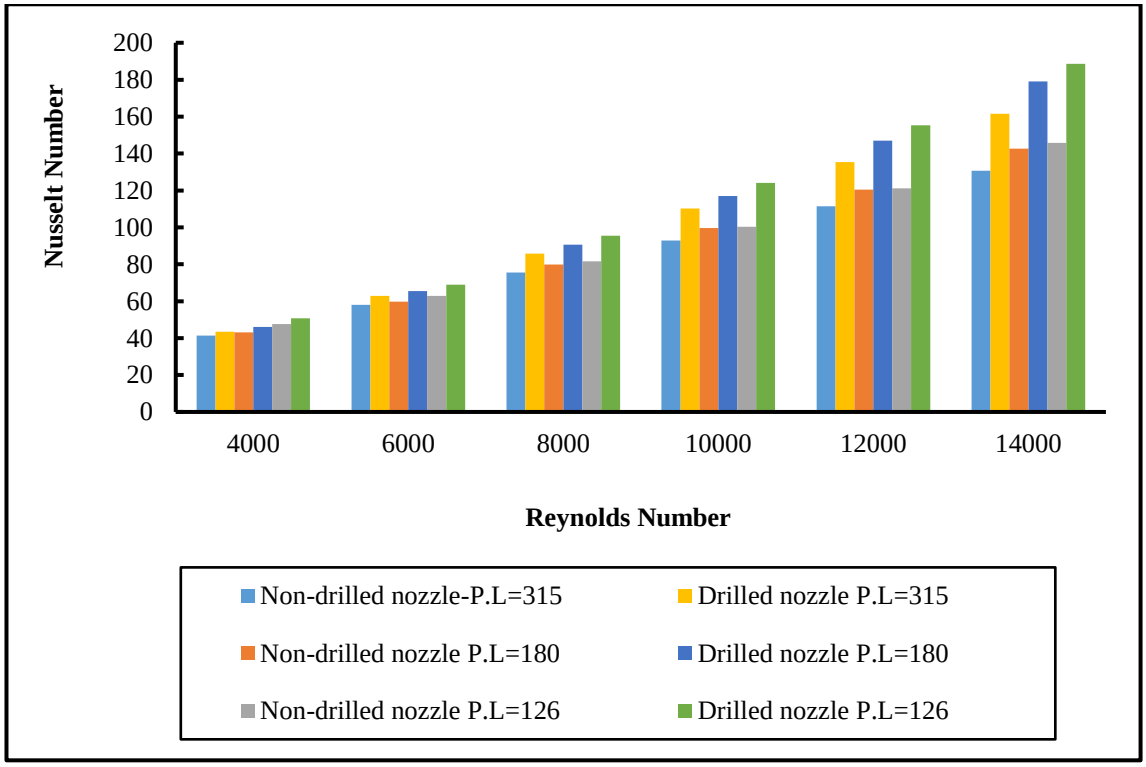


Figure 3.22. Comparison of Nusselt number and Reynolds Number for the water at different pitch lengths (126mm, 180mm and 315 mm) between drilled and non-drilled nozzle

3.3.1.2. Friction factor

The variation of the friction factor in across the test section as a function of Reynolds number is illustrated in Figure 3.23. It can be concluded that the friction factor obtained from three different pitch lengths are in a similar trend and increase with the increasing Reynolds number and lowers with decreases in the pitch length of drilled nozzle with reverse/turbulent current for three different pitch lengths. Generally, it is much more than that with axial current. This is resulted from the energy loss of dynamic pressure of the liquid because of the higher facet region and the behavior caused by the reverse current. Furthermore, the pressure drop is quite likely to occur by the relationship of the pressure drives with inertial drives in the boundary tier.

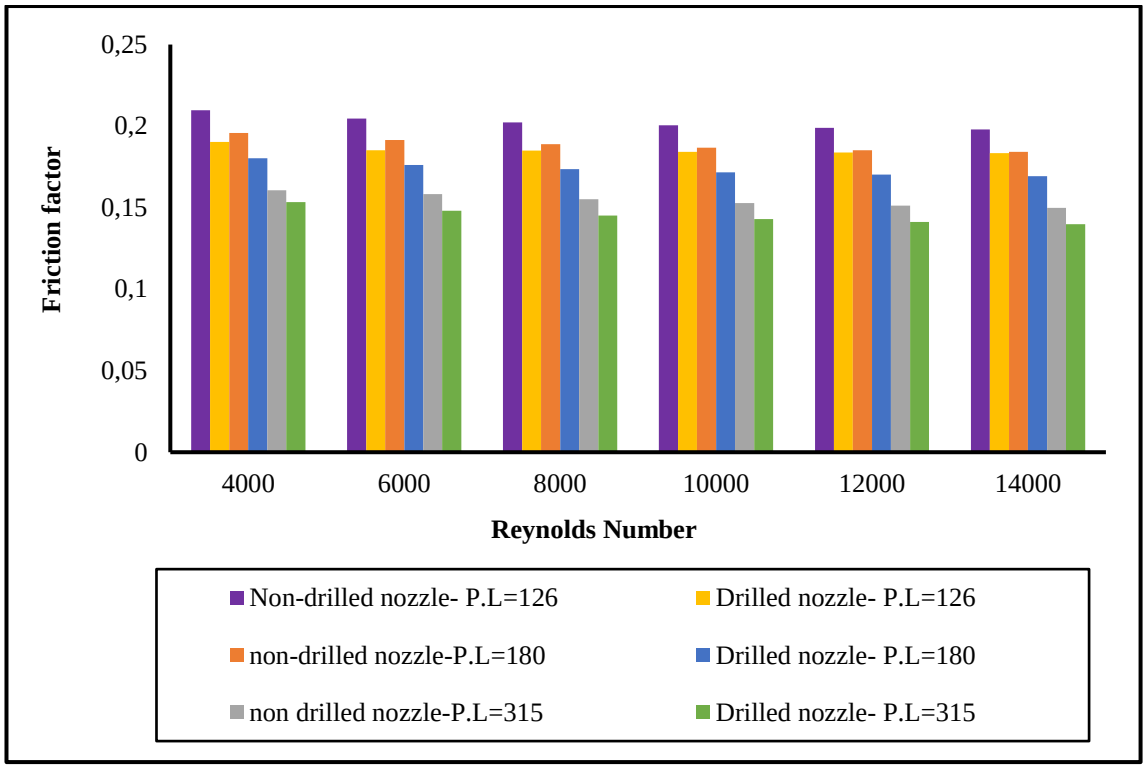


Figure 3.23. Comparison of friction factor and Reynolds Number for water between drilled nozzle and non-drilled nozzle at varying pitch length (126mm, 180mm and 315 mm)

3.3.1.3. Performance Enhancement Factor

The performance enhancement factor results associated with the use of the drilled nozzle inserted and water based on the same pumping power criteria are presented in figures 3.24 to Fig.3.26. Evidently, thermal performance factor increased as the pitch length of nozzle decreased and is higher than the smooth tube. Enhancement efficiencies at Re=14000 is 1.28, 1.24 and 1.15, for pitch length of 126 mm, 180 mm, and 315 mm, respectively. This argues that nozzle turbulators are feasible with regard to the energy saving at higher Reynolds numbers.

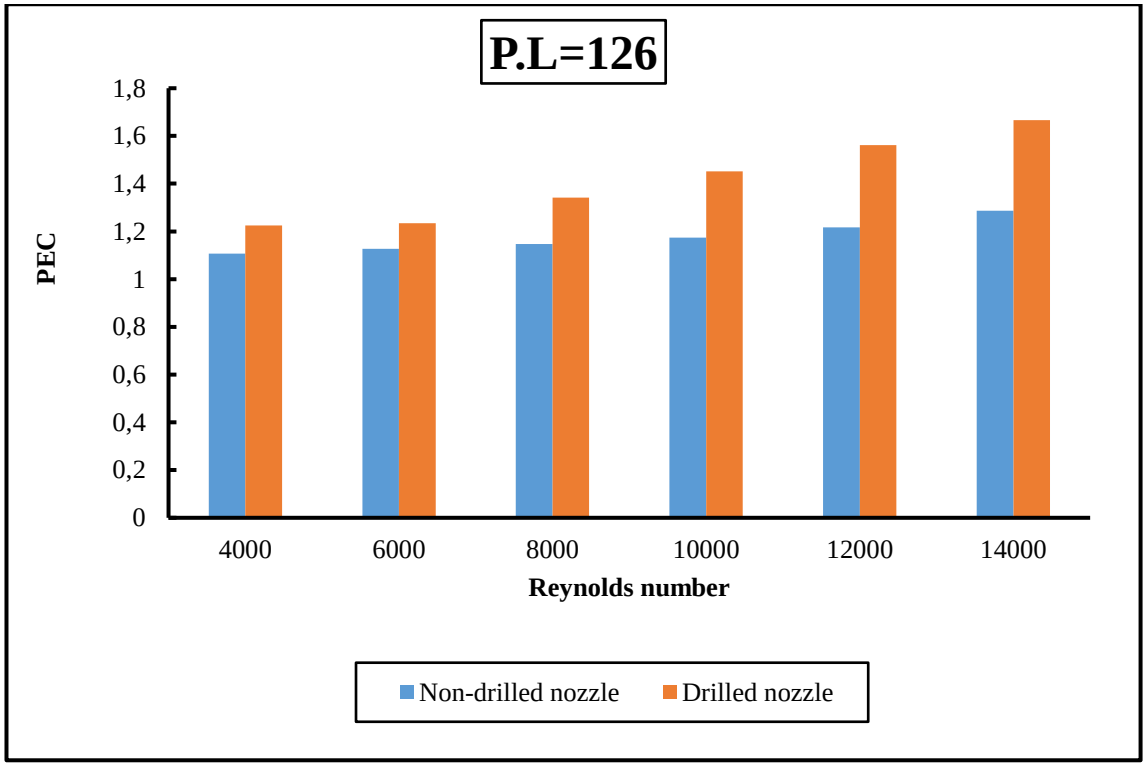


Figure 3.24. Comparison of drilled nozzle with non-drilled nozzle inserted on tube on thermal performance factor for water flow at pitch length of 126mm

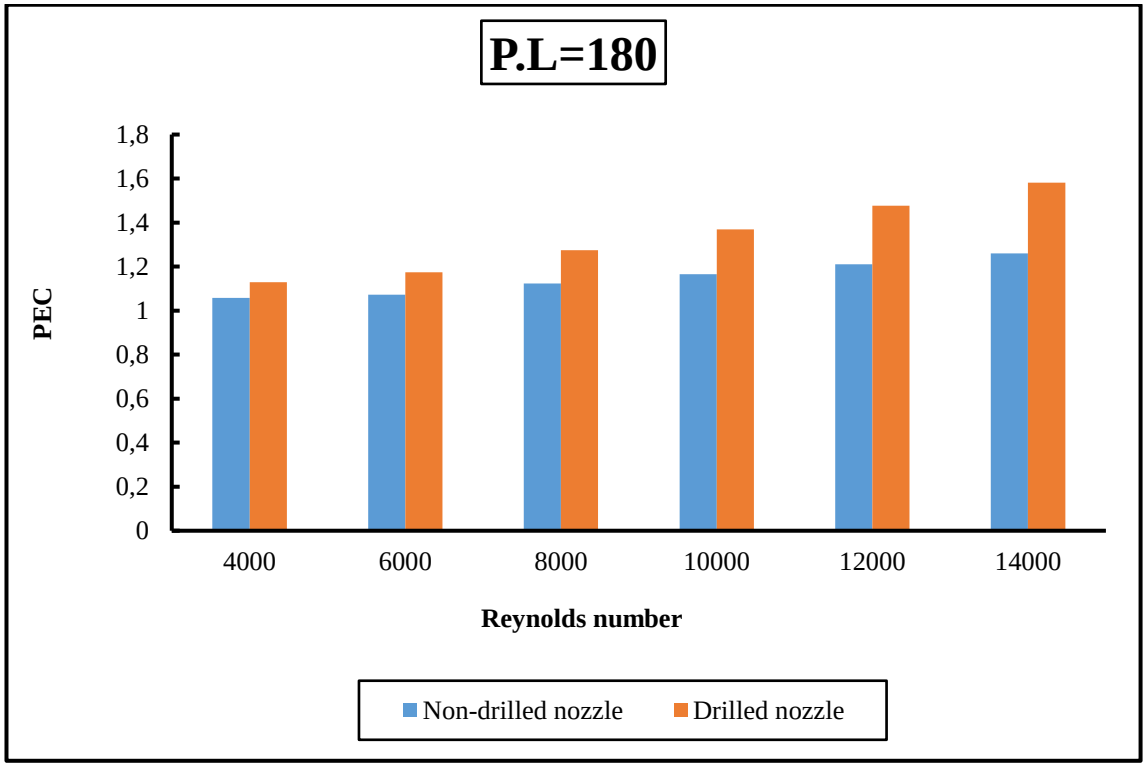


Figure 3.25. Comparison of drilled nozzle with non-drilled nozzle inserted on tube on thermal performance factor for water flow at pitch length of 180mm

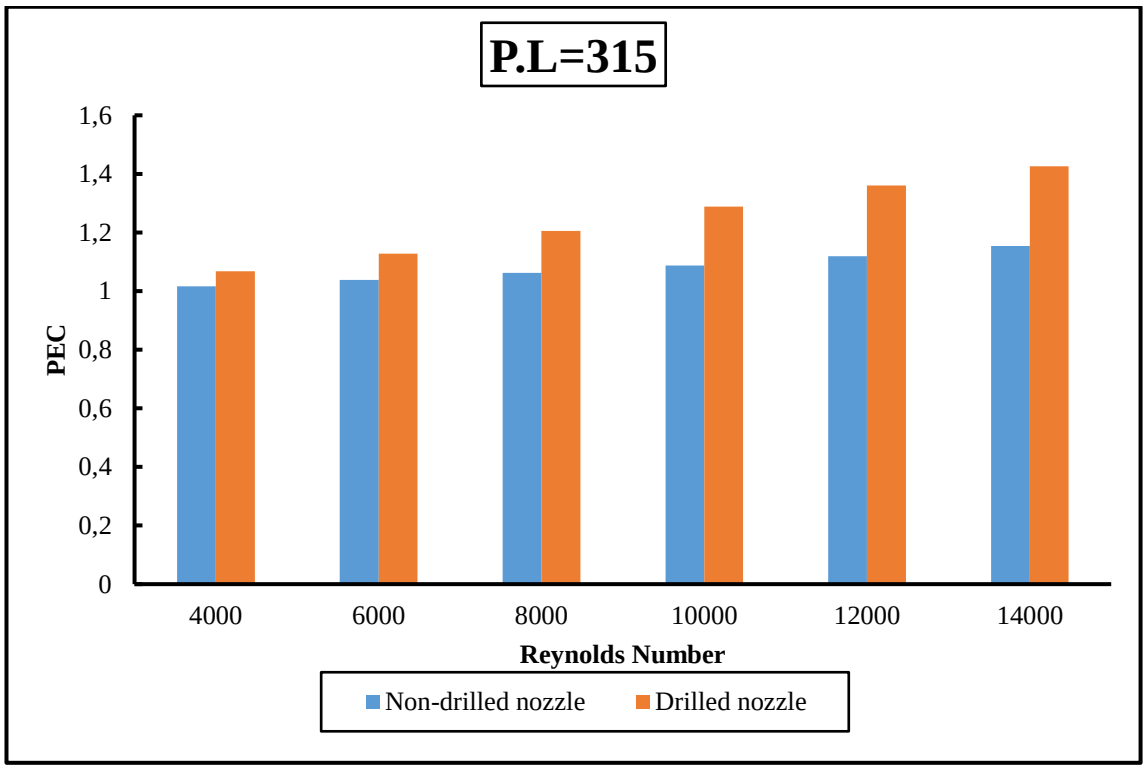


Figure 3.26. Comparison of drilled nozzle with non-drilled nozzle inserted on tube on thermal performance factor for water flow at pitch length of 315mm

3.3.2. Nanofluid flow

3.3.2.1. Convective Heat Transfer

The impact of the volume density of TiO2/water nanofluid on “convective heat transfer coefficient” of the tube with the non-drilled nozzle embedded. For the studied range, the convective heat transfer parameter increased with rising TiO2 density, and all TiO2/water nanofluids provided higher convective heat transfer parameter than water as the base liquid. The higher heat transfer by nanofluids arises from, as outlined in Figure 3.27, the comparison of pitch length of the embedded drilled nozzles through volume fraction of 2.0% nanofluid current.

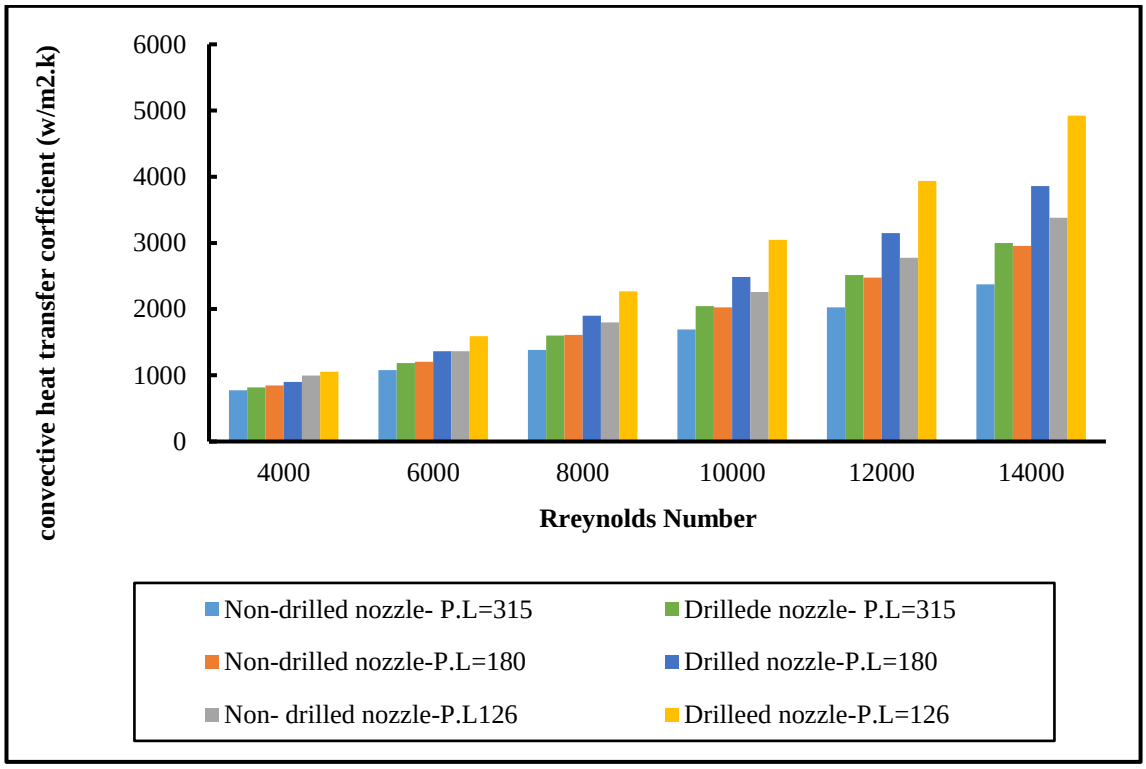


Figure 3.27. Comparison of drilled nozzle with non-drilled nozzle inserted on tube on thermal performance factor for nanofluid flow at constant volume fraction of 2.0%

3.3.2.2. Pressure Drop

When the results are examined in terms of hydraulic characteristics, it is beneficial to use pressure drop property of the considered configurations. Increment of volume fraction of TiO_2 in water increases the pressure drop penalty. In a similar vein, inserting drilled nozzle and decreasing the pitch length of the drilled nozzles increase the pressure drop penalty. It is likely to expect this result as any inserts in the tube become an obstacle to the flow. Thus, friction increases and outlet pressure decreases much more than the inlet pressure. These results are summarized in Figure 3.28. Which compares the pitch length of the inserted nozzles through volume fraction of 2.0% nanofluid flow

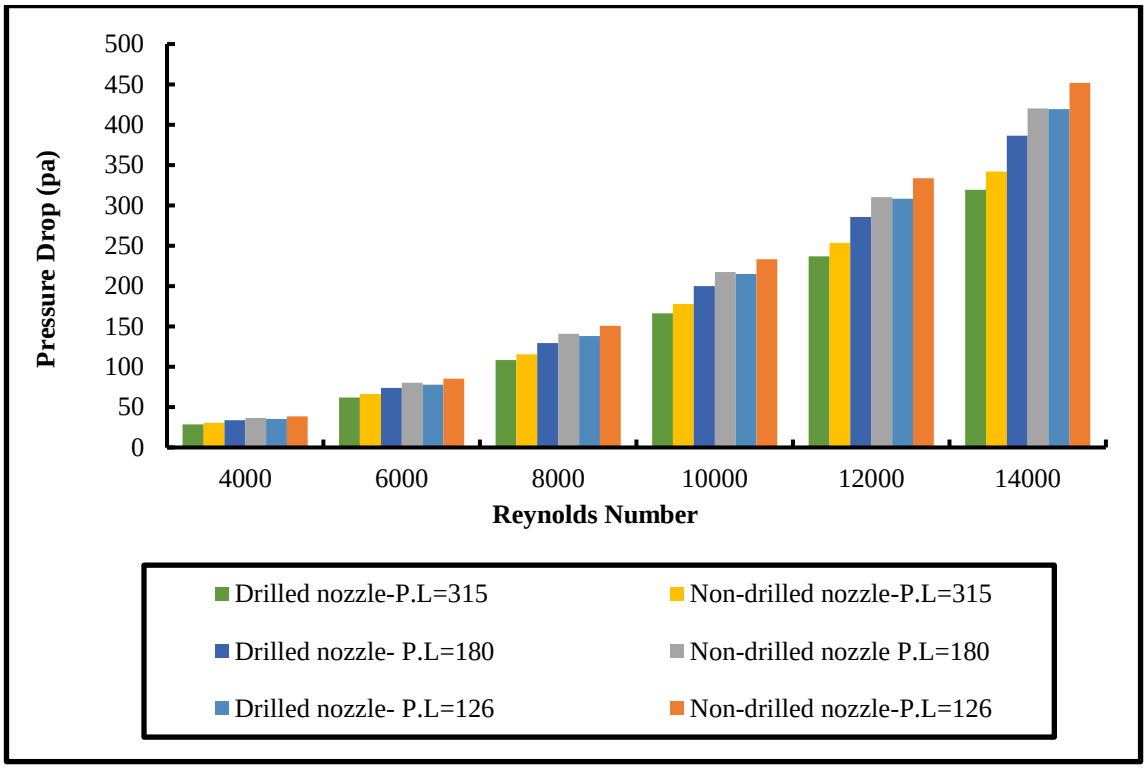


Figure 3.28. Comparison of drilled nozzle with non-drilled nozzle inserted on for nanofluid flow at constant volume fraction of 2.0% in terms of pressure drop versus Reynolds number

3.3.2.3 Performance Enhancement Factor

Thermal performance factor results for pitch lengths of the drilled nozzle (126, 180 and 315 mm) and volume fraction of TiO_2 in water of 0.2%, 0.6%, 1%, 1.5% and 2% are outlined in figures 3.29, 3.30 and 3.31. The analysis data suggest that the thermal performance rises with decreasing pitch length and rising volume fraction. Performance enhancement efficiencies ranges are 1.74-2.92, 1.47-2.3 and 1.38-1.78, for pitch lengths of 126 mm, 180 mm, and 315 mm, respectively and all volume frictions.

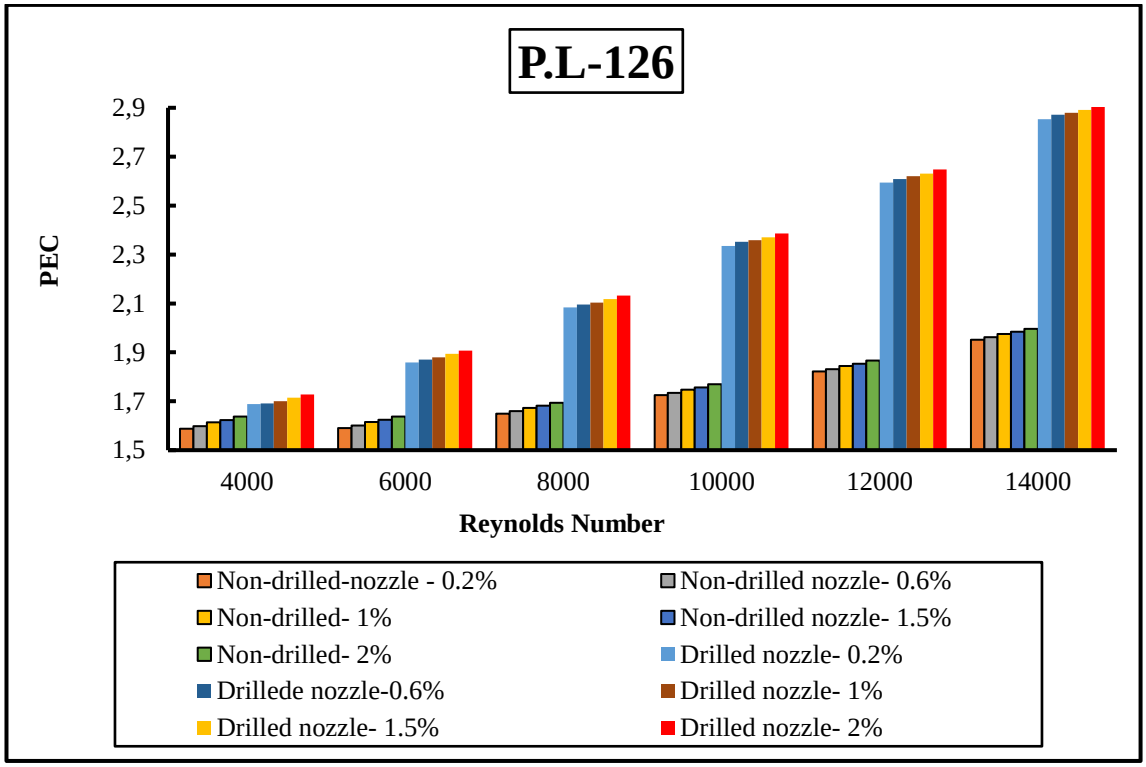


Figure 3.29. Comparison of drilled nozzle with non-drilled nozzle inserted on tube on thermal performance coefficient and volume friction on thermal performance factor for pitch length of 126 mm

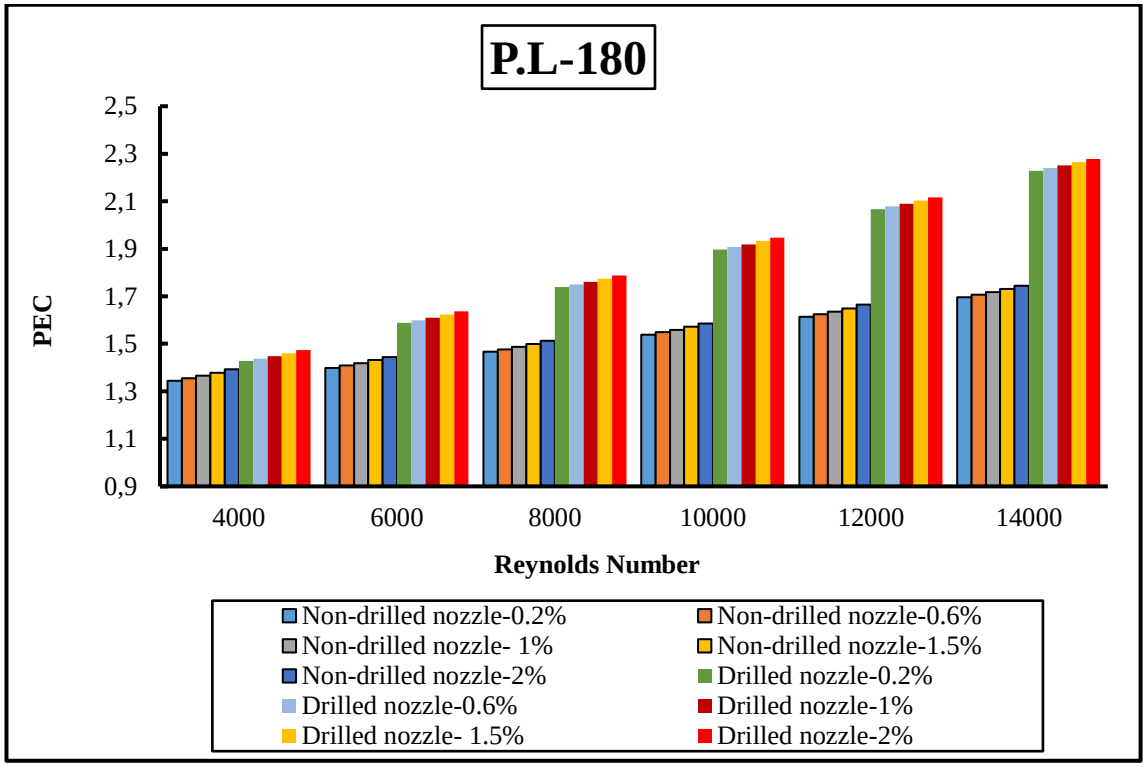


Figure 3.30. Comparison of drilled nozzle with non-drilled nozzle inserted on tube on thermal performance coefficient and volume friction on thermal performance factor for pitch length of 180 mm

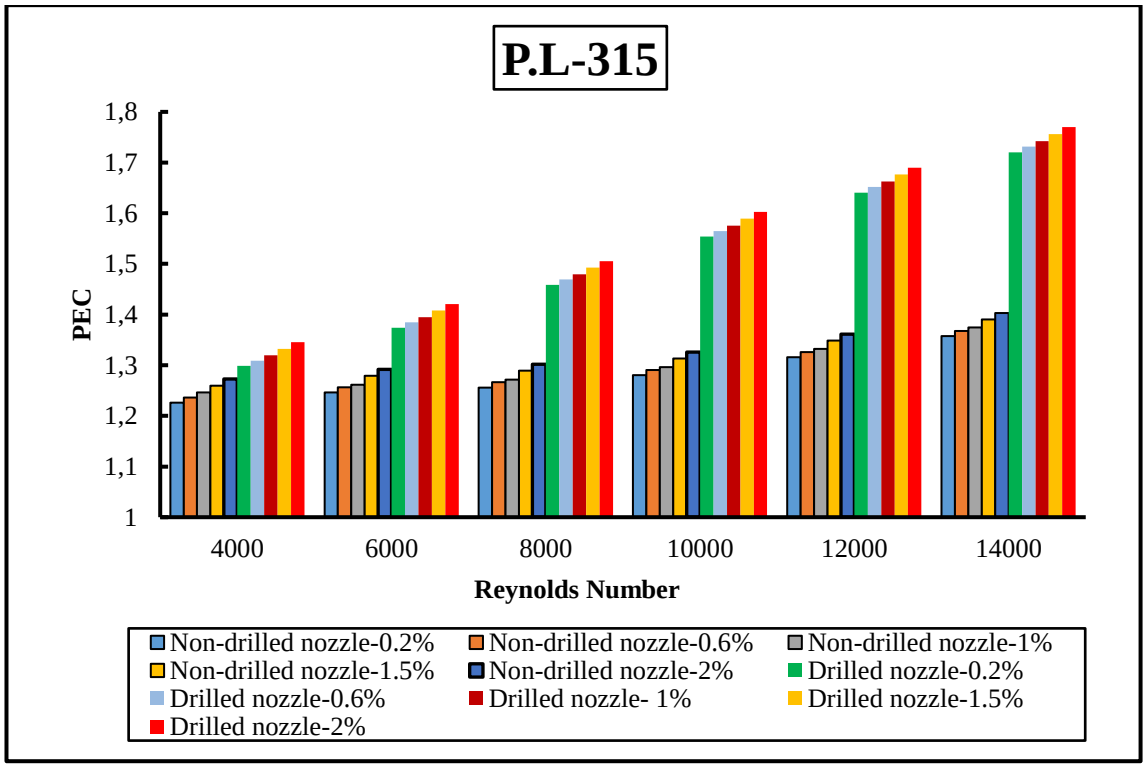


Figure 3.31. Comparison of drilled nozzle with non-drilled nozzle inserted on tube on thermal performance coefficient and volume friction on thermal performance factor for pitch length of 315mm

In order to easily understand the effect of nanofluid in smooth tube on the heat transfer and hydraulic performance and comparison with the drilled nozzle embedded, Figure 3.32 and Figure 3.33 can be examined visually. Total pressure contour of the considered cases is illustrated in Figure 3.32. Using nanofluid current in the tube leads to decrease in the outlet pressure. As a result, pressure drop penalty increases, so as to supply the same current conditions, more pumping power is required.

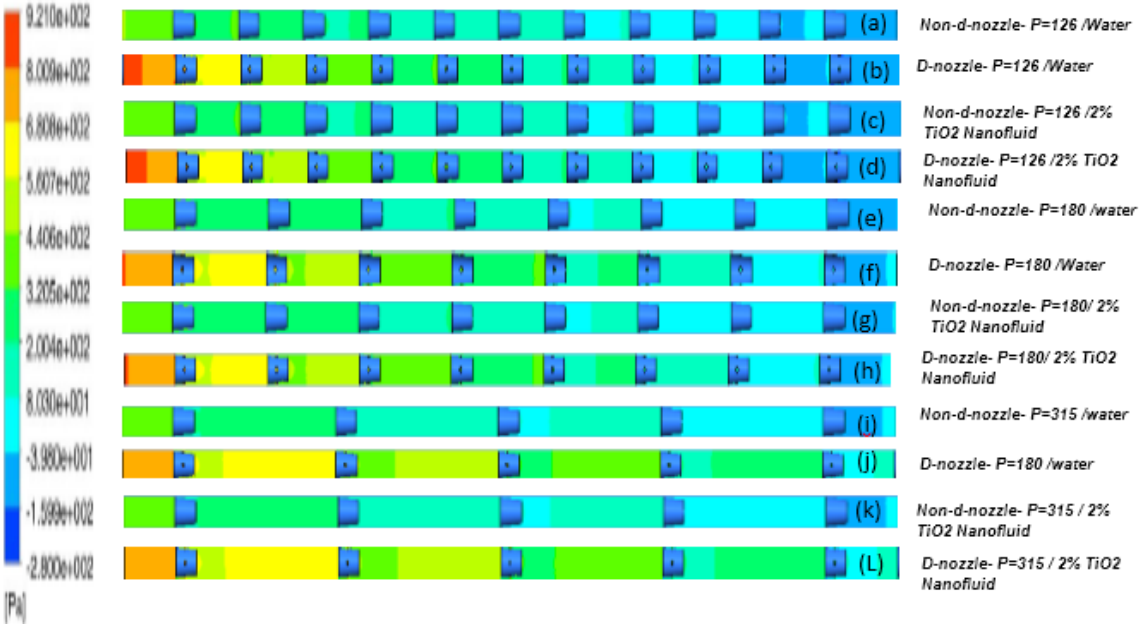


Figure 3.32. Pressure contours of considered configurations for total pressure (a) Non-drilled- nozzle P.L=126mm/water. (b) Drilled-nozzle P.L=126mm/water. (c) Non-drilled- nozzle P.L=126mm/2% TiO2 nanofluid, (d) Drilled-nozzle P.L=126mm/2% TiO2 nanofluid, (e) Non-drilled- nozzle P.L=180mm/water, (f) Drilled- nozzle P.L=180mm/water., (g) Non-drilled- nozzle P.L=180 mm/2% TiO2 nanofluid, (h) Drilled- nozzle P.L=180mm/2% TiO2 nanofluid, (i) Non-drilled- nozzle P.L=315mm/water, (j) Drilled- nozzle P.L=315 mm/water, (k) Non-drilled- nozzle P.L=315mm/2% TiO2 nanofluid, and (l) Drilled- nozzle P.L=315mm/2% TiO2 nanofluid**.**

The total temperature contours of the considered cases are outlined in Figure 3.33. As can be seen in this figure, due to using nanofluid flow and comparison between drilled nozzle inserted inside the tube and non-drilled nozzle, temperature distribution adjacent the wall decreases and influences the heat transfer performance positively.

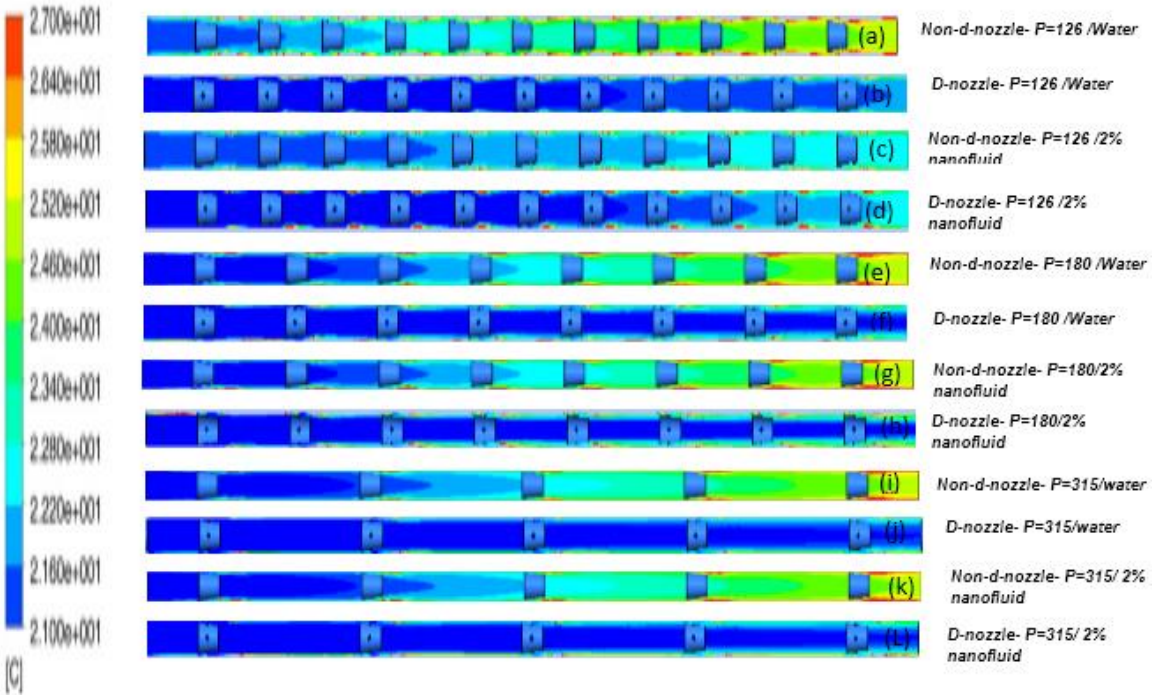


Figure 3.33. Temperature contours of considered configurations for total (a) Non-drilled- nozzle P.L=126mm/water. (b) Drilled-nozzle P.L=126mm/water. (c) Non-drilled- nozzle P.L=126mm/2% TiO2 nanofluid, (d) Drilled-nozzle P.L=126mm/2% TiO2 nanofluid, (e) Non-drilled- nozzle P.L=180mm/water, (f) Drilled- nozzle P.L=180mm/water., (g) Non-drilled- nozzle P.L=180 mm/2% TiO2 nanofluid, (h) Drilled- nozzle P.L=180mm/2% TiO2 nanofluid, (i) Non-drilled- nozzle P.L=315mm/water, (j) Drilled- nozzle P.L=315 mm/water, (k) Non-drilled- nozzle P.L=315mm/2% TiO2 nanofluid, and (l) Drilled- nozzle P.L=315mm/2% TiO2 nanofluid**.**

The velocity vector of the considered cases is illustrated in Figure 3.34. As can be understood from this figure, due to using nanofluid flow and comparison between the drilled nozzle inserted inside the tube and non-drilled nozzle, velocity distribution adjacent the wall collected the nanofluid and increased the velocity between the wall of drilled nozzle and the wall of tube which has an effect on the heat transfer performance positively, because of the increases in Reynolds number.

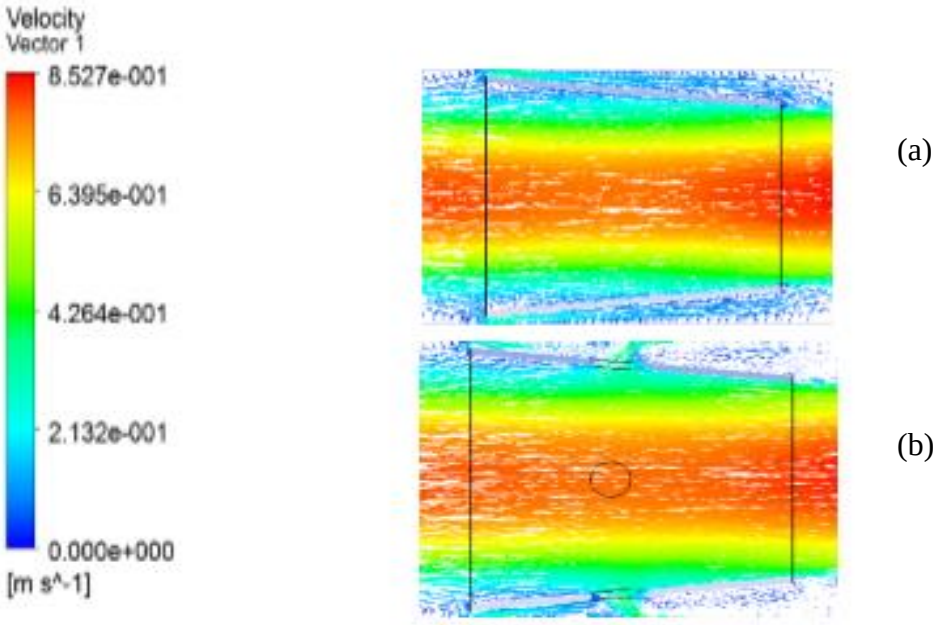


Figure 3.34. Velocity vector (a) Non-drilled nozzle (b) Drilled nozzle for nanofluid flow at 2% TiO2/Water and Reynolds number 14000

CHAPTER- 4

CONCLUSION AND RECOMMENDATIONS

4.1. CONCLUSION

A quantitative investigation regarding the thermal performance of inserting two types of nozzle was conducted including non-drilled nozzles and Drilled nozzle with three different pitch lengths (126, 180 and 315mm) through a water-based TiO2 nanofluid flowing into a horizontal tube. The considered nanofluid volume fractions were limited from 0.2% to 2.0%. A uniform constant heat flux of 50 kW/m^2K was employed on the outer surface of the tube. The k-ω standard turbulent model was opted to simulate the turbulent flow, and the analyses were implemented for the Reynolds number range of 4000 to 14,000.

In terms of physical reasons

- Inserting a non-drilled nozzle in a tube increases the convective heat transfer when it is compared to the smooth tube with increases in Reynolds number and decreases with increasing pitch length of nozzle. In addition, a maximum convective heat transfer coefficient in non-drilled nozzle is 29% greater than the smooth tube at flow water through at Reynolds number of 14000 and pitch length of 126 mm. The main reason of increasing convective heat transfer is destruction of the boundary layer and emergence of secondary flow in the non-drilled nozzle between the wall of smooth tube and the wall of nozzle.
- Inserting drilled nozzle in a tube increases the convective heat transfer when it's compared to the non-drilled nozzle with increases in Reynolds number and decreases with increasing pitch length of nozzle. Also, a maximum convective heat transfer coefficient in drilled nozzle is 28% larger than the non-drilled

nozzle at flow water through at Reynolds number of 14000 and pitch length of 126 mm. The main motive of the increasing convective heat transfer is that the boundary layer destroyed and secondary flow emerges in the drilled nozzle through the hole of the nozzle which increases the turbulence flow between the wall of smooth tube and the wall of nozzle.

- Inserting non-drilled nozzle in a tube increases the pressure drop when it's compared to the smooth tube with decreases in Reynolds number and rises with decreasing pitch length of nozzle. Furthermore, a maximum pressure drop in non- drilled nozzle is 6 times with the smooth tube at flow water through at Reynolds number of 14000. The major reason of the increasing pressure drop is that flow in the tube inserted with non-drilled nozzle shocked the wall surface of the nozzle and decreased the potential energy.
- Inserting drilled nozzle in a tube decreases pressure drop when it's compared to the non-drilled nozzle with increases in Reynolds number and goes up with decreasing pitch length of the nozzle. Besides, a maximum pressure drop in drilled nozzle is 8% less than that of non-drilled nozzle at flow water through at Reynolds number of 14000 and pitch length of 126 mm. The main reason of the increasing pressure drop is accumulation of the flow between the non-drilled nozzle surface and the wall of the tube with greater effect than the drilled nozzle
- The performance enhancement coefficient rises with the increases in the Reynolds number and decreases with the pitch length of nozzle for water flow. In addition, a maximum of the performance enhancement coefficient in non-drilled nozzle is 1.3 in pitch length of 126 mm and at Reynolds number of 14000.
- The performance enhancement coefficient rises with the increases in the Reynolds number and decreases with the pitch length of nozzle for water flow. Furthermore, a maximum of the performance enhancement coefficient in drilled nozzle is 1.3 in pitch length of 126 mm) and at Reynolds number of 14000, and it's higher than the non-drilled nozzle at the identical Reynolds number and the pitch length.

In terms of chemical reasons

- Adding nanoparticle up to volume fraction of 2.0% into the water also increases the heat transfer. This result is mainly resulted from the rise in thermal conductivity of the nanofluid, and thus, the more effective emergence of heat transfer among the molecules.

- Adding nanoparticle into the water slightly increases the pressure drop in comparison with the heat transfer. The reason of the increasing pressure drop is engaged with the increasing viscosity and density of the nanofluid.

Table 4.1. Most advantages and Most Disadvantages for Convective heat transfer coefficient, Pressure drop and Performance Enhancement Factor.

	Most Advantages Configuration					Most Disadvantages Configuration				
	Value	Re	φ	P.L (mm)	Tube type	Value	Re	φ	P.L (mm)	Tube type
Convective heat transfer coefficient (W/m^2K)	4924.7	14000	2%	126	Drilled nozzle	609.5	4000	0%	-	Smooth tube
ΔP *(Pa)*	7.02	4000	0%	-	Smooth tube	451.8	14000	2%	126	Non-drilled nozzle
PEC	2.9	14000	2%	126	Drilled nozzle	1	4000-14000	0%	-	Smooth tube

4.2. RECOMMENDATIONS

1. The next study needs to be done to explore the heat transfer and flow of nanofluid in a circular tube under laminar and turbulent flow with modified nozzle inserts together with nanofluid experimentally and quantitatively and further studies can be conducted experimentally because all quantitative studies provide a prediction about the real results.

2. Nanofluids can be investigated in detail with regard to the heat transfer and thermal flow using a two-phase approach.

3. Thermal -physical properties information for different types of essential fluids like water, engine oil and R-134a are very rare. The heat transfer of nanofluids should be investigated on a large scale. They have a higher Brandtel number, and lower thermal

conductivity, which provides more nanofluid, enhanced heat transfer potentials so promote new and numerical experiments in this matter are required.

4. Other studies can investigate heat transfer and thermal current using a different hole in a nozzle such as a triangle, square or ellipse.

5. The measuring studies should be conducted by considering the arguments. The results can be used to estimate the heat transfer parameter of nanofluids. Then, the links with the wide application ranges of analyzes can be derived and can be compared with experimental studies.

6. A crucial focus for further research should be specifying the key energy transport mechanisms in nanofluids.

7. The further studies can aim to obtain the desirable nanoparticle products, helpful nanoparticle production techniques for the nanofluid research to achieve large improvement of conductivity with a minor concentration of particles that thoroughly sustained the Newtonian behavior of the fluid.

8. The future studies can utilize the nanofluid as a clean and viable renewable energy source. Their use can alleviate the devastating outcomes of greenhouse gas emissions, global warming, and environmental degradation.

9. In practical applications, the fluid flow is usually in the turbulent regime as higher heat transfer is obtained via the turbulent flow. Thus, there is a need to fully understanding the overall effect of various turbulent models on the heat transfer results of nanofluid and inserts.

REFERENCES

1. Bergles.A., E., 1981. Application of heat transfer Augmentation. **Hemisphere pub.com**.
2. Webb, R.L., 2005. Principles of Enhanced Heat transfer, no.1.c, **Taylor Francis**.
3. Mahesh Jadhan, R.A, D.B, A.B, M.M, Review on Enhancement of heat transfer by Active Method, **Int.Journal of Eng. &Tech**.PISS2347-5161.
4. Usui H, Sano Y, Iwashita K, Isozaki A., 1984. Heat transfer enhancement e!ects by combined use of internally grooved rough surfaces and twisted tapes. Heat transfer-**Japanese Research 13**(4):19-32.
5. Usui H, Sano Y, Iwashita K, Isozaki A., 1986. Enhancement of heat transfer by a combination of an internally grooved rough tube and a twisted tape**. International Chemical Engineering 26**(1):97-104.
6. Aksoy, S., Calikoglu, E., Aras, H., and Karakoc, N., 2013. Energy Management and Policy, Anadolu Universitesi, 219s.
7. Agarwal S. K. and M. Raja rao, 1996. "Heat transfer augmentation for the flow of a viscous liquid in circular tubes using the twisted tape inserts", **Int. J. Heat Mass Transfer**, **Vol. 39**, No. 17, 3547-3557.
8. Gunes S., V. Ozceyhan, O. Buyukalaca, 2010. The experimental investigation of heat Transfer and pressure drop in a tube with coiled wire inserts placed separately from the tube wall, **Applied Thermal Engineering 30**(0) 1719-1725.
9. Promvonge P., Eiamsa S., 2007. Heat transfer and turbulent flow friction factor in a circular tube fitted with conical- nozzle turbulators.**Int.communication in Heat and Mass Transfer** 3472-82.
10. Akeel A.M, B.A.M, R.J.M, 2014. Heat transfer Enhancement in a Tube Fitted with Nozzle Turbulators Perforated Nozzle – Turbulators, With Different Hole Shape, **Eng. &Tech.Journal**, and **Vol.32**, part A.
11. Kebliuski P., Eastaman J.A., Cahill D.G., 2005. Nanofluids for the thermal transport, **Mater. Today.8** (6) 36-44.
12. J.C.Maxwell, 1954. Treatise on Electricity and Magnetism, Dover, New York.

13. S.U.S.Choi, 1995. Enhancing thermal conductivity of fluids with nanoparticale, ASME.FED.231- 99.

14. M. Kostic, Nanofluds, 2004. Advanced flow and heat transfer fluids, Northern Illionis University.

15. Murshed,S.M.S,Leong,K.C,and Yang,C.,2006. Determination of the effective thermal diffusivity of nanofluids by the double hot-wire technique,**Journal of physics D: Applied physics,vol.39**,no.24,pp.5316-5322

16. The Thermophyiscal Properties Research Center (TPRC), 1970. Thermophysical Properties of Matter-Specific Heat (monometallic solid), **vol.5**, Purduce University.

17. Das, S.K., Chio, S.U., Y.U., W., Pradeep, T. 2008. Nanofluids: Science and technology .ed.John wiley&Sons.

18. Timofeeva,E.V.,Routbort,J.L.,and Singh,D., 2009.Partical Properties of Alumina nanofluids .**Journal of Applied physics,vol.106**,no.1,pp.014304-1-10.

19. Boluk,Y.,Lahiji,R.,Zhao,L.,and McDermott,M.T.,2011.Suspension viscosities and shape parameters of cellulose nano crystals(CNC),Colloids and surfaces A: **physicochem,Eng.Aspects,vol.337**,pp297-303.

20. Rubio-Hernandez,F.J.,Ayucar-Rubio,M.F,Vlaazquez-Navarro, J.F., and Galindo Rosales, F.J.,2006. Intrinsic viscosity of SiO2, Al2O3 and TiO2 aqueous suspensions, **Journal of colloied and Interface Science, 298**, 967-972.

21. Syam Sundar, L., Venkata Ramana,E.,Singh,M.K.,and De Sousa,A.C.M,2012. Viscosity of low volume concentrations of magnetic Fe3O4 nanoparticales dispersed in ethylene glycol and water mixture, **chemical physics Letter, 554,** 236-242.

22. Liu Yang. K.D., 2017. A comprehensive review on heat transfer characteristics of TiO2 nanofluids, **Int.Journal of heat and mass transfer, 108**(0)11-31.

23. Yanjiao Li., J.Z., S.T., E.S, S.X., 2009. A review on development of nanofluid preparation and characterization, **Journal. Powder Technology**.196.

24. J.A. Eastman, S.U.S. Choi, 2001. Anomalously increased effective thermal conductivities of ethylene glycol-based nanofluids containing copper nanoparticles, **Appl. Phys.Lett**. 78 718–720.

25. Min-Sheng Liu, MarkChing-Cheng Lin, C.Y. Tsai, Chi-Chuan Wang, 2006. Enhancement of thermal conductivity with cu for nanofluids using chemical reduction method, **Int. J. Heat Mass Transfer 49** (0) 3028–3033.

26. Y. Xuan, Q. Li, Heat transfer enhancement of nanofluids, **Int. J. Heat Mass Transfer21** (2000) 58–64.

27. T.K. Hong, H.S. Yang, C.J. Choi, 2005. Study of the enhanced thermal conductivity of Fe-nanofluids, J. Appl. Phys. 97 (064311) 1–4.

28. H.E. Patel, S.K. Das, T. Sundararagan, A.S. Nair, B. Geoge, T. Pradeep, 2003. Thermal conductivities of naked and monolayer protected metal nanoparticle based nanofluids: manifestation of anomalous enhancement and chemical effects, **Appl. Phys. Lett. 83** -2931–2933.

29. Shawn A. Putnam, David G. Cahill, Paul V. Braun, 2006. Thermal conductivity of Nanoparticle suspensions, **J. Appl. Phys. 99** (084308) 1–6.

30. H. Zhu, C. Zhang, S. Liu, 2006. Effects of nanoparticle clustering and alignment on Thermal conductivities of Fe3O4 aqueous nanofluids, **Appl. Phys. Lett. 89** (23123) 1–3.

31. S.M.S. Murshed, K.C. Leong, C. Yang, 2005. Enhanced thermal conductivity of TiO2–water based nanofluid, **Int. J. Therm. Sci. 44** -367–373.

32. H. Xie, J.Wang, T. Xi, Y. Liu, F. Ai, 2002. Thermal conductivity enhancement of suspensions containing nanosized alumina particle, **J. Appl. Phys. 91**-4568–4572.

33. X. Zhang, H. Gu, M. Fujii, 2006. Experimental study on the effective thermal conductivity and thermal diffusivity of Nanofluid, **Int. J. Thermophys. 27**-569–580.

34. H.Q. Xie, et al., 2001. Study on the thermal conductivity of SiC nanofluids, **J. Chin. Ceram.Soc. 29**- 361–364 (in Chinese).

35. M.S. Liu, M.C. Lin, I.Te. Huang, C.C. Wang, 2005. Enhancement of thermal conductivity with carbon nanotube for nanofluids, **Int. Commun. Heat Mass Transf. 32-** 1202–1210.

36. S.U.S. Choi, Z.G. Zhang, W. Yu, F.E. Lockwood, E.A. Grulke, 2001. Anomalous thermal conductivity enhancement in nanotube suspensions, **Appl. Phys. Lett. 79-** 2252–2254.

37. Huaqing Xie, Hohyun Lee, Wonjin Youn, Mansoo Choi, 2003. Nanofluids containing multiwalled carbon nanotubes and their enhanced thermal conductivities, **J. Appl. Phys. 94** 4967–4971.

38. B. Yang, Z.H. Han, 2006. Thermal conductivity enhancement in water-in-FC72 nanoemulsion fluids, **Appl. Phys. Lett. 88** (261914) 1–3.

39. R Saidur, K Y Leong & H A Mohammad. 2011. A Review on Applications and challenges of Nanofluids, **Renewable and Sustainable Energy Reviews, 15**(5), pp1646–1668.

40. G. H. Jiinkhan, A. E. Bergles, V. Nirmalan, T. Ravigururajan, 1985. Investigation of Turbulators for Fire Tube Boilers, **Journal of Heat Transfer, MAY Vol**. 107/355.

41. Manglik, R., Bergles, A. 1993a. Heat transfer and pressure drop correlations for Twisted-tape inserts in isothermal tubes: part II—transition and turbulent flows, **Journal of Heat Transfer, 115**, 890-896.

42. Manglik, R.M., Bergles, A.E. 1993b. Heat transfer and pressure drop correlationsfor twisted-tape inserts in isothermal tubes: part I—laminar flows, Journal of heat transfer, 115, 881-889.

43. Al-Fahed, S., Chakroun, W. 1996. Effect of tube-tape clearance on heat transfer for fully developed turbulent flow in a horizontal isothermal tube, **International journal of heat and fluid flow, 17**, 173-178.

44. S. K. Saha. A. Dutta, 2001. Thermohydraulic Study of Laminar Swirl Flow Through a Circular Tube Fitted with Twisted Tapes, **Journal of Heat Transfer, JUNE, Vol**. 123.

45. Kenan Y., Bayram S., Suat C., 2004. Flow-induced vibration analysis of conical rings used for heat transfer enhancement in heat exchanger, **Applied Energy 78** (0) 273–288.

46. Smith E., Chinaruk T., Pongjet P., 2006. Experimental investigation of heat transfer and flow friction in a circular tube fitted with regularly spaced twisted elements, **Int.Communications in heat and mass transfer, 33**-1225-1233.

47. Pongjet P., Smith E.-ard, 2007.Heat transfer augmentation in a circular tube using V-nozzle turbulator inserts and snail entry, **Experimental Thermal and Fluid Science 32-**332–340.

48. Veysel O., Sibel G., Orhan B., Necdet Alt., 2008. Heat transfer enhancement in a tube using circular cross sectional rings separated from wall, **Applied Energy 85-** 988–1001.

49. Anil S. Y., 2009.Effect of Half Length Twisted-Tape Turbulators on Heat Transfer and Pressure Drop Characteristics inside a Double Pipe U-Bend Heat Exchanger, **Jordan Journal of Mechanical and Industrial Engineering Volume 3**, Number 1, March. Pages 17- 22.

50. Panida S., Smith E., 2012. Visualization of Flow and Heat Transfer in Tube with Twisted Tape Consisting of Alternate Axis**, (ICCMS 2012) IPCSIT vol.22**.

51. Bofeng B., Wen L., 2015. A numerical study on helical vortices induced by a short twisted tape in a circular pipe, **Case StudiesinThermalEngineering, 5-**134–142.

52. Muhammad R., Suhaimi H., Aklilu T., 2015. Experimental Investigation on Heat transfer Enhancement by using Porous Twisted Plate as an Insert in a Fitted Tube, **ARPN Journal of Engineering and Applied Sciences VOL. 10**, NO 21, NOVEMBER

53. Smith E., Kwanchai N., Khwanchit W., Kittisak Y., Chinaruk T.,2015. Thermohydraulic Performance of Heat Exchanger Tube Equipped with Single-, Double-, and Triple-Helical Twisted Tapes, **Chemical Engineering Communications, 202**:606–615.

54. Toygun D., Orhan K., Veysel O., 2016. Numerical Investigation to Enhance Heat Transfer in a Circular Tube with Nozzles Formed Sinusoidal Geometry, **International Journal of Scientific and Technological Research Vol 2**, No.1.

55. Amnart B., Withada J., 2016.Turbulent Forced Convection and Heat Transfer Characteristic in a Circular Tube with Modified-Twisted Tapes, **Hindawi Publishing Corporation Journal of thermodynamics Volume**, Article ID 8235375, 16 pages.

56. V. Tirupati R., A. Rupesh V. R., T. Dharma R., 2017. Augmentation Heat Transfer in Circular Tube using Conical Ring and Twisted Tape Insert, **International Journal of Scientific Research Engineering & Technology (IJSRET), ISSN 2278 – 0882 Volume 6**, Issue 1, January.

57. Bock C. Pak, Young I. Cho**,** 1998**.** Hydrodynamic and Heat transfer Study of Dispersed Fluids with Submicron Metallic Oxide Particles, **Experimental Heat Transfer, 11**:151-170,

58. Li Q., Xuan Y., 2002. Convective heat transfer and flow characteristics of Cu-water nanofluid, **Science in china (Series E) Vol. 45** No. 4 August.

59. Yimin Xuan, Qiang Li, 2003. Investigation on Convective Heat Transfer and Flow Features of Nanofluids, **Journal of Heat Transfer February Vol. 125**.

60. Yulong D., Dongsheng W., 2004. Experimental investigation into convective heat transfer of nanofluids at the entrance region under laminar flow conditions, **International Journal of Heat and Mass Transfer 47-** 5181–5188.

61. Yulong D., Hajar A., Dongsheng W., Richard A. W., 2006. Heat transfer of aqueous suspensions of carbon nanotubes (CNT nanofluids), **International Journal of Heat and Mass Transfer 49-** 240–250.

62. Yurong He., Yi Jin, Haisheng Chen, Yulong D., Daqiang C., 2007. Huilin Lu, Heat transfer and flow behaviour of aqueous suspensions of TiO2 nanoparticles (nanofluids) flowing upward through a vertical pipe, **International Journal of Heat and Mass Transfer 50** -2272–2281.

63. Apurba K.S., Swarnendu S., Niladri C., 2009. Study of heat transfer due to laminar flow of copper–water nanofluid through two isothermally heated parallel plates, **International Journal of Thermal Sciences 48** -391–400.

64. Weerapun D., Somchai W., 2010.An experimental study on the heat transfer performance and pressure drop of TiO2-water nanofluids flowing under a turbulent flow regime, **International Journal of Heat and Mass Transfer 53**-334–344.

65. R. Ben M., N. Galanis, C.T. Nguyen, 2011. Experimental study of mixed convection with watereAl2O3 nanofluid in inclined tube with uniform wall heat flux**, International Journal of Thermal Sciences 50** (2011) 403-410.

66. Jaafar Al., Satinder T., Mushtaq Al., 2013. Heat transfer through heat exchanger using Al2O3 nanofluid at different concentrations, **Case Studies in Thermal Engineering 1**- 38–44.

67. M.Kh. Abdolbaqi, C.S.N.Azwadi, R.Mamat, 2014. Heat transfer augmentation in the straight channel by using nanofluids, **Case Studies in Thermal Engineering 3**-59–67.

68. W.H. Azmi, K.V. Sharma, P.K. Sarma, Rizalman M., G. Najafi, 2014. Heat transfer and friction factor of water based TiO2 and SiO2 nanofluids under turbulent flow in a tube, **International Communications in Heat and Mass Transfer 59**-30–38.

69. Oronzio M., Sergio N., Daniele R., Salvatore T., 2014. A Numerical Analysis on Nanofluid Mixed Convection in Triangular Cross-Sectioned Ducts Heated by a Uniform Heat Flux, **Hindawi Publishing Corporation Advances in Mechanical Engineering Article** ID 292973. Accepted 3 November.

70. Cong Qi, Yongliang Wan, Lin L., Zhonghao R., Yimin Li, 2016. Numerical and Experimental Investigation Into the Effects of Nanoparticle Mass Fraction and Bubble Size on Boiling Heat Transfer of TiO2–Water Nanofluid, **Journal of Heat TransferAUGUST, Vol. 138**.

71. Toygun D., Veysel O., 2016. Thermal Performance analyses of water based CU-TiO2 Hybrid Nanofluid flow in a Horizontal Tube, Fuels, **Fire and Combustion in Engineering Journal Volume 4**, December

72. E. E.Bajestan, M. C. Moghadam, H. Niazmand, W. Daungthongsuk, S.Wongwises , 2016. Experimental and numerical investigation of nanofluids heat transfer characteristics for application in solar heat exchangers**, International Journal of Heat and Mass Transfer 92**: 1041–1052.

73. K.V. Sharma, L. Syam Sundar, P.K. Sarma, 2009. Estimation of heat transfer coefficient and friction factor in the transition flow with low volume concentration of Al2O3 nanofluid flowing in a circular tube and with twisted tape insert, **International Communications in Heat and Mass Transfer 36-** 503–507.

74. L. Syam Sundar, K.V. Sharma, 2010. Heat transfer enhancements of low volume concentration Al2O3 nanofluid and with longitudinal strip inserts in a circular tube, **International Journal of Heat and Mass Transfer 53-** 4280–4286.

75. Khwanchit Wongcharee, Smith Eiamsa-ard, 2011. Enhancement of heat transfer using CuO/water nanofluid and twisted tape with alternate axis, **International Communications in Heat and Mass Transfer 38-** 742–748.

76. S. Suresh, K.P. Venkitaraj, P. Selvakumar, 2011 Comparative study on thermal performance of helical screw tape inserts in laminar flow using Al2O3/water and CuO/water nanofluids, **Superlattices and Microstructures 49-** 608–622.

77. M. Chandrasekhar, S. Suresh, A. Chandra Bose, 2011. Experimental Studies on Heat Transfer and Friction Factor Characteristics of Al2O3/Water Nanofluid in a Circular Pipe under Transition Flow with Wire Coil Inserts, **Heat Transfer Engineering, 32**(6): 485–496.

78. M. Saeedinia, M.A. Akhavan- Behabadi, M. Nasr, 2012.Experimental study on heat transfer and pressure drop of nanofluid flow in a horizontal coiled wire inserted tube under constant heat flux, **Experimental Thermal and Fluid Science 36** 158–168.

79. M. Kahani, S. Zeinali Heris, S. M. Mousavi,2013.Effects of Curvature Ratio and Coil Pitch Spacing on Heat Transfer Performance of Al2O3/Water Nanofluid Laminar Flow through Helical Coils, **Journal of Dispersion Science and Technology, 34**:1704–1712.

80. W.H. Azmi, K.V. Sharma, P.K. Sarma, Rizalman Mamat, Shahrani Anuar,2014. Comparison of convective heat transfer coefficient and friction factor of TiO2 nanofluid flow in a tube with twisted tape inserts, **International Journal of Thermal Sciences 81**- 84-93.

81. W.H. Azmi, K.V. Sharma, P.K. Sarma, Rizalman Mamat, Shahrani Anuar,L. SyamSundar,2014. Numerical validation of experimental heat transfer coefficient with SiO2 nanofluid flowing in a tube with twisted tape inserts, **Applied Thermal Engineering 73**:294-304.

82. M. T. Naik, L. S. Sundar, 2014. Heat Transfer and Friction FactorWith Water / Propylene Glycol-Based CuO Nanofluid in Circular Tube with Helical Inserts under Transition Flow Regime, **Heat Transfer Engineering, 35** (1):53–62**.**

83. P.V. Durga Prasad, A.V.S.S.K.S. Gupta, M. Sreeramulu, L. Syam Sundar, M.K. Singh, Antonio C.M. Sousa,2015, Experimental study of heat transfer and friction factor of Al2O3 nanofluid in U tube heat exchanger with helical tape inserts , **Experimental Thermal and Fluid Science 62**:141-150.

84. S. Eiamsa-ard, K. Kiatkittipong, W. Jedsadaratanachai, 2015. Heat transfer enhancement of TiO2/water nanofluid in a heat exchanger tube equipped with overlapped dual twisted-tapes, Engineering Science and Technology, **an International Journal** xxx 1-15.

85. Jaypal Mali, Girish Patil, A. R. Acharya, A. T. Pise, 2016. Heat Transfer Enhancement with Centrally Hollow Twisted Tape and AL2O3/ Water Based Nanofluid in Tubular Heat Exchanger, International Journal of Innovations in Engineering, **Research and Technology,IJIERT-ICITER-16**,ISSN:2394-3696 .

86. Hamed Safikhani, Ebrahim Hajian, Rafat Mohammadi, 2017. Numerical simulation of nanofluid flow over diamond-shaped elements in tandem in laminar and turbulent flow, **Trans. Phenom. Nano Micro Scales, 5**(2): 102-110.

87. K. N. Pavan, S. Suresh, M., Sekhar M, 2017. Experimental Investigation on Enhancement of Heat Transfer Rate in Heat Exchangers using Plain and Punched Twisted Tape Inserts and Nanofluid Employing Al2O3 Particles, **Indian Journal of Science and Technology, Vol 10**(25).

88. L. Syam Sundar, P. Bhramara, N.T. Ravi Kumar, Manoj K. Singh, Antonio C.M. Sousa,2017. Experimental heat transfer, friction factor and effectiveness analysis of Fe3O4 nanofluid flow in a horizontal plain tube with return bend and wire coil inserts, **International Journal of Heat and Mass Transfer 109**:440–453.

89. Fariba B., Majid S.-Avval , Mohammad S., Abbass A.,2017. Numerical investigation of nanofluid heat transfer in helically coiled tubes using the four-equation model, **Advanced Powder Technology** xxx: xxx–xxx.

90. Mostafa M., M. R. Tavakoli, Mohamad A. M., Arash G., Mohammad R. S.,2017. Experimental and numerical investigation on forced convection heat transfer and pressure drop in helically coiled pipes using TiO2/water nanofluid, **International Journal of Refrigeration S0**140-7007:30383-8.

91. Y. A. CENGEL, Cimbala, J.M., 2008, 929p, Fluid Mechanics Fundamentals and Applications, **McGraw-Hill Companies Inc**.

92. Johan.F.D.,Janusz M.G.,John A.S.,2011.Fluid Mechanics. **Prentice Hall**.6 edition.

93. Holman, J.P, 2010. Heat Transfer, **McGraw-Hill Companies Inc**.10 edition.

94. Y. A. CENGEL, Cimbala, J.M., 2008, 929p, HEAT TRANSFER\A Practical Approach, **McGraw-Hill Companies Inc**. 2 edition.

95. V.L.Streeter, E.B.Wylie, 1985.Fluid Mechanics, **McGraw-Hill Companies Inc**.8 edition.

96. Petukhov B. S., 1970. “Heat Transfer and Friction in Turbulent Pipe Flow with Variable Physical Properties.” **In Advances in Heat Transfer, ed. T. F. Irvine and J. P. Hartnett, Vol. 6**. New York: Academic Press.

97. Colburn. A. P., 1933. Transactions of the AIChE 26, p. 174.

98. Dittus F. W., Boelter L. M. K.., 1930. University of California Publications on Engineering 2, (p: 433).

99. Kays W. M., Crawford M. E.., 1993. Convective Heat and Mass Transfer. 3rd ed. New York: **McGraw-Hill**.

100. Gnielinski V., 1976. “New Equations for Heat and Mass Transfer in Turbulent Pipe and Channel Flow.” **International Chemical Engineering 16**, pp. 359–368.

101. Prandtl L.1904. Über Flüssigkeitsbewegung bei sehr kleiner Reibung (Motion of fluids with very little viscosity), **in Verhandlungen des III Internationalen Mathematiker-Kongresses, Heidelberg, (B G Teubner, Leipzig),** 484-491.

102. Nusselt W., 1915.The Fundamental Law of Heat Transfer**.** Das Grundgesetz des Wärmeüberganges, **Gesundheits-Ingenieur, vol. 38**, no. 42, pp. 477-482, 490-496.

103. Moody L. F., 1944. “Friction Factors for Pipe Flows.” **Transactions of the ASME 66**, pp. 671–684.

104. Mc. Adams. W.H, 1954. Heat transmission. **McGraw-Hill**.

105. Blasius H., 1913.Das Ahnlichkeitsgesetz bei Ribungsorgangen in Fluissigkeiten, **Frsch.Arb.Ing.-Wes**., No.131, Berlin.

106. Nikuradse J., 1932.GesetzmaBigkeiten der Turbulanten Stromung in Glatten Rohren, **Forsch.Arb.Ing.-Wes**., NO: 356.

107. Fluent v.14.5 User Guide, Fluent Corporation, Lebanon, **New Hampshire**, 2006.

108. ANSYS, 2013.Meshing User's GuideANSYS South pointe 275 Technology Drive Canonsburg, PA 15317 ANSYS, Inc. ansysinfo@ansys.com http://www.ansys.com.

109. Kayhani M.H., Soltanzadeh H., Heyhat M.M., Nazari M., Kowsary F., 2012. Exprimantal study of convective heat transfer and pressure drop of TiO2/water nanofluid, **, Int. J. Heat Mass Transfer 39**: 456-462.

110. Zhou S. Q., Ni R., 2008, Measurement of the specific heat capacity of water based Al2O3 nanofluid, **Applied Physics Letters, Vol. 92**, 093123-1.

111. Drew D.A., S.L. Passman, 1999. Theory of Multi-Component Fluids, Springer, Berlin.

112. Timofeeva E.V., Gavrilov A.N., McCloskey J.M., Tolmachev Y.V., 2007. Thermal conductivity and particle agglomeration in alumina nanofluids: **experiment and theory, Phy. Rev. 76**- 061203.

CURRICULUM VITAE

PERSONAL DATA

Name and Surename:	:	Natiq AL-AMERI
Nationality	:	Iraq (Iraqi)
Birth Date and Place	:	December 2, 1978, Baghdad
Marital Status	:	Married
Tel:	:	+90 5531306866 (Turkya) : +9647711209688 (Iraq)
Fax	:	-
email	:	eng.natiq6813@gmail.com
Address		Mevlana Mah.Tavlusun Cad. Feslegen Sok No:9,Seza Residance, Talas/KAYSERİ

EDUCATION

Degree	Institute	Date of Graduation
Bachelor's	Baghdad Univercity- Engeenering faculaty	2001
High School	AL-Karkh Secondary school	1997

PROFESSIONAL EXPERIENCE

Year	Institute	Mission
2008- Currently	Ministry of Municipalities and Works / Directorate of Water Baghdad Governorate	Head of Resident Engineer Department for Husseiniya Water Networks Project
2007–2008	Ministry of Municipalities and Works / Directorate General Water	Head of Machinery and Equipment Department
2005-2007	Ministry of Municipalities and Works / Directorate of Municipalities of Baghdad Governorate	Directorate of the Municipality of Diyala Bridge
2003-2005	Ministry of Public Works / General Construction Directorate	Engineer

LANGUAGE

Arabic, English and Turkish.

SELECTED PUBLICATIONS

1. ALAMERI N., ÖZCEYHAN V., DAGDEVIR T., KEKLIKCIOGLU O. " A Numerıcal Study Of The Effect Of Nozzle Insert In A Horızontal Tube By Usıng Water Based TiO_2- Nanofluıd On Heat Transfer" ULIBTK'17 21. Ulusal Isı Bilimi ve Tekniği Kongresi, ÇORUM, (2017).
2. ALAMERI N., ÖZCEYHAN V., DAGDEVIR T., KEKLIKCIOGLU O. "Numerical Study Of The Effect Of Drilled Nozzle Inserted In A Tube Through Water Based TiO_2- Nanofluid On Heat Transfer Performance", 4^{th} International Conference On Computatıonal And Experımental Scıence And Engıneerıng (ICCESEN-2017)2017, Antalya-Turkey, (2017).